PHYSICOCHEMICAL AND TRIBOLOGICAL ANALYSIS OF CHEMICALLY MODIFIED MICROALGAE OIL BLENDS FOR MALAYSIAN CONDITIONS

CHEAH MEI YEE

FACULTY OF ENGINEERING
UNIVERSITY OF MALAYA
KUALA LUMPUR

2019

PHYSICOCHEMICAL AND TRIBOLOGICAL ANALYSIS OF CHEMICALLY MODIFIED MICROALGAE OIL BLENDS FOR MALAYSIAN CONDITIONS

CHEAH MEI YEE

THESIS SUBMITTED IN FULFILMENT OF THE REQUIREMENTS FOR THE DEGREE OF DOCTOR OF PHILOSOPHY

FACULTY OF ENGINEERING
UNIVERSITY OF MALAYA
KUALA LUMPUR

2019

UNIVERSITY OF MALAYA

ORIGINAL LITERARY WORK DECLARATION

Name of Candidate: Cheah Mei Yee

Matric No: KHA100013

Name of Degree: Doctor of Philosophy

Title of Project Paper/Research Report/Dissertation/Thesis (“this Work”):

Physicochemical and tribological analysis of chemically modified microalgae oil blends for Malaysian conditions

Field of Study: Biofuel

I do solemnly and sincerely declare that:

(1) I am the sole author/writer of this Work;
(2) This Work is original;
(3) Any use of any work in which copyright exists was done by way of fair dealing and for permitted purposes and any excerpt or extract from, or reference to or reproduction of any copyright work has been disclosed expressly and sufficiently and the title of the Work and its authorship have been acknowledged in this Work;
(4) I do not have any actual knowledge nor do I ought reasonably to know that the making of this work constitutes an infringement of any copyright work;
(5) I hereby assign all and every rights in the copyright to this Work to the University of Malaya (“UM”), who henceforth shall be owner of the copyright in this Work and that any reproduction or use in any form or by any means whatsoever is prohibited without the written consent of UM having been first had and obtained;
(6) I am fully aware that if in the course of making this Work I have infringed any copyright whether intentionally or otherwise, I may be subject to legal action or any other action as may be determined by UM.

Candidate’s Signature Date:

Subscribed and solemnly declared before,

Witness’s Signature Date:

Name:

Designation:

PHYSICOCHEMICAL AND TRIBOLOGICAL ANALYSIS OF CHEMICALLY MODIFIED MICROALGAE OIL BLENDS FOR MALAYSIAN CONDITIONS

ABSTRACT

Many health and environmental issues like skin and respiratory disease due to groundwater contamination, greenhouse gasses, and toxic smog have been linked to the usage of fossil-based lubricant and fuel. This growing demand for greener alternatives has led scientist to microalgae, an ancient organism with more than 100,000 species. In order to bioprospecting local microalgae species that will eradicate the issue of alien species invasion of local ecosystem, we have identified and isolated five local freshwater microalgae species. Their suitability (including two purchased species) for biolubricant production were assessed from the growth, biomass productivity and lipid composition aspects. The oil extraction process, chemical modification and the physicochemical properties of the selected species were investigated, followed by the tribological performance evaluation as a biolubricant and as an additive in diesel and in a commercial full synthetic lubricant (FFL). It was found that *Chlorella* sp. and *Ankistrodesmus* sp. exhibited comparable growth rate and lipid yield (higher than other tested species). However, *Chlorella* sp. was selected over *Ankistrodesmus* sp. due to its lipid composition as this species contained higher amount of long carbon chain fatty acids and unsaturation. The higher amount of long carbon chain fatty acids and unsaturation are found to produce thicker lubricating film and exhibit better cold weather performance, two important properties for biolubricant application. The lipid yield has been successfully increased by changing the extraction solvent from petroleum ether to chloroform: methanol (2:1). Additionally, chemical modification can be used to reduce the acidity of the extracted oil as free fatty acids were converted into esters. Results indicate that chemically modified microalgae oil (MMO) can be used as friction modifier. We observed a decline in friction coefficient (COF) when blending percentage is increased compared with pure polyalphaolefin (PAO) (used as base-oil) sample, though the further increase in blending percentage (above 10%) ceased to cause any further improvement on the COF. On the aspect of wear prevention and performance in extreme pressure condition, MMO-10 showed notable results that were comparable to a FFL. It exhibited a load-wear index (an important load carrying parameter for an EP additive) that was similar to that of a commercial lubricant. Our analyses further revealed that MMO-10 was thermally stable and exhibited better combustion than PAO, and the oxidation stability of PAO was extended to more than 24 folds with MMO addition. The presence of oxygen-containing compounds and natural antioxidants would be the reasons for such observations. When MMO was used as additives in diesel, significant wear reduction was observed compared with pure diesel. However, no further improvement on the wear were observed with the increase of MMO above 8%. Further, the fluctuations of COF and wear with the increase of MMO-10 percentage indicates that the interactions between MMO-10 and FFL were more complex though blending at 2% and below enhances the wear and COF of pure FFL. In conclusion, chemically modified microalgae oil (particularly, MMO-10) is an effective friction modifier and has shown great potential as an anti-wear and EP additives for lubricant.

Keywords: microalgae; biolubricant; growth; fatty acid profile; friction and wear

ANALISIS FISIKOKIMIA DAN TRIBOLOGI MINYAK MIKROALGA YANG TELAH DIUBAHSUAI SECARA KIMIA UNTUK KEGUNAAN DI MALAYSIA

ABSTRAK

Banyak isu kesihatan dan alam sekitar seperti penyakit kulit dan pernafasan akibat kontaminasi air bawah tanah, gas rumah hijau serta asap toksik telah dikaitkan dengan penggunaan pelincir dan bahan api berasaskan fosil. Permintaan yang semakin meningkat untuk alternatif yang lebih hijau telah membawa saintis kepada mikroalga, satu organisma purba yang mengandungi lebih daripada 100,000 spesies untuk dieksploitasi. Untuk tujuan bioprospeksi, spesies mikroalgae tempatan yang akan membasmi isu pencerobohan spesies asing terhadap ekosistem tempatan, kami telah mengenal pasti dan mengasingkan lima spesies mikroalga air tawar tempatan dan menguji kesesuaian mereka untuk pengeluaran pelincir bio. Kesesuaian mikroalga (termasuk dua spesis yang dibeli) untuk pengeluaran biolubricant dinilai dari aspek pertumbuhan, produktiviti biomas dan komposisi minyak. Proses pengekstrakan minyak, pengubahsuaian kimia dan sifat fizikokimia spesies terpilih akan diselidik. Kami juga menguji penggunaan minyak microalga sebagai biopelincir dan juga sebagai aditif pengubah geseran untuk diesel dan pelincir sintetik penuh komersial (FFL). Adalah didapati bahawa *Chlorella* sp. dan *Ankistrodesmus* sp. mempamerkan kadar pertumbuhan dan hasil lipid yang setara (lebih tinggi daripada spesies lain yang diuji). Walau bagaimanapun, *Chlorella* sp. akhirnya dipilih kerana komposisi lipidnya yang lebih sesuai untuk penghasilan pelincir. Ini adalah kerana spesis ini mengandungi jumlah yang tinggi bagi asid lemak rantai karbon panjang dan asid lemak tidak tepu. Kedua-dua sifat ini didapati boleh menghasilkan filem pelincir yang lebih tebal dan mempamerkan prestasi cuaca sejuk yang lebih baik, antara dua sifat penting untuk aplikasi pelincir bio. Selain itu, kami dapati bahawa, dengan mengubah pelarut pengekstrakan yang digunakan daripada *ether petroleum* kepada *chloroform: methanol* (2: 1), kedapatan lipid berjaya dinaikkan dengan signifikan. Selain itu, pengubahsuaian kimia boleh digunakan untuk mengurangkan keasidan minyak yang diekstrak, apabila asid lemak bebas ditukarkan menjadi ester. Keputusan menunjukkan bahawa minyak mikroalgae yang diubahsuai secara kimia (MMO) boleh digunakan sebagai pengubah geseran. Hasil kajian menunjukkan penurunan pekali geseran (COF) apabila peratusan campuran ditingkatkan berbanding dengan polyalphaolefin (PAO) (digunakan sebagai minyak asas). Sungguhpun begitu, peningkatan dalam peratusan pengadunan melebihi 10%, tidak lagi menyebabkan penurunan lanjut COF. Selain itu, dari aspek pencegahan hausan dan prestasi pelincir dalam keadaan yang melampau, penggabungan MMO-10 menunjukkan hasil yang ketara, yang setanding dengan pelincir sintetik penuh (FFL) yang boleh didapati secara komersil. MMO-10 mempamerkan indeks beban-hausan (satu parameter penting untuk bahan tambah EP) yang hampir serupa dengan FFL. Analisis seterusnya telah menunjukkan bahawa MMO-10 adalah stabil dan mempamerkan pembakaran yang lebih baik berbanding PAO. Di samping itu, MMO-10 juga menunjukkan kestabilan pengoksidaan yang lebih baik daripada PAO. Tempoh kestabilan pengoksidaan PAO berjaya diperpanjangkan dengan kadar 24 kali ganda dengan penambahan MMO. Ini adalah kerana terdapat sebatian beroksigen dan antioksidan semulajadi dalam MMO. Apabila MMO digunakan sebagai aditif dalam diesel, pengurangan COF yang ketara didapati jika dibandingkan dengan diesel tulen. Bagaimanapun, tiada penambahbaikan COF diperolehi apabila peratusan MMO ditingkatkan melebihi 8%. Selain itu, kedapatan COF yang turun naik dan kadar hausan yang meningkat apabila kandungan MMO-10 yang digunapakai dinaikkan melebihi 2% menunjukkan bahawa interaksi antara MMO-10 dan FFL adalah amat kompleks. Hasil kajian ini menyimpulkan bahawa minyak mikroalga yang diubahsuai secara kimia (terutamanya, MMO-10) merupakan pengubah geseran, pencegah hausan dan bahan tambah EP yang berkesan dan berpotensi tinggi untuk digunakan sebagai aditif pelincir.

Kata kunci: mikroalga; pelincir bio; pertumbuhan; profil asid lemak; geseran dan hausan

ACKNOWLEDGEMENTS

I would like to dedicate my thesis to my late father and brother. I love you all.

To my supervisors Emeritus Prof. Ir. Dr. Masjuki Hj. Hassan and Prof. Datin Seri Dr. Hjh. Aishah Hj. Salleh, thank you for putting up with my slow progress and for all the support and guidance provided.

Special appreciation to Dr. Ong Hwai Chyuan, Dr. Nurin Wahidah Mohd Zulkifli, Dr. Mahendra Varman, Assoc. Prof. Dr. Md. Abul Kalam, Assoc. Prof. Dr. Chong Wen Tong, Assoc. Prof. Ir. Dr. Ang Bee Chin and Mr. Poh Sin Chew.

To Dr. Lim Hong Chang from Tunku Abdul Rahman University College, thank you for assisting in the phylogeny tree generation and relevant description.

Thank you to Mr. Sulaiman Bin Ariffin (Wak Leman), Mr. Faisal Hadi Bin Mohd Amizam from ISB, Mr. Mohd Fauzi Bin Bakri Hashim and Mr. Mohd Syukri Bin Ab Razak.

To my fellow lab mates Dr. How Heoy Geok, Dr. Teoh Yew Heng, Mr. Leang So Khuong, Mr. Mohd Nur Ashraf Bin Mohd Yusoff, Madam Siti Safiyah Binti Nor Azman, Madam Jassinnee Milano, Mr. Muhammad Syahir Amzar Bin Zulkifli and Mr. Muhammad Harith Bin Hasnul thank you for all the help extended.

The author gratefully acknowledges the financial support provided by the Ministry of Education (MOE), Malaysia, and University of Malaya through the following grants: PS121/2010B, RG112-11AET, RP016-2012B, and UM.C/HIR/MOHE/ENG/60.

TABLE OF CONTENTS

LIST OF FIGURES

LIST OF TABLES

LIST OF SYMBOLS AND ABBREVIATIONS

COF	:	Coefficient of friction
F_f	:	Frictional force experienced by the two contacting bodies in motion
F_N	:	Normal force pressing the same two bodies together
μ	:	Coefficient of friction in tribology
η	:	Viscosity
V	:	Rotational speed
P	:	Load
HD	:	Hydrodynamic
EHD	:	Elastohydrodynamic
USD	:	United States dollar
TLL	:	Total lost lubricants
FA	:	Fatty acid
EU	:	European Union
USA	:	United States of America
+	:	Positive influence
-	:	Negative influence
COOH	:	Carboxylic acid
C-OH	:	Carboxyl group
$COOCH_3$	:	Methyl ester
C=O	:	Carbonyl group
C-O-C	:	Ether group
VI	:	Viscosity index
UV	:	Ultraviolet radiation
β	:	Beta
C	:	Carbon

H	:	Hydrogen
PP	:	Pour point
CP	:	Cloud point
n	:	An amount of substance in chemical physics
$-COO^-$	:	Charged carboxyl group
R	:	Organic group
TMP	:	Trimethylolpropane
US DOE	:	United States Department of Energy
CO_2	:	Carbon dioxide
NO_3^-	:	Nitrate ion
NO_2^-	:	Nitrite ion
NH_4^-	:	Ammonium ion
PO_4^{3-}	:	Phosphate ion
Hg(II)	:	Mercury (II) ion
Cd(II)	:	Cadmium (II) ion
Pb(II)	:	Lead (II) ion
TBT	:	Tributyltin
Cd	:	Cadmium
N	:	Nitrogen
P	:	Phosphorus
Co	:	Cobalt
Zn	:	Zinc
Mn	:	Manganese
Ni	:	Nickel
Pb	:	Lead
Cu(II)	:	Copper (II) ion
Fe(II)	:	Iron (II) ion
Ni(II)	:	Nickel (II) ion

Zn(II)	:	Zinc (II) ion
Cr(VI)	:	Chromium (VI) ion
U	:	Uranium
Cu	:	Copper
KF/Al_2O_3	:	Potassium fluoride on alumina
KF/HZSM-5	:	Potassium fluoride on HZSM-5 zeolite
AEO	:	Upgraded KF/Al_2O_3 oil
HEO	:	Upgraded KF/HZSM-5 oil
Fe_2O_3	:	Iron (III) oxide
Ra	:	Surface roughness
AMO	:	Esterified bio-oil using KF/Al_2O_3 as the catalyst
HMO	:	Esterified bio-oil using KF/HZSM-5 as the catalyst
MeOH-SBO	:	Crude *Spirulina* sp. bio-oil and methanol blends (MeOH-SBO)
M	:	Molar
$NaNO_3$	:	Sodium nitrate
K_2HPO_4	:	Dipotassium phosphate
$MgSO_4.7H_2O$	:	Magnesium sulfate heptahydrate
$CaCl_2.2H_2O$	:	Calcium chloride Dihydrate
Na_2CO_3	:	Sodium carbonate
$Na_2SiO_3.9H_2O$	:	Sodium metasilicate nonahydrate
$MgNa_2EDTA.3H_2O$	:	Magnesium disodium ethylenediaminetetraacetate trihydrate
H_3BO_3	:	Boric acid
$ZnSO_4.7H_2O$	:	Zinc sulfate heptahydrate
$CuSO_4.5H_2O$	:	Copper(II) sulfate pentahydrate
$Na_2MoO_4.2H_2O$	:	Sodium molybdate dihydrate
$Co(NO_3)_2.6H_2O$	:	Cobalt(II) nitrate hexahydrate
NaCl	:	Sodium chloride
KH_2PO_4	:	Monopotassium phosphate

$Na_2EDTA.\ 2H_2O$	Disodium ethylenediaminetetraacetate dihydrate
KOH	Potassium hydroxide
$FeSO_4.7H_2O$	Iron(II) sulfate heptahydrate
H_2SO_4	Sulfuric acid
$MnCl_2$	Manganese(II) chloride
MoO_3	Molybdenum trioxide
Vitamin B1	Thiamine HCl
Vitamin B12	Cyanocobalamin
18S	18 Svedberg units
rRNA	Ribosomal ribonucleic acid
gDNA	Genomic DNA
DNA	Deoxyribonucleic acid
PCR	Polymerase chain reaction
rDNA	Ribosomal DNA
NCBI	National Center for Biotechnology Information
nt	Nucleotide
SSU	Small subunit
MP	Maximum parsimony
ML	Maximum likelihood
BI	Bayesian inference
TBR	Tree-bisection-reconnection
AIC	Akaike information criterion
TIM2+I+G	Transition model 2 + proportion of invariable sites + gamma distribution
ESS	Effective samples size
PP	Posterior probability
OD	Optical density
μ	Specific growth rate in predictive microbiology

N_1	:	Biomass at time1 (t1)
N_2	:	Biomass at time2 (t2)
t1	:	At time1
t2	:	At time2
P	:	Microalgae biomass productivity
N1	:	Biomass at time1
N2	:	Biomass at time2
FAME	:	Fatty acid methyl ester
GC	:	Gas chromatography
FID	:	Flame ionization detector
C:M	:	Chloroform: Methanol
IV	:	Iodine value
A_i	:	Fatty acid composition of each component
D	:	Number of double bonds
M_{wi}	:	Molecular mass of each component
KV	:	Kinematic viscosity
V_{mix}	:	Kinematic viscosity of the biodiesel sample (mixture of fatty acid alkyl esters)
A_c	:	Relative amount (%/100) of the individual neat ester in the mixture
CFPP	:	Cold filter plugging point
PAME	:	Palmitic acid methyl ester content (wt%)
wt%	:	Weight percentage
sp.	:	Species
v/v	:	Volume/volume
rpm	:	Revolutions per minute
CMO	:	Crude *Chlorella* sp. microalgae oil
MMO	:	Modified microalgae oil
PAO	:	Polyalphaolefin

OIT : Oxidative induction time

DMO : Diesel-MMO blends

FMO : FFL-MMO-10 blends

FFL : Full synthetic lubricant

SEM : Scanning electron microscope

EDS : Energy-dispersive X-ray spectrometer

WSD : Wear scar diameter

EHL : Elastrohydrodynamic lubrication

λ : Film thickness ratio

α : Dynamic viscosity

σ : Surface roughness of the two contacting surfaces

η_o : Dynamic viscosity at atmospheric pressure

μ : Coefficient of friction

ν : Kinematic viscosity

E : Modulus elasticity of the solids

E' : Modulus elasticity of the interacting solids

h_{min} : Minimum film thickness

H_{min} : Dimensionless minimum film thickness

k : Ellipticity ratio

R : Radius of the ball

R' : Reduced radius

u : Mean speed of contacts

U : Dimensionless speed parameter

σ_q : Composite surface roughness

W : Dimensionless load parameter

FTP : Flash temperature parameter

d : Mean wear scar diameter

LIST OF APPENDICES

CHAPTER 1: INTRODUCTION

1.1 Background

Lubrication is applied to reduce friction and wear between the rubbing surfaces, and the substance that performs the work is called a lubricant. Unproductive friction and wear will lead to the failure of mechanical systems, a pertinent issue facing the industrial and transportation sectors. The global lubricant market was valued at USD 118.89 billion in 2016 and it is forecasted to reach 45.4 million metric tons in 2019, with a projected rise of 2% per year (Research Grand View, 2018). This demand is further supported by the rapid expansion of transportation and industrialization in China and India, the world's two giant economies (The Freedonia Group, 2015).

Additionally, industrial lubricants can be categorized by application; generally, process oils and general industrial oils dominate the market by volume. Process oils refer to special oils that are used in the chemical and technical industries either as raw materials or as an aid to processing. On the other hand, general industrial oils are like hydraulic fluids, turbine oils, gear oils, compressor and refrigeration fluids. Figure 1.1 shows the 2016 market volume of industrial lubricant by applications and according to a market survey by Research Grand View (2018), the demand for industrial lubricants expected to grow further in the near future.

On the other hand, Figure 1.2 illustrates the demand for lubricant in Southeast Asia from 2014 to 2019 where the compound annual growth rate (CAGR) is projected at 4.7% within this period. Malaysia's lubricant's demand is estimated to increase from 247 in 2014 to 287 million liters in 2019 (Ng & Law, 2017).

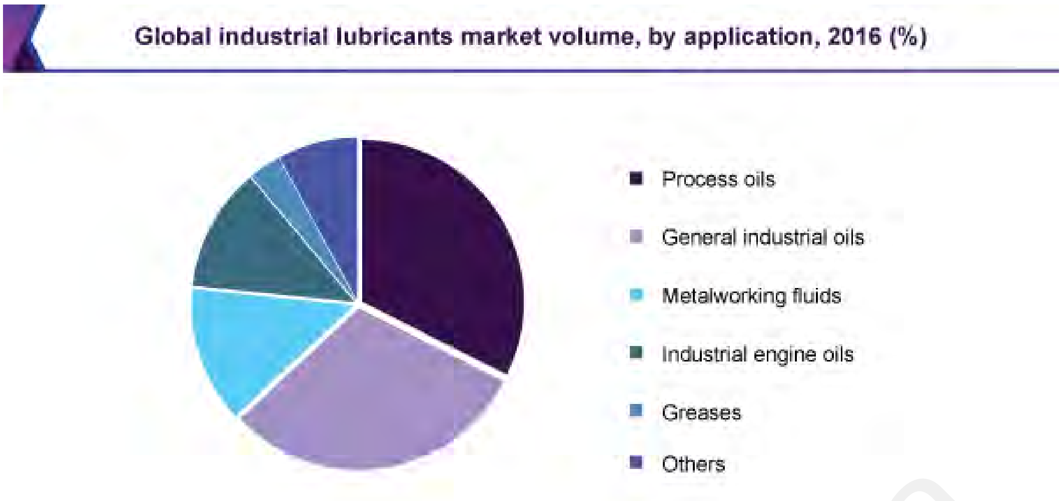

Figure 1.1: Global industrial lubricants market volume 2016 (Research Grand View, 2018)

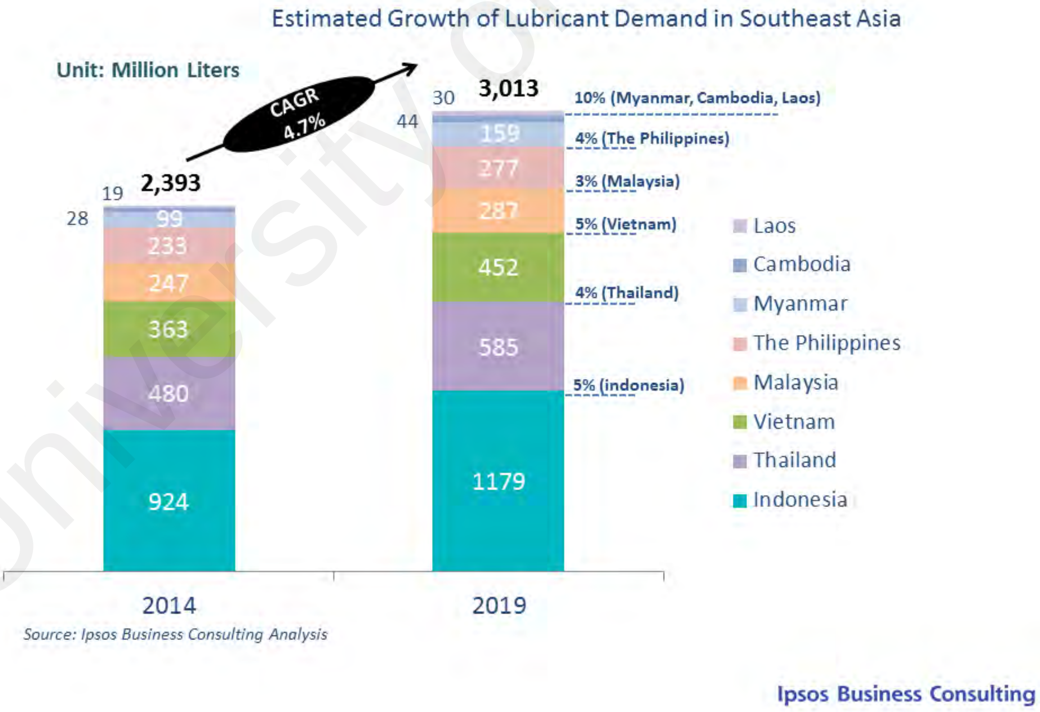

Figure 1.2: Estimated growth of lubricant demand in Southeast Asia (Ng & Law, 2017)

Today, lubricants are formulated not only to reduce friction, but serving various needs like wear debris removal, corrosion inhibition, act as a coolant, wear prevention, etc. (Syahir et al., 2017). Furthermore, normal conventional lubricants are produced from petroleum, however, various environmental and health issues have arisen due to the complexity of lubricant formulations in order to cater to various demands (Figure 1.3).

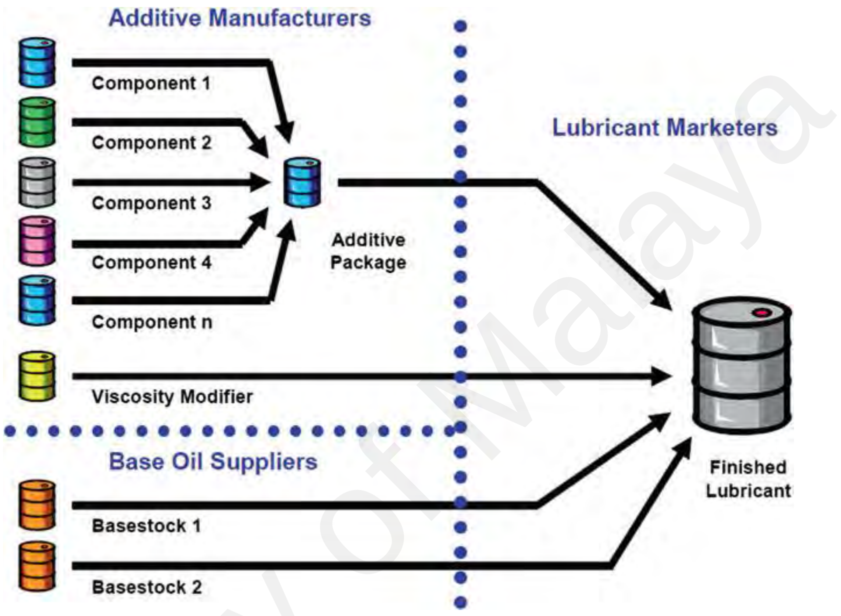

Figure 1.3: Additives in lubricant (Madanhire & Mbohwa, 2016)

The release of these hazardous chemicals, either accidentally or due to defective parts, have negatively affected the environment. Environmentally sensitive areas like near water resources and often ground water will be adversely impacted if proper disposal is not implemented. Exposure to these chemicals is found to cause health issues, excessive or long-term exposure can even lead to death. Kidney damage is associated with heavy metal exposure such as lead and chromium, and benzene are known to be carcinogenic (Madanhire & Mbohwa, 2016; Wedeen & Qian, 1991; Zainal et al., 2018). Additionally, flu-like symptoms such as fatigue, headache, nausea, and eye irritation are likely to go unnoticed.

Due to the growing concerns regarding health and environmental issues, much effort is being made to produce biolubricants to replace petroleum-derived lubricants. Biolubricants which are typically produced from vegetable oils are more desirable since they are highly biodegradable and non-toxic, which are ideal to replace conventional lubricants especially for use in environmentally sensitive areas. Besides that, more countries are imposing stricter policies for lubricant usage.

The biolubricants market is projected to grow from an estimated USD 2.47 billion in 2017 to USD 3.36 billion by 2022 with a CAGR of 6.4%. Apart from the implementation of regulating polices (like EU Ecolabel) in the market like the US and EU, new biolubricant R&D firms are projected to further catalyze the biolubricants market during these period (Markets and Markets, 2018).

Biolubricant is generally derived from vegetable oil, with triglyceride dominating almost 98% of total lipid composition (Rudnick, 2009). Usually, oil crops like canola, coconut, corn, olive, palm, and rapeseed are used to produce biolubricants (Syahir et al., 2017). But due to food security issues concerning vegetable-based biolubricant, the need to produce them from alternative feedstock that is both renewable and sustainable is much preferred.

The quest for alternative feedstock has led researchers to microalgae, one of the earth's earliest occupants. These organisms are collectively referred to as algae, and can be grouped into macro- and microalgae. Macroalgae as its name suggested, are made up of bigger size algae like seaweed and kelp. On the other hand, microalgae are microscopic in size.

Microalgae fulfill this need and these microorganisms offer the following advantages over edible vegetable oils:

a) microalgae have high lipid production,
b) microalgae can be cultivated in ponds which can be built on marginal lands, thereby reducing competition for arable lands suitable for food crops, some microalgae species can tolerate a wide range of water salinity including seawater and municipal wastewater which facilitates its cultivation,
c) microalgae have higher photosynthetic efficiency compared with terrestrial plants, resulting in quick microalgae growth and,
d) microalgae can be harvested daily throughout the year, rather than in seasons.

Microalgae which consist of many different taxonomic divisions can be applied in various industries (Figure 1.4), as food and feeds, as bio-filter for pollutant removal (Maity et al., 2014), for the production of nutraceutical and pigments, and for the production of biofuel and biolubricant.

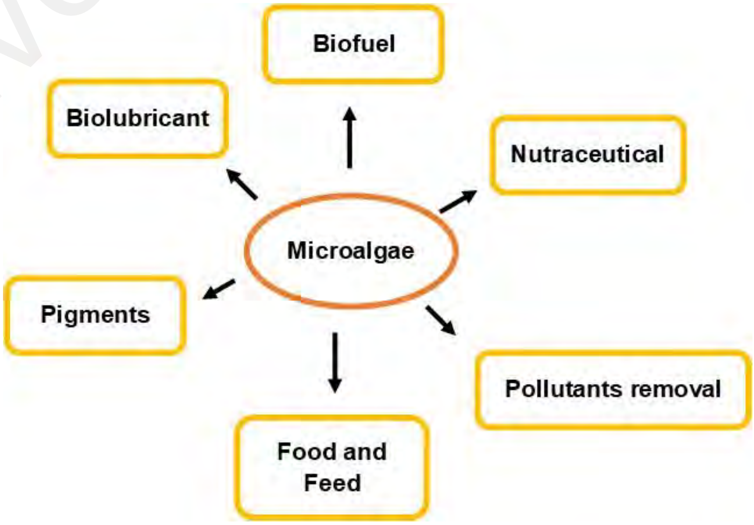

Figure 1.4: Applications of microalgae in different industry

Owing to microalgae’s diversified applications, Credence Research (2017) has forecasted that the algae products market is projected to reach USD 44.7 billion by 2023, with a CAGR of above 5.2% from 2016 to 2023. Meanwhile, Figure 1.5 illustrates the global distribution of private companies producing commercial food and feed products from microalgae. Evidently, the majority of them are producing the high-value nutraceutical products like docosahexaenoic acid (DHA), eicosapentaenoic acid (EPA), β-carotene and astaxanthin.

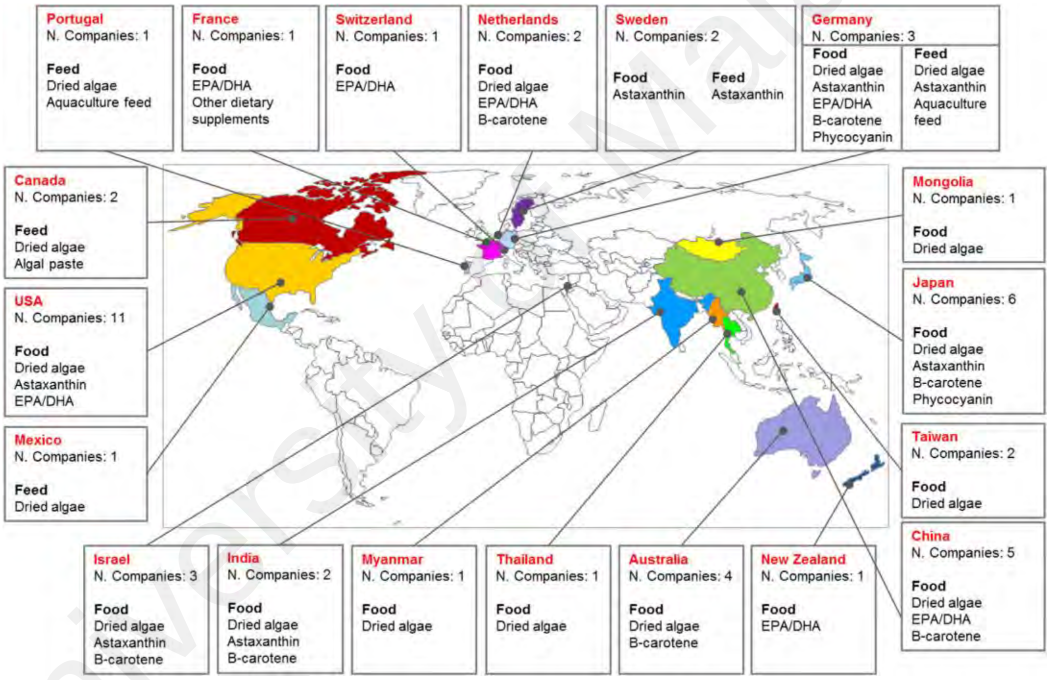

Figure 1.5: Global distribution of private companies producing commercial food and feed products derived from microalgae (Vigani et al., 2015)

1.2 Problem statement

Looking at the benefits that could be offered by microalgae, many researchers have concluded that an integrated system that could recycle waste carbon dioxide from flue gas and remediate municipal wastewater as cultivation resources form the best production design. The biomass attained from the system will be used as feedstock. However, because the introduction of foreign species may cause serious ecological problems and threats to the local biodiversity, it would be ideal to find indigenous species for such applications.

Secondly, despite a large number of studies available in the scientific literature on microalgae, most of these studies are focused on the production of biodiesels, bioethanols, and biohydrogen from microalgae, optimization of the process parameters for biofuel production, as well as the life cycle assessment of microalgae biofuels. To date, little is known regarding the friction and wear characteristics of microalgae-based biolubricants, and these characteristics are the motivation of this work. Table 1.1 tabulates the friction and wear responses of various vegetable oil-based biodiesel and biolubricant. Evidently, promising improvements of COF and wear are obtained with the addition of vegetable oil and vegetable biodiesel into diesel or lubricant base oil. Moreover, the inclusions of solid nanolubricants or ionic liquid are shown to further enhance these properties. Because the content of the fatty acids varies by oil sources that in turn, affect the resultant product properties, different types of chemical modification have been applied to produce the best performing lubricant. As with many of the vegetable oil crops that have been reintroduced as biolubricant, the same approach may also be adopted for microalgae oil based biolubricant.

Table 1.1: The friction and wear responses of various vegetable oil-based biodiesel and biolubricant

Sample	Equipment	Testing condition	Findings	References
Rapeseed oil with Stearic acid-capped cerium borate composite nanoparticles (SA/$CeBO_3$)	FBT	Rotary speed: 1500 r/min, load: 392 N, duration: 30 min, temperature: RT	COF and WSD decrease with the increase of SA/$CeBO_3$ to up about 2.0%, beyond which sharp increase of COF and WSD were detected.	(Boshui et al., 2015)
Diesel, *Calophyllum inophyllum*, palm biodiesel, and their blends	FBT	Load: 40 kg, speed: 600, 900, 1200 and 1500 rpm, temperature: 75°C, duration: 3600s	The average COF of pure *C. inophyllum* and palm biodiesel were 28.8 and 23.4% lower than diesel respectively. The WSD of biodiesel and biodiesel blends at different temperatures and loads were lower than the WSD detected on diesel. PB20 exhibited good lubrication performance and has the lowest WSD among all the tested samples.	(Mosarof et al., 2016)
Rubber seed oil (RSO), coconut oil, sunflower oil, and SAE20W40 lubricant	FBT	ASTM D4172-94	RSO has the lowest WSD when compared with coconut and sunflower oils (vegetable oil). However, RSO's WSD is still higher than SAE20W40.	(Aravind et al., 2015)

Table 1.1, continued

Cottonseed oil methyl ester (COME), blends and diesel	FBT	Load: 40 kg and 80 kg, speed: 1800 rpm, temperature: RT (27°C), 45°C, 60°C and 75°C, duration: 300s	The COF decreases with the increase of COME concentration. The COF of COME100 were lower by 28.06, 19.49, 7.49 and 3.65% when compared with DL100, COME10, COME20, and COME50. The WSD of COME100 were lower than that of DL100, COME10, COME20, and COME50 by 47.6%, 33.3%, 32.1%, and 21.42%, respectively.	(Jamshaid et al., 2019)
TMP palm (CMPO) with 1wt% CuO, 1wt% MoS2, 1wt% Surfactant (oleic acid)	FBT	ASTM 2783	CuO and MoS_2 enhanced the AW/EP of pure CMPO by 1.5 times. MoS_2 offers better AW/EP performance than CuO due to better dispersion. Surfactant aids the dispersant of nanoparticles and reduces wear compared with pure CMPO.	(Gulzar et al., 2015)
TMP jatropha (MJO) with phosphonium-based ionic liquid (PIL) and ammonium-ionic liquid (AIL)	FBT	ASTM 2783	AIL and PIL offered good synergistic effect on the tribological performance of MJO. 10wt% and 1wt% are the percentages needed for AIL and PIL to enhanced MJO lubrication. 10 wt% AIL is better at corrosion prevention in comparison to 1wt% PIL.	(Amiril et al., 2018)

Table 1.1, continued

Rapeseed oil (RSO) with GO-D and GO-T Graphene oxide reacted with 1-dodecanethiol (GO-D) and tert-dodecyl mercaptan (GO-T).	FBT	China GB 3142-82 Temperature: RT, rotational velocity: 1450 rpm, duration: 30 min., load: 98 N, 196 N, 294 N, 392 N.	GO-D and GO-T exhibited excellent anti-friction, anti-wear properties, and extreme pressure performance. The addition of GO-D at 0.2 wt% reduces the COF by 44.5% and WSD by 40.1%.	(G. Zhang et al., 2018)
Waste cooking oil (WCO) biodiesel	HFRR	Load applied: 9.8 N, stroke length: 1mm, frequency: 20 Hz, duration: 180 min., temperature: 105 °C.	Improved COF and WSD were detected with 10% blending of SAE20W40 with WCO biodiesel.	(Paramvir Singh & Goel, 2018)
Jatropha oil (JO), engine mineral oil (EMO) and 20% JO blend in EMO (B20)	HFRR	Oil temperature (°C): 26, 100, load [N]: 20, contact pressure (GPa): 0.99, test duration (minutes): 20, mean sliding distance (m): 136, Reciprocating frequency (Hz): 4.7, Mean sliding velocity (m/s): 0.11, Max. sliding velocity (m/s): 0.22, Stroke length (mm): 12.	JO is more susceptible to thermo-oxidation compared with EMO and B20, where a significant increase of viscosity is detected JO. Thermo-oxidation causes the increase of COF for JO and B20. The COF of EMO (fresh or aged) were lower than the COF detected for both JO and B20. The WSD of EMO is higher than JO after thermo-oxidation. Smearing was detected for all oil samples but severe scuffing was detected using fresh JO at 100 °C.	(Farfan-Cabrera et al., 2019)

Table 1.1, continued

Soybean biodiesel blends from 0-100% with petrol diesel	HFRR Steel-steel, Steel-ZrO_2, Steel-diamond coated wafer	ISO 12156	Diamond coating is more effective in friction and wears reduction, evidenced from the lower detected COF and indistinguishable wear scar. The impact of biodiesel concentration on COF was not remarkable. Biodiesel concentration affects the wear scar on the steel ball in steel-ZrO_2 tribo-pair due to wear debris removal by the flow of biodiesel. Diamond coating is suitable for use in biodiesel environment but ZrO_2 not suitable for use in biodiesel environment.	(H. Xiao et al., 2019)
Coconut oil as base oil with Copper (Cu) and Silver (Ag) nanoparticles in concentrations of 0.1%, 0.25%, 0.5% and 1%.	Pin-on-disk wear testing machine	Sliding velocity (m/s) 1.4, disc material: EN 31-b; 60 HRC, disk diameter (mm): 55, pin material: Aluminium 6063, wear scar diameter: 22 mm, 42 mm, load (kgf): 1.5 kgf, rotational speed of motor (rpm): 47 at (d = 42 mm), 1228 at (d = 22 mm), Sliding distance (m): 1000 m.	The addition of Cu or Ag nanoparticles decreases the COF of virgin coconut oil (base oil) at the optimum concentration of 0.25%. The recorded COF was higher for nanoparticles addition of above 0.25%.	(Khan et al., 2019)
Jatropha curcas L. oil (JCL), rapeseed methyl ester oil (RME), hydrotreated rapeseed oil (HVO)	Pin-on-disc wear testing machine	Oscillation frequency:10 and 20 Hz, load: 10 N and 19 N, stroke: 8 mm, duration: 30 min.	JCL has the lowest COF among the three oils examined, followed by RME and HVO. HVO exhibited the lowest wear but with the highest surface roughness.	(Ruggiero et al., 2017)

Note: FBT = four-ball tribotester, HFRR = High-frequency reciprocating rig, COF = coefficient of friction, WSD = wear scar diameter, RT = room temperature.

1.3 Objectives

The main aim of this research is to assess the potential of using microalgae oil for biolubricant application. The first step involves getting the suitable feedstock, local species is preferred to prevent alien species invasion. Then, it is important to evaluate their suitability from the growth, lipid yield, lipid composition, and expected physicochemical properties aspects for biolubricant application. This is followed by the processes investigations, which include extraction and chemical modification. The resultant product's physicochemical properties will be assessed. Lastly, the actual tribological performance of the produced modified microalgae oil will be evaluated as both biolubricant, and additive in diesel and a commercial formulated lubricant. The research objectives can be summarized as follows:

a) To identify, isolate and culture potential microalgae feedstock for biolubricant production.
b) To analyze the lipid composition and the physicochemical properties of the isolated microalgae oil.
c) To investigate the process of extraction, chemical modification and the physicochemical properties of microalgae oil based biolubricant.
d) To investigate the tribological performance of the produced microalgae oil as a biolubricant and its effect as an additive for diesel and in a commercial full synthetic lubricant.

1.4 Contribution of this study

The findings presented in this thesis will be of great interest to other researchers, academics or individuals who share an interest in microalgae-based biolubricant. The conclusions drawn will further the knowledge related to the exploitation of microalgae biolubricant for engine and machinery applications, particularly in Malaysia.

1.5 Thesis outline

Chapter 1 provides an overview of the current situation pertaining to biolubricant utilization and its accompanying issues. This is followed by the objectives of this study.

Chapter 2 consists of a brief development of biolubricants, technical issues accompanying their usage and mitigation measures proposed, and the reasons that bring about the exploitation of microalgae.

Chapter 3 outlines the materials and methods used to conduct the experiments and analysis pertaining to the stated objectives.

Chapter 4 shows the obtained results and the reasons for such observations are deliberated. Comparisons with the work of other researcher are also included and discussed in this section.

Chapter 5 concludes the findings obtained in this study. Recommendations for future work are also included.

1.6 Research limitation

Species used in this study were limited to the five locally isolated species and the two purchased local species. For lipid productivity evaluation, the cultivation was carried out under normal growth conditions using established culturing media, where no optimization study is conducted. For the chemical modification process, only the two-step esterification followed by transesterification is employed, other properties' enhancement modifications like hydrogenation and epoxidation are not explored.

CHAPTER 2: LITERATURE REVIEW

This chapter presents the past literature and current development that relates to the investigation of this study. A brief background on tribology, wear and friction was included. Lubrication and the different types of lubrication regime were discussed. The application of fossil-based lubricant and the issues associated with its usage were detailed. This is followed by the introduction of biolubricant as an alternative to conventional lubricant, factors that contribute to a biolubricant lubricity, additional issues facing biolubricant and the proposed solutions were included. Also covered are the advantage of exploiting microalgae as a feedstock for biolubricant production, the limiting factors for growth and lipid production, and lastly the current development of microalgae-based biolubricant.

2.1 Tribology

Tribology is an interdisciplinary science and engineering of interacting surfaces in relative motion, it involves the study and application of the principles of friction, lubrication and wear (Hutchings, 1992). Tribology research could be of macroscale like the movement of the continental shelf to as small as nanoscale like tiny insects' movement (Gwidon W. Stachowiak, 2017).

2.1.1 Friction

Friction is the resistance to motion between two bodies in contact, which could be of solid surfaces, fluid layers, and material elements. Kinetic friction acts on an object that slides on a surface, whereas static friction occurs when friction prevents the object from moving. Generally, friction can be categorized into three modes: solid, mixed and fluid friction, refer to Figure 2.1

solid friction — the two bodies in direct contact with each other.

mixed friction — the two bodies are separate intermittently where some parts are in direct contact while others are separated by a fluid film.

fluid friction — the two bodies are separated by fluid film that could be of solid, liquid, or gas.

Figure 2.1: Different modes of friction

The coefficient of friction (COF), $\mu = \frac{F_f}{F_N}$ where F_f is the frictional force experienced by the two contacting bodies in motion and F_N is the normal force pressing the same two bodies together. A higher coefficient of friction denotes a greater frictional force, and vice versa.

2.1.2 Wear

Wear is the damage that occurred on solid surfaces. When motion with friction occurs, heat is generated where kinetic energy is converted to thermal energy. Productive friction application such as traction of tire on road surfaces, or during braking, is desirable (Bhushan, 2013). However, friction will also lead to wear, the gradual removal or deformation of material at solid surfaces (Brown Jr, 1971). Productive wear includes machining, polishing, pencil writing, etc. where the loss of materials is expected, in order to achieve a final product. On the other hand, unproductive friction and wear may cause the failure of a mechanical system when essential components deform or fail, such as in gears, clutches, bearings, human joints, etc. (Bhushan, 2013; Chethan et al., 2018). Wear is known to shorten the lifespan of materials. Both friction and wear will lead to the failure of mechanical systems, which is a perennial concern in the industrial and transportation sectors. Table 2.1 describes the different types of common wear. The most common types of wear that are often found in machinery are abrasive, fatigue, corrosive, and adhesive wear, which may occur in isolation or as a complex interaction, refer to Figure 2.2.

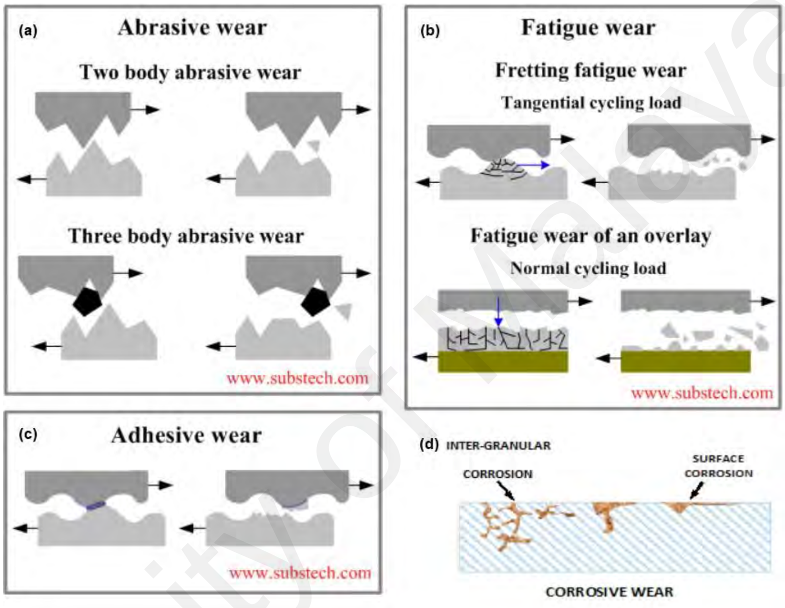

Figure 2.2: Mechanisms of wear: (a-c) abrasive wear, fatigue wear, adhesive wear (Kopeliovich, 2018), and (d) corrosive wear (JGS LLC, 2014)

Table 2.1: Types of common wear

Wear type	Wear mechanism	Reference
Abrasive	It occurs when hard grits or asperities from one surface slides on a softer surface. The interface is damage due to plastic deformation or fracture. There are two modes of abrasive wear, namely two-body and three-body abrasive wear. In two-body wear, hard particles remove material from the other softer surface, for example, in grinding, cutting and machining. Meanwhile, three-body wear occurs when a hard particle (grit) is trapped between the mating surfaces. Research has found that the increase in hardness of materials reduces the wear loss in three-body wear. In the three-body wear, both sliding and rolling friction occurs. Productive example of this mode can be seen in metal polishing.	(Bhushan, 2013; Dwyer-Joyce et al., 1994; Kusano & Hutchings, 2003; Kusumoto et al., 2019)

Table 2.1, continued

Fatigue	During friction, when the applied load is higher than the fatigue strength of the material, fatigue wear occurs. Repeated high loading contact between the asperities causes high-localized stress on the contact point that leads to severe plastic deformation on surfaces. These cyclic loading of sliding or rolling, with or without lubrication will lead to the formation and propagation of cracks under the stressed surfaces. If the cycles continue, large pits will form due to the break-up of large fragments from the surfaces. However, before such a critical point is reached, wear is negligible. For example, spalling of ball bearing race. Research has found that gradient structure layers can enhance the resistant to fatigue-wear on rails. The increase of surface yield strength will effectively reduce the surface displacements in a fixed gradient layer condition.	(G. Stachowiak & Batchelor, 2013; J. Wang & Zhou, 2018)
Adhesive	Adhesion (or bonding) occurs between two sliding surfaces at the asperity contacts. Fragment detachment will occurs when the sliding force shears the contacts (bonding). These fragments may reattach to the other surface as sliding continues. Past studies have found that shearing may occur at the origin or at the weakest point between the two bodies. The total displacement of the fragment may form loose particles; in addition, loose particles may also form due to fatigue. In industrial manufacturing practice, this is referred to as galling. Adhesive wear happened repeatedly, especially in a heavy-loaded gearing system. It is indicated by tooth plasticizing and metal adhesion during the intermittent breakdown of the lubricating film. This phenomenon changes the surface integrity and load distribution. The continual removal of gear surface materials will lead to transmission inaccuracy and when excessive materials were removed, vibration, noise, and heat will be generated, if this situation continued, system failure is imminent.	(Archard, 1953; Rabinowicz & Tanner, 1966; H. Wang et al., 2019)
Corrosive/ chemical	Corrosive wear happens when a surface is damaged due to exposure to reactive corrosive substances, such as due to exposure to strong acid or alkali, and even moisture. When oxidative wear occurs, a thin layer of oxides is formed on the exposed surfaces, if sliding is absent; this layer may actually provide protection to the exposed surfaces by forming a tribofilm. Generally, chemical wear is one of the main operation concern of the mining, and chemical processing industry. For oil-based drilling, the reduction of corrosive (due to salts and other corrosive compounds) and abrasive wear (from the silica in drilling fluid) is critical to prolonging the service life of the drilling tools. It is found that the use of liquid friction reduction additives containing long hydrocarbon tails with high metal affinity polar heads displayed out performed additives that contained molybdenum dialkyldithiocarbamate where less wear was detected.	(Bhushan, 2013; Humood et al., 2019)

2.2 Lubrication

Lubrication is applied to reduce friction and wear between the rubbing surfaces, and the substance that performs the work is called a lubricant. When a fluid is used to separate two rubbing surfaces, lubricated friction occurs. Thus, it is important to ensure that adequate lubrication is at work to prevent destructive rubbing of components that will lead to system failure.

The Stribeck diagram illustrates (Figure 2.3) the relationship between friction, viscosity, speed, and load. Stribeck variable, a lubrication parameter is a dimensionless Sommerfeld number and it is given as $Stribeck\ variable = \frac{\eta V}{P}$, where η = viscosity, V = rotational speed, and P = load. Table 2.2 describes the characteristics of different lubrication regime.

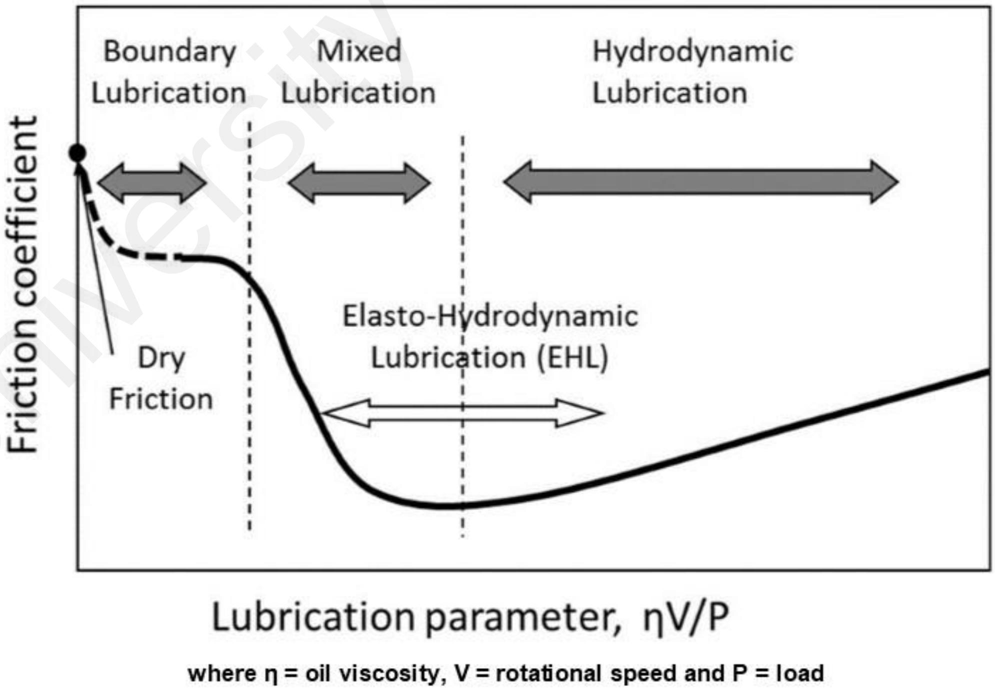

Figure 2.3: Stribeck diagram (Kondo et al., 2013)

Table 2.2: Different types of lubrication regime

Stribeck variable	Lubrication regime	Description	Example	Reference
High value	Hydrodynamic (HD)	HD lubrication is also referred to as full fluid-film lubrication. In this regime, the oil film that separates the two solid surfaces carries the load, resulting in low friction. The surface characteristics (i.e. surface roughness, asperities, etc.) are not important because the rubbing surfaces are not in direct contact, whereas the fluid properties would impose a greater impact. However, current research shows that surface texturing are beneficial for friction reduction. High Stribeck variable is indicated by: • high fluid viscosity • high rotational speed • low load	Hydrodynamic journal, thrust bearings	(Bhushan, 2013; Hamrock et al., 2004; Rosenkranz et al., 2019; Uddin et al., 2017)
Moderately high	Elastohydrodynamic (EHD)	It is a subset of HD lubrication with a thinner film thickness than HD. The EHD film supports the load similar to HD film. In some cases, the asperities between the two solid surfaces are actually touching; therefore, in this scenario, boundary lubricant is used for surface protection. In EHD lubrication, adhesive wear is common in start-stop operation, corrosive wear may also occur due to the surface-lubricant interaction, and fatigue wears mostly happened to heavily loaded bearings. Current research found that dimples configuration decreases the lift-off speed and promote full-film EHD conditions, where shallower texture designed (~0.5μm) reduces friction compared with un-textured material while deeper features design (> 1μm) resulted in negative affect.	Contact point of ball bearings, gear tooth	(Bhushan, 2013; Boidi et al., 2019; Hamrock & Dowson, 1981; Hamrock et al., 2004)

Table 2.2, continued

Moderately low	Mixed lubrication	Mixed lubrication refers to the transition area between HD/EHD and boundary lubrication. Here, both lubrication mechanism may be at work concurrently. Given that the fluid film only provides partial support, hence solid-solid contacts are more frequent. In poor lubrication condition: adhesion, metal transfer, wear particle formation and seizure are likely. The used of boundary lubricant may prevent adhesion during asperities contact. Researchers also found that turbulence may cause the increase of friction coefficient, slightly increase of the minimum nominal film thickness, and reduces the transition speed during the transition from mixed-lubrication to hydrodynamic lubrication regime.	Liquid lubricated bearings	(Bhushan, 2013; Lv et al., 2018)
Low value	Boundary lubrication	In this regime, the solid surfaces are in close contact. Due to the close proximity, the interaction between the lubricant and the solid asperities dominates the contact, thus rendering the surface characteristics crucial. Boundary lubrication failure is normally defined by adhesive and corrosive wear. In order to minimize wear, a sacrificial thin and easily sheared film is formed by boundary lubricant with anti-wear or extreme pressure additives. Important properties of this sacrificial film are melting point, shear strength, hardness, and formation rate. In recent years, nanoparticles such as molybdenum disulfide (MoS_2), graphene, multiwall carbon nanotubes (MWCNT), fullerene, and titanium dioxide were found to be effective additives for surface friction reduction and wear loss prevention. The lubricant bulk flow properties like viscosity are not important. Low Stribeck variable is indicated by: • low fluid viscosity • low rotational speed • high load	Fuel injection system, cam-tappet	(Bhushan, 2013; Booser, 1997; Upadhyay & Kumar, 2019)

2.3 Conventional lubricant

Nowadays, lubricants are formulated not only to reduce friction, but also to remove wear debris, clean components, and prevent corrosion. Lubricants also serve as coolants. Lubricants are typically formulated from petroleum (Mannekote et al., 2017).

However, due to the complexity of lubricant formulations in order to cater to various demands, some components of the lubricants are less degradable than others. For this reason, any accidental (as in human errors or defective parts) or intentional release (as in total-loss lubricants) of these hazardous chemicals are detrimental to the environment (Mannekote et al., 2017; Mobarak, Niza Mohamad, et al., 2014; Syahir et al., 2017).

According to (Research Grand View, 2018), the global lubricants market size was valued at USD 118.89 billion in 2016 and world lubricants demand is projected to reach 45.4 million metric tons in 2019 (an estimated rise of 2 percent per year). The expanding number of motor vehicles in use and continued industrialization, such as in China and India, are expected to catalyze this growing demand (The Freedonia Group, 2015).

Additionally, more countries are enforcing stricter regulations on the use and disposal of lubricants when more than half of all lubricants used worldwide were reported to have contributed to environmental pollution through lubrication total-loss, spillage, and evaporation (Rudnick, 2013). Stricter rules and environmental issues will drive the demand for environmentally friendly bio-based lubricants.

2.4 Biolubricant

Biolubricant refers to lubricant that is derived from biological materials like plant oil and animal fats, in partial or in whole. They are highly biodegradable meaning its usage will help bring down the cost of maintenance, storage, and disposal - requirements of conventional lubricants. They are an ideal environmental-friendly substitution for total lost lubricants (TLL) particularly in delicate regions, like in or near water resources. In addition, many European countries have started imposing the usage of biolubricants in environmentally sensitive areas (Kraft, 2011). Table xx tabulates the current biolubricant available in the market.

Generally, biolubricant is derived from vegetable oil with triglyceride dominating almost 98% of total lipid composition (Rudnick, 2009). Triglyceride is an ester molecule that consists of one glycerol molecule linked to three fatty acids (Figure 2.4). Fatty acid (FA) is a carboxylic acid with a long aliphatic chain that could be either saturated or unsaturated. FA chain usually consists of 76-77% carbon, 11-12% hydrogen and 10-12% oxygen based on weight (Ruhul et al., 2016). Studies have found that fatty acids content varies by oil sources and these differences in turn, affect the resultant product properties. The following section will discuss the important physicochemical properties of biolubricant.

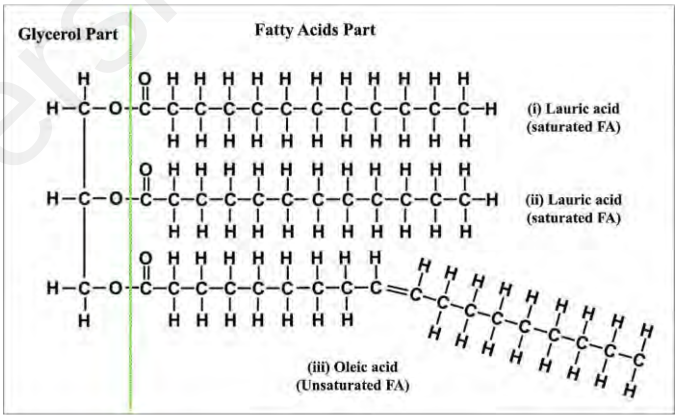

Figure 2.4: Triglyceride (Syahir et al., 2017)

Table 2.3: Biolubricants in the market (Zainal et al., 2018)

Manufacturer	Trade Name	Manufacturing region	Applications
Total	Bio-Mold-7	UK	Concrete demolding oil
Fuchs	Locolub eco	USA/Europe	Grease, hydraulic fluid, gear oil, bar and chain oil
Castrol	Castrol Biolube 2T	UK	Two-stroke engine oil
Mobil	Mobil EAL	USA/Europe	Grease, hydraulic fluid and refrigeration oil
Shell	Ecolube	USA	Hydraulic fluid
Houghton International Inc.	Cosmolubric/ Hydrodrive	UK	Hydraulic oil
Morris Lubricants	Supergreen Air-O-Lube	UK	Air mist lubricant
Selenia	Arbor 46 Bio-V	UK	Hydraulic oil
Solar Lubricants	Arborol	UK	Chain and bar lubricant
Rock Oil	BD-Rock Drill Oil	UK	Hydraulic oil and rock drill oil
Aztec Oils	Biohyd & Biochain	UK	Hydraulic and chainsaw oil
Teklube TS	Safra Range	UK	Metalworking fluid
Cargill Industrial Oils & Lubricants	Novus	USA/Europe/Japan	Hydraulic fluids, cutting oil, gear oil, metalworking oil, bar and chain oil
International Lubricants Inc.	Lubegard	USA/Europe	Hydraulic fluid, gear oil and metalworking oil
Bioblend Lubricants International	Bioblend	USA/Europe	Grease, hydraulic fluid, gear oil, bar and chain oil
Karlshamns-Binol AB	Binol	USA/Europe	Hydraulic fluid, metalworking oil, bar and chain oil

Table 2.3, continued

Renewable Lubricants	Biogrease/oil	USA	Grease, hydraulic fluid, cutting oil, transmission oil, gear oil, metalworking oils, bar and chain oil, turbine drip oil, vacuum pump oil and crankcase oil
Chevron Texaco	Biostar (Rando)	USA/Belgium	Hydraulic fluid
Environmental Lubricants Manufacturing Inc.	SoyTrak, SoyEasy	USA	Grease, hydraulic fluid, cutting oil, gear oil, metalworking oils, bar and chain oil
Moton Chemicals	Biolube	Europe	Grease, turbine drip oil, bar and chain oil

Table 2.4: Fatty acid profile of vegetable oil used for biolubricant production (Smith et al., 2010; Zainal et al., 2018)

Vegetable oil	Fatty acid (%)														Saturated (%)	Unsaturated (%)	Producing country/ region
	6:0	8:0	10:0	12:0	14:0	16:0	16:1	18:0	18:1	18:2	18:3	20:0	22:0	22:1			
Canola						3.9	0.2	1.9	64.1	18.7	9.2	0.6	0.2		6.6	92.2	EU, Canada, China, India, Australia
Coconut	0.5	8.0	6.4	48.5	17.6	8.4		2.5	6.5	1.5		0.1			92.0	8.0	Indonesia, India, Philippines, Sri Lanka

Table 2.4, continued

Corn			12.2	0.1	2.2	27.5	57	0.9	0.1			14.5	85.5	USA, China, Brazil, Argentina, Mexico, Ukraine
Olive			13.7	1.2	2.5	71.1	10.0	0.6	0.9			17.1	82.9	Spain, Italy, Greece
Palm	0.3	1.1	45.1	0.1	4.7	38.5	9.4	0.3	0.2			51.4	48.3	Malaysia, Indonesia
Rapeseed		0.1	2.8	0.2	1.3	21.8	14.6	7.3	0.7	0.4	34.8			EU, Canada, USA, Australia, China, India
Safflower		0.1	6.5		2.4	13.1	77.7		0.2			9.2	90.8	Kazakhtan, India, USA, Mexico, Argentina, Turkey
Soybean		0.1	10.9	0.1	4.2	25.0	52.7	6.2	0.3	0.1				USA, Argentina, Brazil, China, India
Sunflower	0.5	0.2	6.8	0.1	4.7	18.6	68.2	0.5	0.4			12.6	87.4	Rusia, EU, Ukraine, Argentina

2.4.1 Physicochemical properties of biolubricant

Considering that most of the biolubricant are vegetable oil-based, therefore, the properties of the lubricant will be in the direct effect of the physical and chemical structures of the compounds it constitutes (Table 2.4). Past literature has concluded that the affected critical parameters are the viscosity, oxidation stability, and cold flow properties (Knothe, 2005; Ramos et al., 2009; Sajjadi et al., 2016). The effect of the chemical structure of the fatty acid on these parameters are discussed below (Table 2.5).

Table 2.5: Critical biolubricant properties

Parameters	Increase chain length	Increase branching	Increase degree of unsaturation	Reasons and implications
Viscosity	+	-	+	High viscosity will increase oil temperature and induced drag due to random intermolecular interactions between the carbon chains (Knothe & Steidley, 2005). Therefore, these interactions will increase as the chain length increases. Viscosity also increases in the presence of heteroatom such as oxygen. Additionally, the study has found that the order of effect of oxygenated moieties on viscosity is as follows: COOH $\approx$ C-OH > $COOCH_3$ $\approx$ C=O > C-O-C > no oxygenated compound (Knothe & Steidley, 2005). In addition, when the unsaturation is high, the affinity to polymerize is higher, leading to fluidity loss. Double bond configuration influence viscosity where trans double bond configuration giving a higher viscosity (almost similar to that of saturated compounds) than cis (Kaufmann & Funke, 1938; Teeter & Cowan, 1956). It can be foreseen that, the resultant biolubricant from waste cooking oil would have viscosity due to the high amount of hydrogenated and trans fats it contains. However, the positions of double bonds are less of a problem, so were the branching of the ester moiety. Thereby, viscosity is dependable on chain length, double bonds (position, number and configuration) and, the nature of oxygenated moieties. In order to counter issues associated with high unsaturation but retaining the benefits of unsaturation, partial or/and selective hydrogenation has gained tremendous interest (Adu-Mensah et al., 2019)
Viscosity index	+	-	+	Viscosity index (VI) is a measurement of a substance's viscosity in relation to temperature. High VI is important because it indicates a lubricant's usability over a wide range of temperature. Generally, the vegetable oil-based lubricant has a higher VI than mineral oil due to the triglycerides it contained (Masjuki et al., 1999; Silitonga et al., 2013).

Table 2.5, continued

Oxidative stability	+	+	-	Oxidation stability is associated with the service life of a lubricant. Low oxidative stability will lead to lubricant's thickening and the formation of plastic-like compounds due to polymerization (Zainal et al., 2018). The vegetable oil-based lubricant has lower oxidation stability compared with synthetic esters due to the presence of unsaturated fatty acids, particularly polyunsaturated fatty acids (Rudnick, 2013) and unsaturated fatty acid are susceptible to autoxidation (Pullen & Saeed, 2012; Z. Yang et al., 2013). Autoxidation is any oxidation that occurs in the presence of oxygen (and sometimes UV radiation) that forms peroxides and hydroperoxides (Figure 2.5). Further, the presence of β-CH (Figure 2.6) that is easily cleavage will lead to the breakdown of the whole molecular structure of esters, forming free fatty acids a precursor for autoxidation (Wagner et al., 2001). The presence and location of double bonds in the fatty acid chains will also determine the susceptibility and rate of autoxidation (Frankel, 2014), in this case, the bis-allylic positions (common in polyunsaturated fatty acids) are more vulnerable to autoxidation than the allylic positions (refer Figure 2.7).
Low temperature properties	-	+	+	Low pour point (PP) indicates the usability of a lubricant under low temperature. Generally, when the pour point is not sufficiently low, the restrictive flow of lubricant will lead to excessive friction, wear and heat in the system, that in turn leads to equipment damage and system failure, especially during start-up (Mobarak, Mohamad, et al., 2014). The presence of long saturated chains impart good durability, due to increasing intermolecular interactions; but it is also due to this reason that causes poor low-temperature properties of a biolubricant (Fox & Stachowiak, 2007; Sukjit et al., 2019). Meanwhile, branched esters impart lower melting points in the neat form. Studies have demonstrated that branched-chain esters have lowered cloud point (CP) and PP (Table 2.6) but the cost of production would be increase as isopropanol is more costly than methanol. Studies have found that the higher the degree of unsaturation, the better the PP but in turn will have an adverse effect on the oxidation stability (Jayadas & Nair, 2006; Quinchia et al., 2012).

Notes: "+" = positive influence, "-" = negative influence.

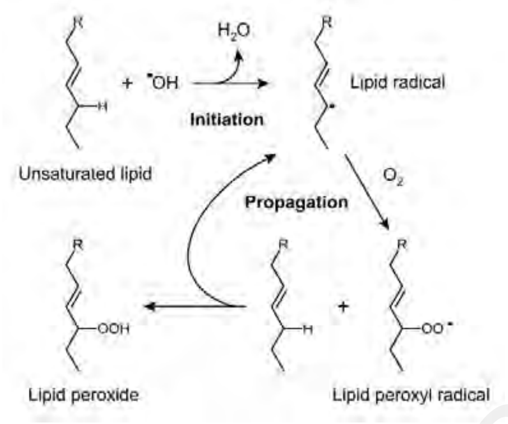

Figure 2.5: Mechanism of unsaturated fatty acid autoxidation (Medina-Meza et al., 2014; Young & McEneny, 2001)

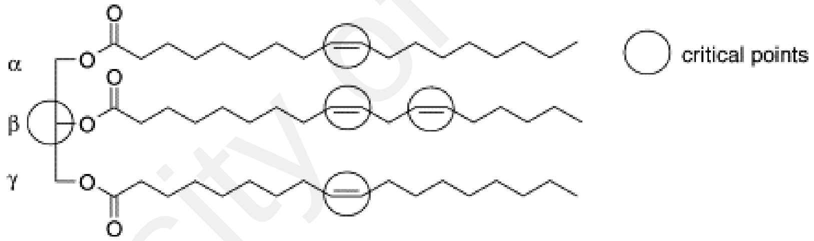

Figure 2.6: Reactive sites of vegetable oil-based esters: double bonds and β-CH (Wagner et al., 2001)

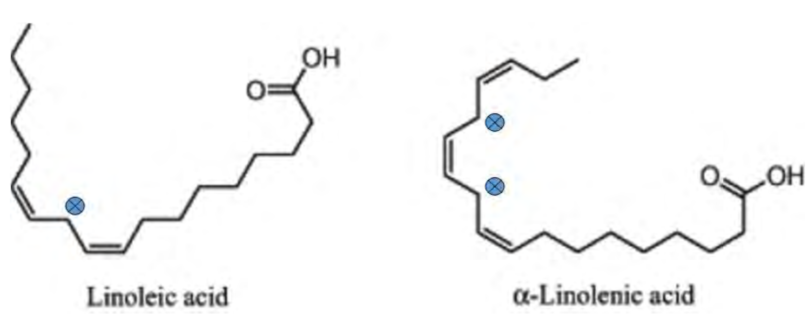

Figure 2.7: Position of bis-allylic carbons in linoleic acid (C18:2) at C11 and linolenic acid (C18:3) at C11 and C13

Table 2.6: CP and PP of esters of common feedstock (Knothe et al., 2015; Smith et al., 2010)

Oil or fat	Ester	Cloud point (°C)	Pour point (°C)
Canola	Methyl	1	-9
Canola	Ethyl	-1	-6
Canola	Isopropyl	7	-12
Canola	n-Butyl	-6	-16
Coconut	Ethyl	5	-3
Corn	Methyl	-3	-3
Olive	Methyl	-2	-3
Palm	Methyl	13	16
Palm	Ethyl	8	6
Safflower	Methyl	–	-6
Safflower	Ethyl	-6	-6
Soybean	Methyl	0	-2
Soybean	Ethyl	1	-4
Soybean	Isopropyl	-9	-12
Soybean	n-Butyl	-3	-7
Soybean	2-Butyl	-12	-15
Sunflower	Methyl	2	-3
Sunflower	Ethyl	-1	-5
Beef tallow	Methyl	17	15
Beef tallow	Ethyl	15	12
Beef tallow	n-Propyl	12	9
Beef tallow	Isopropyl	8	0
Beef tallow	n-Butyl	9	6
Beef tallow	Isobutyl	8	3

2.4.2 Factors affecting the lubricity of biolubricant

Lubricity is the measure of the reduction in friction and/or wear by a lubricant that cannot be directly measured because it is not a material property. A lubricant's performance, however, can be quantified by measuring the wear scar caused by a wear-inducing object in a given time period. Other related factors like surface area, temperature, and pressure can be specified in the evaluation. For example, when two lubricants having the same viscosity but one resulted in a smaller wear scar compared with the other, it can be deduced that the smaller-wear scar lubricant has a higher lubricity than the other does. Studies have found that generally, biolubricant lubricity is affected by chain length, chain branching, degree of unsaturation and polarity (Zahid et al., 2017), refer to Figure 2.8.

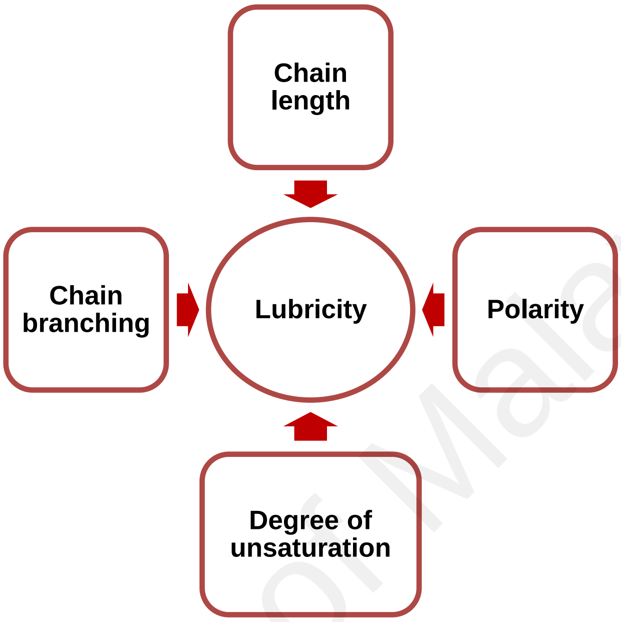

Figure 2.8: Factors affecting the lubricity of biolubricant

2.4.2.1 Carbon chain length

In a boundary lubrication condition, the coefficient of friction (COF) is found to be influenced by the fatty acid carbon chain length (Geller & Goodrum, 2004; Srivastava & Prasad, 2000). It is believed that the arrangement of fatty acid on the matting surfaces plays an important role in contributing to the observation. The adsorption of the polar carboxyl head on the solid surface, leaving the alkyl non-polar tail facing the opposite surface has created a molecular barrier between the rubbing surfaces (A. Adhvaryu et al., 2004), refer Figure 2.9.

Additionally, long carbon chain (Figure 2.9 (b)) will create a thicker film compared with the short ones (Figure 2.9 (c)) (Biresaw et al., 2003; N.W.M. Zulkifli et al., 2013).

In a study by G.W. Stachowiak& Batchelor (2005), it is found that the transition temperature of friction in fatty acids will increase when their molecular weight increases, further, they concluded that the minimum carbon chain length for effective lubrication is n = 9, shorter than that, no lubrication improvement is observed.

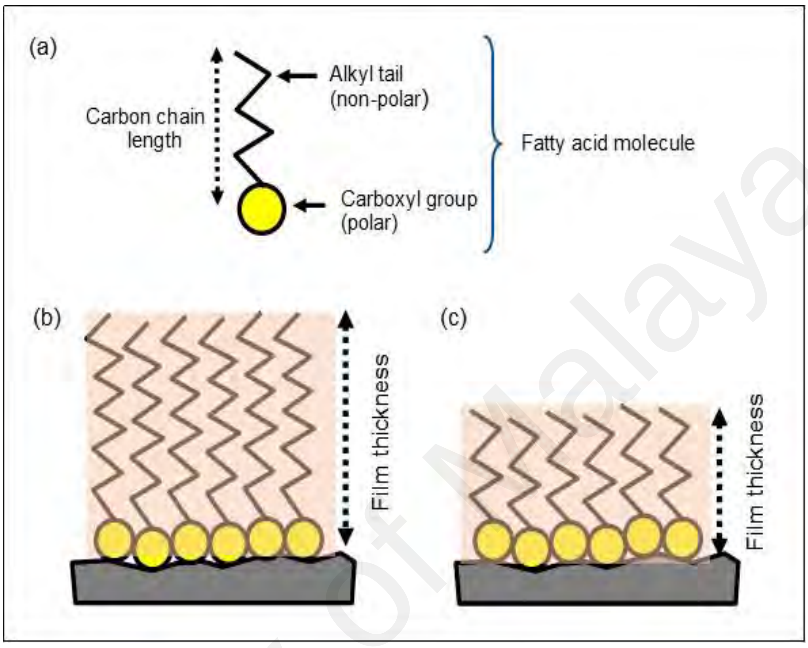

Figure 2.9: Film thickness attributed to carbon chain length: (a) fatty acid molecule, (b) long carbon chain, and (c) short carbon chain

2.4.2.2 Chain branching

The friction between fluid particles due to fluid viscosity causes shear stress. Shear stress is one of the factors influencing fluid film lubrication. In addition, shear stress is dependent on ester structure, and long, linear chain ester is found to have lower shear stress than branching ester (Chang et al., 1992; Hamrock et al., 2004; Konishi & Perez, 1997; Macias-Rodriguez & Marangoni, 2018). Excessive branching will disrupt the adhesion of the molecule on the sliding surface (Ahmed et al., 2015), hence increasing direct metal-to-metal contact (G. Stachowiak & Batchelor, 2013). For example, in a study by (Muraki, 1987) using both ring and branched chain structures, friction is shown to increase when the degree of branching increases. Similarly, J. Zhang et al. (2016) also found that linear-shaped base oil molecules with flexible bonds will perform better in terms of friction compared with base oil having molecules with bulky side groups or rings.

On the other hand, steric hindrance provided by the branching at the polar region will be able to shield the molecule from physical and chemical interactions (Chan et al., 2018). Steric hindrance inhibits the stacking of molecules thus preventing crystallization at low temperature (Ahmed et al., 2015). Epoxidized oil and polyol ester will instead form microcrystalline structure that allows the molecules to glide over one another, resulting in better fluidity and therefore better low-temperature performance (Erhan et al., 2006; Jiang et al., 2015). In addition, increase lubricity and load carrying capacity have been reported (Kania et al., 2018) as branching helps stabilize the tribofilm from breaking apart (Martins et al., 2006).

2.4.2.3 Polarity

Polarity is a separation of electric charge leading to a molecule having an electric dipole or multipole moment; this contributes to the asymmetrical configuration of the molecule. Polarity in ester molecule is caused by the charged carboxyl group ($-COO^-$) on one end and a non-polar hydrocarbon tail at the other. The polar carboxyl group can adsorb strongly on to metallic surfaces while the alkyl hydrocarbon tail provides the scaffold to form a molecular barrier between the rubbing metals (Jiang et al., 2015). This molecular layer is formed when each of the fatty acid molecule line itself up against the metal surfaces (packing); refer to Figure 2.9. A stronger lubricating film with better wear protection can be achieved through chemical modification by increasing the polarity of the functional groups (by substituting them with the more polar functional group). Different functional group exhibits different polarity characteristics, some being more polar than others and, vice versa. For instance, the amide is more polar than acid, and acid being more polar than alcohol and so on; Amide > Acid > Alcohol > Ketone ~ Aldehyde > Amine > Ester > Ether > Alkane (Elmhurst College, 2003). Studies has found that additive that contains long chain hydrocarbon tail with higher metal affinity polar head (probably polyol ester or diester) offers better wear protection than additive with single polar head (probably a monoester) when added into drilling fluid attributed by stronger adsorption of the polar head on the metal surface (Humood et al., 2019).

Solubilizing power is dependent on polarity and vegetable oil is a good solvent for polar substance and additive (as most additive contains oxygen and nitrogen) (Delgado et al., 2017; Dinda et al., 2008). There are also instances where the additive failed to dissolved in vegetable oil-based lubricants due to the lower polarity of the vegetable oil-based biolubricant such as ethyl cellulose. Ethyl cellulose is a natural polymer added as a pour point depressant additive, that is biodegradable and not hazardous according to the Commission Directive 93/21/EEC (Delgado et al., 2017). Its molecules work by disrupting the wax crystallization process. Moreover, if the added additives are not compatible with the ester, it will give rise to the two substances competing against each other for metallic surface attachment, then poorer lubricity performance is likely to happen (Borugadda et al., 2018; Machinery Lubrication, 2018).

2.4.2.4 Degree of unsaturation

The effectiveness of the formed boundary lubrication film is influenced by how well and close the fatty acids pack themselves on the metal surfaces. That, in turn, is directly affected by the structure of the fatty acids. Unsaturation, which gives rise to isomer is found to prevent the packing of fatty acids close to each other. For example, oleic acid has one double bond, and it can exist in the trans or cis forms, refer to Figure 2.10, the cis configuration is unable to form straight chains.

As mentioned previously, the straight long-chain fatty acid is able to form a strong molecular barrier due to the strong adsorption of polar head and the lateral inter-molecule interactions between the carbon tails. Considering this reason, when close packing is hampered by the cis configuration, especially in cases, where there is more than one double bond (as in polyunsaturated fatty acid), the created boundary layer is structurally weaker (Fox et al., 2004; Sukjit et al., 2019).

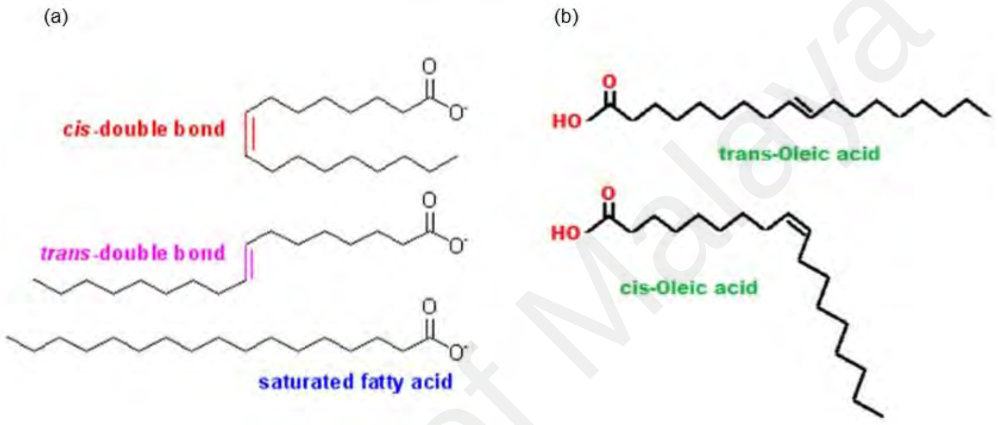

Figure 2.10: (a) Fatty acid (David, 2015) and (b) oleic acid isomers (Nahidian et al., 2018)

2.4.3 Chemical modification

Fatty acids unsaturation is the main cause of oxidation and thermal stability faced by vegetable oil based biolubricant (Knothe, 2005), and many techniques have been employed to counter this, among the widely used are hydrogenation, transesterification, and epoxidation (Chan et al., 2018; McNutt & He, 2016). Figure 2.11 illustrates the different chemical modification pathways.

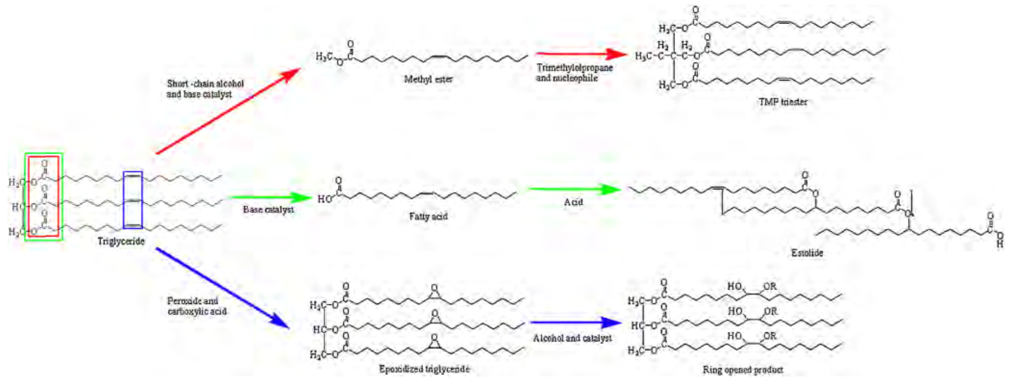

Figure 2.11: Chemical modifications of vegetable oil (McNutt & He, 2016)

2.4.3.1 Hydrogenation

Hydrogenation is a chemical reaction that reduces or saturates an organic compound, in which the double or triple bonds are opened up and filled with hydrogen or another element, usually in the presence of a catalyst like nickel, palladium or platinum, while in non-catalytic hydrogenation, a very high temperature is applied. Selective hydrogenation can be employed to partially reduce fatty acids by using a different type of catalyst. This process is useful for the reduction of polyunsaturated fatty acid to monounsaturated fatty acid in vegetable oil, where fully saturated fatty acids are not desirable, as it will cause deterioration of low-temperature properties such as pour point. Nonetheless, the issue of low conversion percentage arises when partial hydrogenation of multiple types of unsaturated fatty acid is needed in one setting. Different attempts using both heterogeneous and homogeneous catalysts to improve the reaction have been conducted (Adu-Mensah et al., 2019; Pandarus et al., 2012; Pecchia et al., 2013; Zaccheria et al., 2012). This technique has improved the oxidative stability of vegetable oil as a result of reduced unsaturation. But yet this technique also gives rise to another issue, where the newly formed monoenic acid can isomerize into cis and trans configurations that will significantly affect the end product as mentioned earlier (Liu et al., 2018; Nohair et al., 2005; Syahir et al., 2017).

2.4.3.2 Epoxidation

Epoxidation is the chemical reaction that converts the carbon-carbon double bond into oxiranes (epoxides) (Aguilera et al., 2019; Fettes, 1964) in the presence of an acid, enzymes, and metal catalyst (Abdullah & Salimon, 2010). The major advantage of epoxidation is the low-temperature requirement for the reaction, further, epoxidized vegetable oil also exhibits higher oxidative stability, lower acidity and better adsorption to metal surfaces (A Adhvaryu & Erhan, 2002; W. Li & Wang, 2015). However, it also leads to higher viscosity, decrease of viscosity index and increases the pour point of vegetable oil (McNutt & He, 2016). In order to improve the low-temperature properties, further modification like esterification and acetylation can be employed (Hashem et al., 2013). Research indicates that the additional processes like ring opening, followed by esterification and lastly acetylation could greatly enhance the low-temperature properties of vegetable oil with better oxidative and thermal stability, resulting in an overall lubricity improvement (Hwang & Erhan, 2006; Kulkarni et al., 2013; Madankar et al., 2013).

2.4.3.3 Transesterification

Transesterification is a chemical reaction where the organic group R” of an ester is exchanged with the organic group R’ of alcohol in the presence of a catalyst that could be of an acid, base or enzyme (refer to Figure 2.12). The problem brought by the hydrogen atoms in the β position relative to the hydroxyl group in a glycerol molecule can be resolved using transesterification. In the reaction, the glycerol molecule is replaced with another polyhydric alcohol that does not contain the β-hydrogen such as neopentyl glycol, trimethylolpropane (TMP), or pentaerythritol (K. V. Fernandes et al., 2018; Ghazi et al., 2009), the resultant product will be a polyol ester. Polyol ester is an ester with more than one hydroxyl group. The presence of more than one hydroxyl group increases the ester polarity. Thermal and oxidative stability is also improved. Further studies have found that lubricity is enhanced with TMP esters (Yunus et al., 2004; Zahid et al., 2017). However, the requirement for high reaction temperature is the drawback of this process (Koh et al., 2014; Oh et al., 2013).

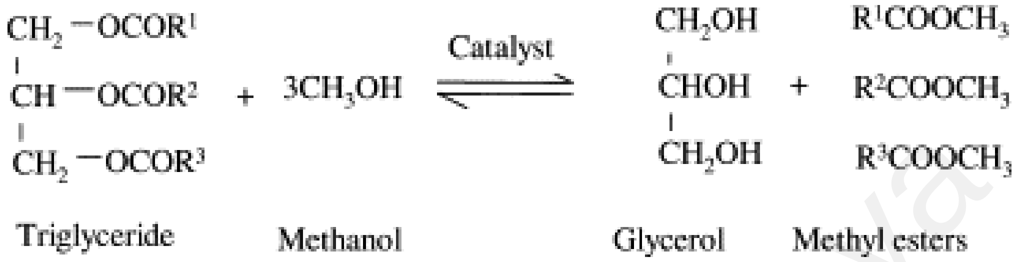

Figure 2.12: The reversible transesterification process (Meher et al., 2006)

2.4.4 Additives

Depending on the application, additives are normally used to counter the limitation posed by the lubricant. Table 2.7 describes the common type of additives found in the lubricant.

Table 2.7: Type of additives (Machinery Lubrication, 2018)

Additive	Purpose	Typical compound	Function
Anti-wear agent	Reduce friction and wear, and prevent scoring and seizure	Zinc dithiophosphates, organic phosphates, and acid phosphates; organic sulfur and chlorine compounds; sulfurized fats, sulfides, and disulfides	Chemical reaction with the metal surface to form a film with lower shear strength than the metal, thereby preventing metal-to-metal contact
Corrosion and rust inhibitor	Prevent corrosion and rusting of metal parts in contact with the lubricant	Zinc dithiophosphates, metal phenolates, basic metal sulfonates, fatty acids and amines	Preferential adsorption of polar constituent on the metal surface to provide a protective film and/or neutralization of corrosive acids

Table 2.7, continued

Detergent	Keep surfaces free of deposits and neutralize corrosive acids	Metallo-organic compounds of barium, calcium and magnesium phenolates, phosphates and sulfonates	Chemical reaction with sludge and varnish precursors to neutralize them and keep them soluble
Dispersant	Keep insoluble soot dispersed in the lubricant	Polymeric alkylthiophosphonates and alkylsuccinimides, organic complexes containing nitrogen compounds	Contaminants are bonded by polar attraction to dispersant molecules, prevented from agglomerating and kept in suspension due to the solubility of dispersant
Friction modifier	Alter coefficient of friction	Organic fatty acids and amines, lard oil, high molecular weight organic phosphorus, and phosphoric acid esters	Preferential adsorption of surface-active material
Pour point depressant	Enable lubricant to flow at low temperatures	Alkylated naphthalene and phenolic polymers, polymethacrylates	Modify wax crystal formation to reduce interlocking
Viscosity improver	Reduce the rate of viscosity change with temperature	Polymers and copolymers of methacrylates, butadiene olefins, and alkylated styrenes	Polymers expand with increasing temperature to counteract oil thinning
Anti-foaming	Prevent lubricant from forming a persistent foam	Silicone polymers and organic copolymers	Reduce surface tension to speed collapse of the foam
Antioxidant	Retard oxidative decomposition	Zinc dithiophosphates, hindered phenols, aromatic amines, sulfurized phenols	Decompose peroxides and terminate free-radical reactions
Metal deactivator	Reduce the catalytic effect of metals on the oxidation rate	Organic complexes containing nitrogen or sulfur, amines, sulfide and phosphites	Form inactive film on metal surfaces by complexing with metallic ions

2.5 Microalgae

Microalgae are microscopic algae that can be found in fresh, brackish and saline water. They can be planktonic species that live in the water column or benthos species (dwelling in the sediment). These unicellular organisms can exist as individual cells, in chains or some can be found aggregated into macroscopic mats. Depending on the species, their sizes can range from a few micrometers (µm) to a few hundred micrometers. Microalgae have no roots, stems, or leaves but their ability to perform photosynthesis produces approximately half of the atmospheric oxygen (Chapman, 2013) and these organisms together with bacteria form the base of the food web and provide energy for all the trophic levels above them.

With over 100,000 species to choose from, microalgae have garnered significant interest as potential biolubricant and biofuel feedstock candidates (Abomohra et al., 2017; Goh et al., 2019; Sadvakasova et al., 2019). There are enormous untapped possibilities to utilize algae in different ways. The primary energy provider, petroleum comes mostly from the Cretaceous deposits of marine algae (Chapman, 2013). Studies have found that the amorphous organic material that was formed under anoxic conditions from phytoplankton (probably dinoflagellate cysts and microalgae *Botryococcus*) or bacterial/archaeal holds a significant role for petroleum generation (Schneider et al., 2019). Now, scientists are pushing to find new ways to exploit algae as the world oil deposits continue to dry up.

2.5.1 Major advantages of microalgae

It all began during the energy crises that occurred in the early and mid-1970s, the US DOE's through the Aquatic Species Program has made tremendous efforts to produce biodiesel from algae. Advances have been made in the aspect of applied biology to the mass production system to resources (land, water, and CO_2) in order to support mass cultivation. However, the final and pertinent aspect of high production cost remained the biggest hindrance especially when the petroleum prices have dropped due to increase output (Sheehan et al., 1998; Sun et al., 2019).

Past studies have found that different types of biofuel can be produced from microalgae such as bio-hydrogen, biodiesel, bio-ethanol, bio-methane, and bio-oil (Table 2.8) and the potential is tremendous. Companies like Cellana Inc. and Terra-via (formerly known as Solazyme) are taking microalgae biodiesel to market. Biofuel is good business, but the health supplement market is more lucrative, especially when the oil prices fall. Thus, many companies have also begun to switch to the more lucrative business where consumers are more willing to spend money on than solely focus on biofuel production. Moreover, in the latter, market competitiveness is gauged by who can offer the lowest price.

Table 2.8: Biofuel production from microalgae (Faried et al., 2017; Maity et al., 2014)

Microalgae	Algae type	Biofuel	Productivity
Arthrospira maxima	Green	Hydrogen, Biodiesel	40–69%
Chlamydomonas reinhardtii	Green	Hydrogen	2.5 mL/h or 11.73 g/L
Chlorella sp.	Green	Ethanol	22.6 g/L
Chlorella protothecoides	Green	Biodiesel	15.5 g/L
Chlorococcum humicola	Green	Ethanol	7.2 - 10 g/L
Chlorococcum infusionum	Green	Ethanol	0.26 g/g
Chlorococcum sp.	Green	Biodiesel	10.0 g/L
Chlorococcum sp.	Green	Ethanol	3.83 g/L
Dunaliella sp.	Green	Ethanol	11.0 mg/g
Haematococcus pluvialis	Red	Biodiesel	420 GJ/ha/year
Neochlorosis oleabundans	Green	Biodiesel	56.0 g/g
Spirulina platensis	Blue-green	Hydrogen	1.8 µmol/mg
S. platensis UTEX 1926	Blue-green	Methane	0.40 m^3/kg

2.5.1.1 CO_2 sequestration

Microalgae's efficiency of converting waste as in carbon (CO_2) into liquid energy as in oil has further driven the exploration of its usage as an alternative biofuel feedstock. The renewed interest of utilizing microalgae for CO_2 capture and storage applications occurred during the crude oil price peak (2002-2008) together with the issue of climate change brought about by the burning of fossil fuels. Microalgae are among the most productive biological systems for generating biomass and capturing carbon. Moreover, the biomass can be harvested 100%, much more than what is possible in terrestrial biomass production systems. It has been reported that carbon dioxide or bicarbonate-capturing efficiencies can reach as high as 90% in open ponds system. Therefore, the emissions from power stations and cement kilns can be connected to the culturing facilities as a carbon source - exploiting microalgae for CO2 sequestration applications. Table 2.9 shows the efficiency of carbon capture by different species of algae. It is found that one of the widely studied algae species for carbon fixation is *Chlorella* sp. from the green algae group.

Table 2.9: CO_2 fixation by algae (Jain et al., 2019; Maity et al., 2014)

Algae species	CO_2 fixation rate (g/L/day) and removal efficiency (%)	Reference
Chlorella vulgaris NIOCCV	0.43 g/L/day	(Jain et al., 2019)
Chlorella minutissima	0.25 g/L/day	(Freitas et al., 2017)
Chlorella sp.	0.51 g/L/day	(Zhao & Su, 2014)
Chlorella sp. mutant MTF-7	0.67 g/L/day	(Chiu et al., 2011)
Chlorella sp.	0.29 g/L/day	(Yadav et al., 2015)
Chlorella sp.	0.10 g/L/day	(Ansari et al., 2017)
Chlorella fusca	0.26-0.30 g/L/day	(Duarte et al., 2017)
Chlorella pyrenoidosa	0.25 g/L/day	(Sydney et al., 2010)
Chlorella pyrenoidosa	0.26 g/L/day	(Tang et al., 2011)
Chlorella sp.	16-58%	(Chiu et al., 2008)
Chlorella sp. *NCTU-2*	63%	(Chiu et al., 2009)
Chlorella sp.	10-50%	(Doucha et al., 2005)

2.5.1.2 Waste-water remediation

Another added benefit of utilizing microalgae as biomass feedstock is its potential as a green pollutant-removal for wastewater (Table 2.10). Eutrophication caused by high contamination of nitrogen and inorganic phosphorus makes a perfect condition for microalgae growth and the resulting biomass could be utilized for biofuel production. The ability of microalgae to uptake heavy metal (Abinandan et al., 2019; Bayramoğlu et al., 2006; Suresh Kumar et al., 2015) has created a win-win situation for wastewater remediation and microalgae cultivation combination to work. However, the selection of local species is still desired because the introduction of non-native species may cause a negative impact on the environment, economy and human health. Very often, an introduced species will either die out or thrive and if they do, native species might be unprepared to defend themselves (Seebens et al., 2016).

Table 2.10: **Pollutant removal by microalgae (Abinandan et al., 2019; Maity et al., 2014; Saranya & Shanthakumar, 2019)**

Microalgae	Pollutant	Reference
Chlorella vulgaris (NRMCF0128)	NH_4^+, PO_4^{3-}, Cr	(Saranya & Shanthakumar, 2019)
Pseudochlorella pringsheimii	NH_4^+, PO_4^{3-}, Cr	(Saranya & Shanthakumar, 2019)
Desmodesmus sp. MAS1	Cu, Fe, Mn, Zn	(Abinandan et al., 2019)
Heterochlorella sp. MAS3	Cu, Fe, Mn, Zn	(Abinandan et al., 2019)
Anabaena, Oscilatoria, Spirulina, S. platensis	NO_3^-, NO_2^-, NH_4^+, PO_4^{3-}	(Markou & Georgakakis, 2011)
Anabaena sp.	2,4,6-trinitrotoluene	(Pavlostathis & Jackson, 2002)
Chlamydomonas reinhardtii	Hg(II), Cd(II), Pb(II)	(Bayramoğlu et al., 2006)
Chlorella sp.	Boron	(Taştan et al., 2012)
Chlorella miniata	Tributyltin (TBT)	(Tam et al., 2002)
Chlorella vulgaris	Azo compounds	(Jinqi & Houtian, 1992)
Chlorella vulgaris	NH_4^+, PO_4^{3-}	(de-Bashan et al., 2002)
Chlorella vulgaris	Cd, Zn,	(Cañizares-Villanueva et al., 2000)
Chlorella vulgaris, Scenedesmus rubescens	N and P	(Shi et al., 2007)
Chlorella salina	Co, Zn, Mn	(Garnham et al., 1992)
Isochrysis galbana	NH_4^+	(Y.-C. Chen, 2003)
Ochromonas danica	phenols	(Semple & Cain, 1996)
Oedogonium hatei	Ni	(Gupta et al., 2010)
Oedogonium sp, *Nostoc* sp.	Pb	(Gupta & Rastogi, 2008)
Oscillatoria sp. *H1*	Cd(II)	(Katırcıoğlu et al., 2008)
Phormidium bigranulatum	Pb(II), Cu(II), Cd(II)	(D. Kumar et al., 2012)
Phormidium laminosum	Cu(II), Fe(II), Ni(II), Zn(II)	(Blanco et al., 1999)

Table 2.10, continued

Scenedesmus quadricauda	Cu(II), Zn(II), Ni(II)	(Bayramoğlu & Yakup Arıca, 2009)
Spirulina platensis	Cr(VI)	(Gokhale et al., 2009)
Chlorella regularis	U	(Nakajima et al., 1982)
Ulva lactuca	Pb(II), Cd(II)	(Sarı & Tuzen, 2008)
Undaria pinnatifida	Ni, Cu	(Z. Chen et al., 2008)

2.5.2 Limiting factors affecting optimal growth for mass production

Earlier research mainly focused on finding the optimum growth conditions for biomass productivity. A few parameters have been identified as limiting factors such as irradiance, CO_2, nutrient, pH, and temperature. Microalgae grow photosynthetically, therefore light becomes a limiting factor. Solar irradiance also varies due to differences in geographical locations and latitudes, and this causes some regions to get minimal sunlight especially during wintertime hampering biomass productivity. Attempts have been made in using artificial light (like light-emitting diode) and the results obtained are quite encouraging, providing opportunity for underground cultivation or at affected regions with seasonal sunlight duration, but a certain cost is incurred when artificial light is used (Altunoz et al., 2017; Ra et al., 2016; C.-Y. Wang et al., 2007).

As mentioned before, CO_2 is the carbon source for photosynthesis. This has prompted microalgae cultivation facilities to use pipe-in flue gases for microalgae growth (Cheng et al., 2016). One of the technical problems to address is to bring down the temperature of the flue gases, before entry into the cultivation photobioreactor or ponds. Other efforts of using different sources of carbon such as glycerol, glucose, xylose, bicarbonate, urea, etc. (Baldisserotto et al., 2016; Leite et al., 2016; Liang et al., 2009; Srinivasan et al., 2018) have also been studied but are presently at laboratory scale.

The optimal temperature for microalgae cultures is generally between 20 and 24 °C but for temperate species; the optimum temperature may differ. Yet, it has been found that some microalgae strains are capable of growing at higher temperatures, between 25 and 50 °C (Onay et al., 2014).

The pH range for most cultured algal species is between 7 and 9, with an optimum range slightly alkaline between 8.2–8.7 as concluded by (Kong et al., 2007). Some microalgae like *Dunaliella* sp. (Srinivasan et al., 2018) may be able to grow at very alkaline environment. Furthermore, the pH of the culturing medium is crucial because it regulates the type of carbon species available for the microalgae (Goldman et al., 1982). Nonetheless, freshwater species may prefer a more neutral pH compared with marine species.

Besides carbon sources, nitrogen and phosphorus are essential nutrients for microalgae growth. Nitrogen and phosphorus are needed for cell growth and cell wall building. When external sources of nitrogen are exhausted, cell growth will be supported by drawing nitrogen from intracellular sources like chlorophyll molecules. Once nitrogen is depleted, cell growth would be disrupted because cell division is an energy-consuming process. In order to conserve energy, lipid storage will take place. Therefore, during cultivation, when substantial biomass is reached, stress as in the form of nitrogen-depletion condition is introduced to stimulate lipid accumulation (George et al., 2014; Griffiths et al., 2012; James et al., 2013; Yantao Li et al., 2011; Yanqun Li et al., 2008; Ren et al., 2013; Xin et al., 2010) .

Although multiple studies have been conducted to find the optimum condition, in many cases, what optimum is to a species might not be optimum to another species. Therefore, it is best to conduct a species-specific assessment using published literature as a base to work on (Griffiths, van Hille, & Harrison, 2012; Han et al., 2017). After species selection, preferably indigenous species, its culturing conditions can be manipulated to obtained high biomass productivity.

2.5.3 Biolubricant from microalgae

The study of friction and wear characteristics of microalgae-based oil is limited because most of the published work are on microalgae biofuel, covering aspects such as growth and cultivation (Doucha et al., 2005; Yanqun Li et al., 2008; H. Xu et al., 2006), lipid accumulation and extraction (Griffiths et al., 2012; Halim et al., 2011; Menegazzo & Fonseca, 2019; Ngangkham et al., 2012; Packer et al., 2011; Ren et al., 2013; J. Yang et al., 2011), biofuel production (Kong et al., 2007; Man Kee Lam & Lee, 2013; Song et al., 2008), and engine performance and emissions (Mostafa & El-Gendy, 2013; Y. Xiao et al., 2015). Past literature pertaining to the tribological properties of microalgae-based oil are summarized in Table 2.11.

Table 2.11: Tribological performance of microalgae-based oil

Microalgae	Sample type	Sample production and treatment	Tribological test condition	Findings	Reference
Spirulina sp.	Bio-oil	Hydrothermal liquefaction of biomass into bio-oil. Bio-oil was upgraded via catalytic esterification using potassium fluoride on alumina (KF/Al_2O_3) and potassium fluoride on HZSM-5 zeolite (KF/HZSM-5) with ethanol.	High-frequency reciprocating rig Reciprocating frequency: 5Hz, slide distance: 80mm, oil feed rate: 25mL/h, sliding velocity: 0.8 m/s, normal load: 350N, duration: 60min. Cast iron cylinder-liner measurement: 122mm x 15.6mm x 6.3 mm, piston ring sample measurement: 8mm x 2mm x 2 mm.	The esterified bio-oils generated lower friction and wear than the ethanol/bio-oils blends. KF/Al_2O_3 performed better than KF/HZSM-5 as a catalyst due to its strong alkalinity. Friction coefficients were reduced by 22% (using AEO) and 10% (using HEO) in comparison to crude bio-oil and ethanol blends. The formed protective lubricating film was more robust in the upgraded oils due to the stronger adsorption of the ester groups on metal surfaces. Tribo-oxide film of Fe_2O_3 was also formed on the metal surfaces.	(Y. Xu, Zheng, et al., 2014)
Spirulina sp.	Bio-oil	Hydrothermal liquefaction of biomass into bio-oil. Bio-oil was upgraded via catalytic esterification using potassium fluoride on alumina (KF/Al_2O_3) and potassium fluoride on HZSM-5 zeolite (KF/HZSM-5) with methanol	High-frequency reciprocating rig Reciprocating frequency: 5Hz, slide distance: 80mm, oil feed rate: 25mL/h, sliding velocity: 0.8 m/s, normal load: 350N, duration: 60min. Cast iron cylinder-liner measurement: cylinder radius 55mm, cylinder measurement: 122mm x 15.6mm x 6.3 mm, cylinder roughness (Ra) <0.3 µm, piston ring measurement: 8mm x 2mm x 2mm, piston ring roughness (Ra) < 0.25 µm.	The friction coefficients of esterified bio-oil HMO and AMO were reduced by 11.4% and 21.6%, respectively, compared with those of MeOH-SBO before esterification. The wear loss was reduced for esterified oil. AMO has better lubricity properties than HMO. The tribological mechanisms of the crude and esterified bio-oils can be ascribed to corrosive wear and boundary lubrication, respectively. The tribo-oxide film and the adsorbed lubricating film serve as protective layers between the frictional pairs. AMO has better lubricity than HMO due to the presence of more ester groups that formed a thicker oil film than HMO.	(Y. Xu, Hu, et al., 2014)

CHAPTER 3: MATERIALS AND METHOD

This chapter details the materials and methods employed in this research study. This project comprised of three main parts, the first part involved obtaining the feedstock. Field sampling was carried out to obtain local microalgae strains to prevent issues associated with foreign species invasion and at the same time, two local strains were also purchased from a local supplier. The next part involved the production of microalgae biolubricant. Crude oil was extracted from biomass and was further upgraded via chemical modification and the last part involved tribological analysis of the produced biolubricant to assess its lubricity performance. Figure 3.1 illustrates the overall methodology of this study.

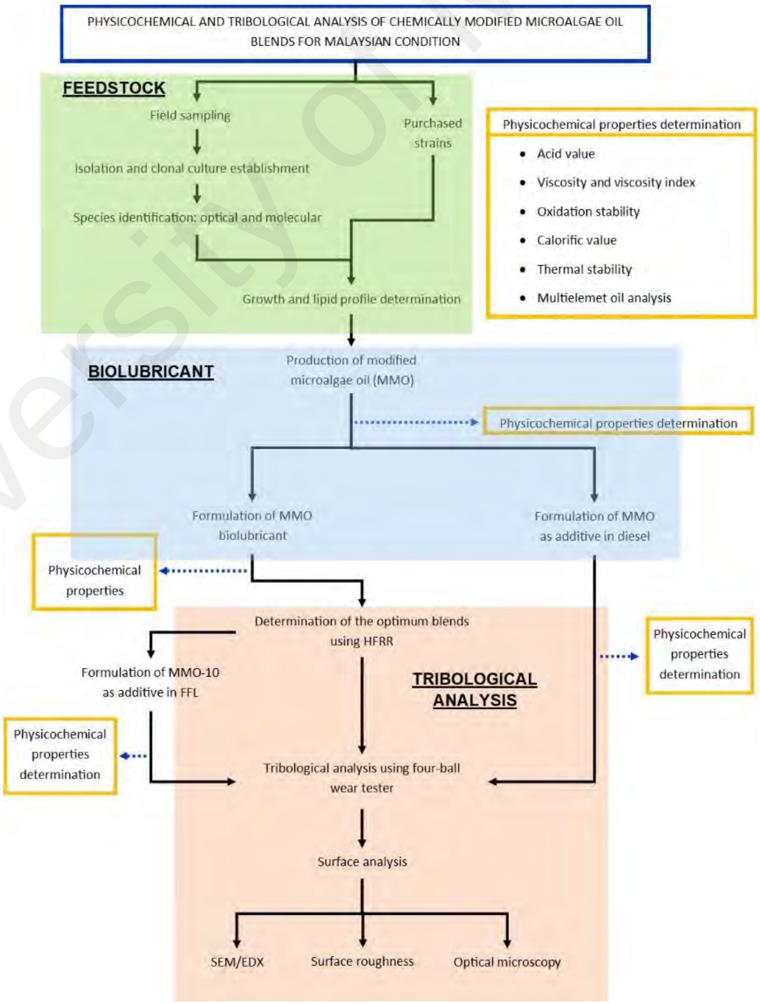

Figure 3.1: Research layout

3.1 Field sampling, isolation, and clonal culture establishment

Plankton samples were collected from Tasik Varsiti, University of Malaya in Kuala Lumpur and Tasik Jaya at Selangor using a 20 mm mesh size plankton net and were brought back live to the laboratory for cell isolation and culturing. Monoclonal cultures were established by micropipeting and streak plating techniques (Figure 3.2). The cells were allowed to divide in the wells before being transferred into culture tubes containing BG11 (modified) medium (Allen & Stanier, 1968; Rippka & Herdman, 1992) and Bold's Basal medium (Bischoff & Bold, 1963; Starr, 1971), refer to Table 3.1. All cultures were maintained at approximately 26 ˚C under a light intensity of 0.9 - 1.3 klux and under a 12:12 h light: dark cycle.

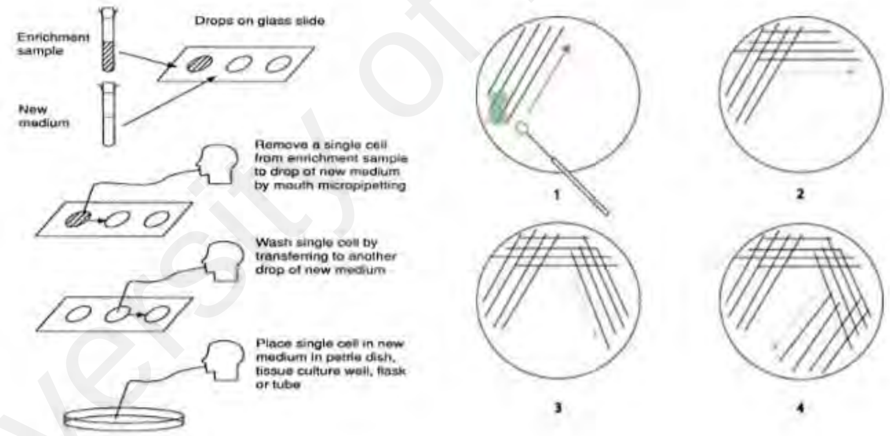

Figure 3.2: (a) micro pipetting technique and (b) plate streaking technique

Table 3.1: Culturing media BG11 (modified) medium and Bold's Basal medium

Medium	Component	Molar Concentration in Final Medium
BG11 (modified) Medium	Fe Citrate solution	
	• Citric acid	3.12 x 10^{-5} M
	• Ferric ammonium citrate	
	$NaNO_3$	1.76 x 10^{-2} M
	K_2HPO_4	2.24 x 10^{-4} M
	$MgSO_4.7H_2O$	3.04 x 10^{-4} M
	$CaCl_2.2H_2O$	1.84 x 10^{-4} M
	Na_2CO_3	1.89 x 10^{-4} M
	$Na_2SiO_3.9H_2O$	2.04 x 10^{-4} M
	Trace element solution	
	• $MgNa_2EDTA.3H_2O$	2.26 x 10^{-6} M
	• H_3BO_3	4.63 x 10^{-5} M
	• $MgSO_4.7H_2O$	1.01 x 10^{-5} M
	• $ZnSO_4.7H_2O$	7.65 x 10^{-7} M
	• $CuSO_4.5H_2O$	3.16 x 10^{-7} M
	• $Na_2MoO_4.2H_2O$	8.68 x 10^{-8} M
	• $Co(NO_3)_2.6H_2O$	1.70 x 10^{-7} M
Bold's Basal Medium	$NaNO_3$	2.94 x 10^{-3} M
	$MgSO_4.7H_2O$	3.04 x 10^{-4} M
	NaCl	4.28 x 10^{-4} M
	K_2HPO_4	4.31 x 10^{-4} M
	KH_2PO_4	1.29 x 10^{-3} M
	$CaCl_2.2H_2O$	1.70 x 10^{-4} M
	H_3BO_3	1.85 x 10-4 M
	EDTA-KOH solution	
	• $Na_2EDTA. 2H_2O$	1.71 x 10^{-4} M
	• KOH	5.53 x 10^{-4} M
	Ferric solution	
	• $FeSO_4.7H_2O$	1.79 x 10^{-5} M
	• H_2SO_4 (concentrated)	(1 ml to acidify)
	Trace element solution	
	• $ZnSO_4.7H_2O$	3.07 x 10^{-5} M
	• $MnCl_2$	7.28 x 10^{-6} M
	• MoO_3	4.93 x 10^{-6} M
	• $CuSO_4.5H_2O$	6.29 x 10^{-6} M
	• $Co(NO_3)_2.6H_2O$	1.68 x 10^{-6} M
	Vitamin Solution (optional)	
	• Vitamin B1 (Thiamine HCl)	2.97 x 10^{-8} M
	• Biotin	1.02 x 10^{-10} M
	• Vitamin B12 (Cyanocobalamin)	1.11 x 10^{-11} M

3.2 Strains identification

3.2.1 Microscopy identification

Once the monoclonal cultures were established, some samples were fixed in formalin solution and viewed under normal light on an Olympus BX51 microscope for identification. Images were captured using a ColorView F12 cooled CCD camera (Soft Imaging System GmbH, Germany) for microscopy identification.

3.2.2 Molecular identification using 18S rRNA gene

Isolates genus were further confirmed using 18S rRNA gene. The gDNA was extracted using commercial bead beating DNA extraction kit followed by PCR using eukaryote 18s rRNA primers (the sequence is not disclosed) due to intelligence proprietary. Next, the PCR product was ligated with vector pJET1.2 (Fermentas) and transformed into JM109 *E. coli* (Promega) according to the manufacturer's protocols. The positive clone was identified using colony PCR, it was followed by sequencing. Sequences obtained were further Blast with sequences from GenBank.

3.2.3 SSU rDNA phylogenetic analysis

The small subunit (SSU) rDNA sequences obtained in this study were deposited in NCBI GenBank nucleotide database, with accession numbers as shown in Table 1. The final dataset consisted of 55 taxa covering species from Chlorophyceae and Trebouxiophyceae based on Leliaert et al. (2012) (Sebayang et al., 2017). Three species from *Tetraselmis* – *T. apiculata* (Butcher) Butcher, *T. convolutae* (Parke & Manton) Norris, Hori and Chihara and *T. inconspicua* Butcher – were defined as outgroup. Sequences with length < 1,600 nt and with ambiguous nucleotides were excluded in the analyses. The sequences were aligned using MUSCLE (Kusumo et al., 2017). The SSU dataset was subjected to maximum parsimony (MP) and maximum likelihood (ML) analyses using PAUP* 4b10 (Rastogi & Yadav, 2003) while Bayesian Inference (BI) was analyzed using MrBayes v3.2.5 (Muratore et al., 2011). MP was performed through heuristic searches with random addition of sequences (1,000 replicates), branch swapping with tree-bisection-reconnection (TBR) and 1,000 bootstrap replicates. For ML analysis, a substitution and rate heterogeneity model was selected using Akaike information criterion (AIC) as implemented in jModelTest 2.0 (Darriba et al., 2012; Shakib & Mekhilef, 2017). The best fitted evolutionary model calculated was TIM2+I+G. ML was performed with 10 random addition sequence replicates, heuristic search using NNI branch swapping and bootstrap at 500 replicates. For Bayesian analysis, the same best-fitted model for ML analysis was used. The effective samples size (ESS) was checked in Bayesian Evolutionary Analysis Sampling Trees (BEAST) v1.8.2 (Kahoul et al., 2017) and further checked in Tracer (http://beast.bio.ed.ac.uk/tracer). The SSU rDNA dataset was performed at 4 × 106 generations per run, sampling every 100 generations and the posterior probability (PP) was estimated with 25% burn-in.

3.3 Microalgae strains cultivation and harvesting

All isolated strains and two purchased strains were cultured in 500 mL and 1 L flask with a working volume of 250 mL and 500 mL each at 26 ˚C under the same light intensity and light: dark cycle until log phase before being transferred into bigger containers with a working volume of 10 L each. Agitations were provided by gently swirling of the flasks once a day and for the bigger volume containers - air bubbling from an aquarium pump. Cells were harvested after 40 days by filtration. Harvested cells were rinsed with distilled deionizer water twice before being dried in an electric oven at 55 ˚C.

3.4 Growth monitoring and growth rate determination

Cells were cultured in 1.5 L flasks with a working volume 1000 mL each at 26 ˚C under the same light intensity and light: dark cycle. Subsamples were conducted every two to three days, 1 ml was subsampled into 1.5 mL pre-weighted micro-centrifuge tube in triplicates. Media were removed by centrifugation and the tubes were placed in an electric oven to remove moisture until a stable mass was obtained. Optical density (OD) reading at 750 nm was used to monitor the growth of the isolated species. The specific growth rate of each strain of microalgae was calculated with the following formula by (Andersen, 2005):

$$\mu = \frac{\ln(\frac{N2}{N1})}{(t2-t1)} \qquad [1]$$

where μ is the specific growth rate (day^{-1}), N_1 and N_2 = biomass measured as dry weight at time1 (t1) and time2 (t2) respectively.

The microalgae biomass productivity was determined by using the following formula by (Vaičiulytė et al., 2014):

$$P = \frac{(N2-N1)}{(t2-t1)} \qquad [2]$$

where P is the biomass productivity (g L^{-1}day^{-1}), N1 and N2 = biomass measured as dry weight at time1 (t1) and time2 (t2), respectively.

3.5 Oil extraction and fatty acid profile determination

Dried biomass samples were ground into smaller size and weighed on a grade 42 filter paper. An empty round bottom flask was pre-weighed. The biomass sample was put into a thimble and reflux with 250 mL petroleum ether at 40-50 °C for 8 hours using a Soxhlet apparatus. After completion, all solvents were evaporated using a rotary evaporator, followed by heat dried for another hour in an electric oven at 105 °C. The extracted oil was cooled in a desiccator and the final weight recorded.

Oil yield is calculated as follows:

$$Oil\ Yield\ (\%) = \left(\frac{Lipid\ extracted\ from\ dry\ biomass}{weight\ of\ dry\ biomass}\right) x\ 100\% \qquad [3]$$

With a condenser attached, methanolic sodium hydroxide was added to transesterify the extracted oil where it was reflux again at 40-50 °C until all fat globules disappeared (usually about 5-15 min). Then, boron trifluoride solution was added and boiling was continued for another 5 min. After that, about 2-5 mL of heptane was added and the mixture was boiled for another 1 min. After completion, several mL of saturated sodium chloride was added to the mixture.

For fatty acid methyl ester (FAME) analysis, the obtained heptane extracts were dried and the residues were dissolved in 100 mL hexane per mg of the original biomass. FAME determination was carried out on an Agilent Gas Chromatography (GC) equipped with an HP88 column and a flame ionization detector (FID). Nitrogen was used as the carrier gas. Temperature program was as follows: 70 °C with a 5 min hold; ramp at 4 °C/min to 240 °C; followed by a 30 min final hold. Instrument conditions were as follows: nitrogen as carrier gas; FID set at 240 °C; air flow of 20 mL/min, non-split, auto-sampler injection volume of 2 µL. FAME identification was carried out by comparison with a certificated standard mixture, Supelco FAME 10 mix 37 (Bellefonte, PA, USA).

3.5.1 Comparative study of lipid extraction using different solvents

Once the highest growth microalgae is determined, the following solvents: (a) Hexane, (b) Hexane: Isopropanol (1:1), (c) Chloroform: Methanol, C: M (1:2), (d) Chloroform: Methanol, C: M (2:1) and (e) Chloroform are used to determine the best solvent for lipid extraction.

3.6 Physicochemical properties estimation

3.6.1 Iodine value

Iodine value (IV) was calculated using the following formula by (Devan & Mahalakshmi, 2009):

$$IV = \sum \frac{254 \ x \ A_i x \ D}{M_{wi}} \qquad [4]$$

where A_i is the fatty acid proposition of each component, D is the number of the double bonds, M_{wi} is the molecular mass of each component.

3.6.2 Kinematic viscosity

Kinematic viscosity (KV) was calculated following formula by (Knothe & Steidley, 2011):

$$V_{mix} = A_c \ x \ V_c \qquad [5]$$

where V_{mix} is the kinematic viscosity of the biodiesel sample (mixture of fatty acid alkyl esters), A_C is the relative amount (%/100) of the individual neat ester in the mixture (as determined by gas chromatography) and V_C is the kinematic viscosity of these esters used to predict kinematic viscosity of a mixture such as biodiesel at a given temperature.

3.6.3 Cold filter plugging point

Cold filter plugging point (CFPP) was calculated using the following formula by (Sarin et al., 2010):

$$CFPP = 0.511 \, x \, PAME - 7.823 \;\; (0 < PAME < 45) \qquad [6]$$

where $PAME$ is the palmitic acid methyl ester content (wt%)

3.7 Production of microalgae-based biolubricants

The production of microalgae-based biolubricant consists of oil extraction from biomass, chemical conversion into chemically modified microalgae oil and the preparation of biolubricant blends.

3.7.1 Extraction of *Chlorella* microalgae oil (CMO)

For large volume lipid extraction from dry microalgae biomass purchased from a local supplier, the modified Folch method (Folch et al., 1951) was used to extract the CMO from 500 g of *Chlorella* sp. biomass using a mixture of chloroform and methanol (2:1, v/v) for 12 h at 500 rpm. This was followed by filtration through a 1-µm polytetrafluoroethylene filter to remove biomass residues. The filtrate was washed with 1% sodium chloride solution at a volume ratio of 8:4:3 (chloroform: methanol: 1% sodium chloride solution). The mixture was shaken and left to settle in a separatory funnel for 12 h. Once the separation process was complete, the bottom layer (CMO) was collected from the separatory funnel by opening the stopcock and the excess solvents were evaporated from the CMO using a rotary evaporator. The extracted CMO was weighed and its acid value was measured.

3.7.2 Acid-catalyzed esterification and alkaline-catalyzed transesterification

As mentioned previously in the literature, CMO cannot be used directly in engines and for machinery because of its high acidity, which will lead to corrosion of the parts. For this reason, acid-catalyzed esterification and alkaline-catalyzed transesterification were carried out in sequence in order to improve the physicochemical properties of the CMO. A two-step reaction is needed when the free fatty acid content is high. Sulfuric acid was used as a catalyst in the first reaction to convert free fatty acids into methyl esters and to prevent the formation of soap. Then, potassium hydroxide was used in the transesterification reaction to convert the rest of the esters into methyl esters.

In acid-catalyzed esterification, the CMO was esterified with 1 (v/v)% of sulfuric acid and 50 (v/v)% of methanol for 2 h at a temperature of 65 °C and stirring speed of 500 rpm. Once the esterification process was complete, the reaction mixture was left to settle overnight in a separatory funnel. Two distinct layers formed in the separatory funnel after the separation process, where the top layer was the esterified oil and the bottom layer was a mixture of glycerin, water, methanol excess, and other impurities. The bottom layer was drained from the separatory funnel. The esterified oil was collected and transferred into a rotary evaporator in order to evaporate the remaining methanol and water.

Next, the esterified microalgae oil was transesterified with 1 (w/w)% of potassium hydroxide (KOH) and 50 (v/v)% of methanol for 2 h at a temperature of 65 °C and stirring speed of 500 rpm. Once the transesterification process was completed, the reaction mixture was left to settle overnight in a separatory funnel. Two distinguishable layers formed in the separatory funnel, where the top layer was the MMO and the bottom layer was a mixture of glycerin and excess methanol. The bottom layer was drained from the separatory funnel and the MMO was transferred into a rotary evaporator in order to evaporate excess methanol. The weight and acid value of the MMO were measured.

3.7.3 Preparation of the modified microalgae oil (MMO) blends

Polyalphaolefin, PAO (Durasyn® Grade 170, INEOS Oligomers LLC, USA) was used as the base oil for the MMO blends. PAO is a polymer made by polymerizing an alpha-olefin and composed of 100% synthetic chemical compound. It is used as a base stock in the production of some synthetic lubricants. Five samples were prepared by blending the PAO with 1, 2, 5, 10, and 20 (v/v)% of MMO.

3.8 Physicochemical properties determination

3.8.1 Fourier transform infrared spectroscopy, gas chromatography, and gas chromatography-mass spectrometry analyses

Fourier transform infrared (FTIR) spectrometer (Model: Spectrum 400, PerkinElmer Instruments LLC, USA) was used to analyze the compositions of the CMO and MMO. The absorption spectra were recorded within a wavenumber range of 4000–400 cm^{-1}.

The fatty acid methyl ester (FAME) content of the MMO was determined using a gas chromatograph with flame ionization detector (GC-FID) (Model: 7890A, Agilent Technologies Inc., USA). Agilent HP-INNOWax column (length × inner diameter × film thickness: 30 m × 0.25 mm × 0.25 μm) was chosen as the capillary column for the GC-FID analysis. The oven temperature was programmed according to the following sequence: (1) hold at 60 °C for 2 min, (2) heat from 60 to 200 °C at 10 °C/min, (3) heat from 200 to 240 °C at 5 °C/min, and (4) hold at 240 °C for 7 min. Nitrogen was used as the carrier gas. The flame ionization detector was set at a temperature of 250 °C, the flow rate was set as 2 mL/min, the type of injector was splitless, and the injection volume was 1 μL. The FAME content of the samples was compared with a certified FAME standard mixture (Supelco® 37 component FAME mix, Supelco Inc., USA).

The compounds present in the MMO were analyzed using gas chromatograph-mass spectrometer (GC-MS) (Model: GCMS-QP2010 Ultra, Shimadzu Corporation, Japan) with a low-bleed column (Model: Rtx-5MS, Restek Corporation, USA, length × inner diameter × film thickness: 30 m × 0.25 mm × 0.25 μm). The injection volume was 1 μL. The oven temperature was programmed according to the following sequence: (1) hold at 60 °C for 2 min, (2) heat from 60 to 200 °C at 10 °C/min, (3) heat from 200 to 250 °C at 5 °C /min, and (4) hold at 250 °C for 7 min. Helium was used as the carrier gas with a split injection ratio of 100:1. The compounds (based on the peak area) were identified from the NIST 02 mass spectral library. The quadrupole mass spectrometer was operated at an interface temperature of 250 °C and ion source temperature of 200 °C with a sample flow rate of 1 mL/min.

3.8.2 Acid value

The acid values of the samples were measured according to the ASTM D664 standard test method using a potentiometric compact titrator (Model: G20, Mettler Toledo, USA). A high value of acid value denotes high corrosiveness. It has a detrimental effect on a lubricant's oxidative stability, that in turn, reducing the shelf life of a lubricant.

3.8.3 Viscosity and viscosity index

The kinematic viscosity, dynamic viscosity, viscosity index and density at 15 °C of the samples were measured according to the ASTM D445, ASTM D2270, and ASTM D1298 standard test methods, respectively, using Stabinger viscometer (Model: SVM 3000^{TM} G2, Anton Paar GmBH, Austria).

3.8.4 Oxidation stability analysis

3.8.4.1 For lubricant

The modified Baader test on DIN 51554 standard, Part 3 was used to evaluate a lubricant's oxidation performance. Lubricant samples were aged for six days in a glass vessel (with constant aeration of 10mL/min) at a constant temperature of 95°C. The differences in the kinematic viscosity of the sample at 48h and at 144 h were used as a relative measurement of its oxidation performance.

In addition, the oxidative induction time (OIT) also provides information about the oxidative stability of materials. ASTM D3895-14 using a DSC (DSC 4000, Perkin Elmer, USA) was used as the test method in this study. Test specimens (PAO and MMO-10) were heated at a constant rate in an inert gas (nitrogen) to a specified temperature, at 200 °C, and then the atmosphere was changed to oxygen at the same flow rate. The specimen was held at isotherm until an oxidative reaction is displayed on the thermal curve. The time taken from the switch to oxygen to the onset of the oxidation reaction is defined as OIT. The end of the induction period is indicated by an abrupt increase in the specimen evolved heat or temperature. The analysis was repeated for isothermal temperatures of 180 °C and 190 °C.

3.8.4.2 For diesel-MMO (DMO) blends

Oxidation stability of DMO was determined using a rancimat (Model: 873, Methrom, Switzerland) according to EN 14112 standard method with a stipulated limitation of 6 h minimum induction period.

3.8.5 Thermal stability analysis

Thermogravimetric analysis was performed using a TGA (Model: TGA 4000, Perkin Elmer, USA). Sample of about 2-50 mg was heated at a constant heating rate of 15 °C /min from 30 °C to 700 °C in an inert environment. Nitrogen gas with a flowrate of 20 ml/ min was used. Sample’s weight loss against time was plotted to determine the decomposition temperature - the extrapolated onset temperature that denotes the temperature at which the weight loss begins. When the weight loss curve is first derivatives, the peak temperature is the inflection point. It represents the point of the greatest rate of change on the weight loss curve and the material remaining behind is the final residue.

3.8.6 Multi-element oil analysis and calorific value

Lubricant oil element analysis was conducted using a multi-element analyzer (Model: MOA, Baird, Canada). Calorific value was determined using a bomb calorimeter (Model: 6100, Paar Instrument Company, USA).

3.9 Tribological analysis

3.9.1 High-frequency reciprocating rig (HFRR)

HFRR is designed to stimulate the bidirectional sliding condition; for example, the motions between the piston-ring/cylinder bore contacts in an internal combustion engine. In this study, a HFRR (Model: TR-281-M8, Ducom Instruments, USA) with pin-on-plate configuration (Figure 3.3) was used to determine the optimum blend of MMO in terms of coefficient of friction (COF) and wear.

ASSAB DF2 carbon steel plate (length × width × thickness: 15 mm × 15 mm × 4 mm) was chosen as the test plate whereas a cylindrical roller bearing (Part no.: RC-6X6 C, SKF, Sweden) was chosen as the pin. Fresh test plate and pin were used for each sample. The COF values were recorded automatically during the tests. The test conditions of the high-frequency reciprocating rig are presented in Table 3.2. PAO and a commercial full synthetic lubricant (FFL) were used as the control samples.

The test plates were washed with acetone and dried in the air prior to the surface morphology and elemental analysis using scanning electron microscope (SEM) integrated with an energy-dispersive X-ray spectrometer (EDS) (Model: Phenom ProX, Phenom-World B.V., The Netherlands). Surface roughness and wear loss of the experimented plate were determined using an optical surface profilometer (Model: Infinite Focus, Alicona Imaging GmbH, Austria).

Table 3.2: Test conditions for the high-frequency reciprocating rig

Test condition	Value
Reciprocating frequency	10 Hz
Temperature	75 °C
Duration	1 h
Load	100 N

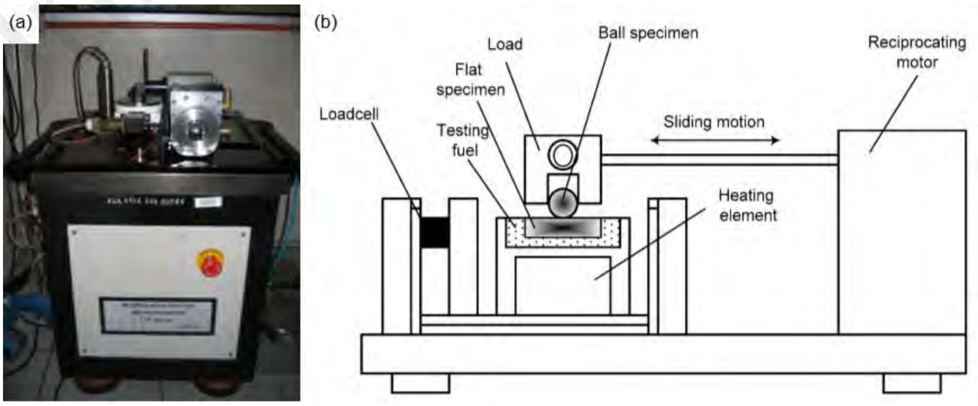

Figure 3.3: (a) HFRR and (b) Schematic diagram of HFRR (Anastopoulos et al., 2017)

3.9.2 Four-ball wear tester

A four-ball wear tester is extensively used by the lubricant industry to characterize a lubricant's lubricating properties, wear, and its chemical interactions particularly at the contact interface. Many lubricant and lubrication related standards such as ASTM were created based on the four-ball application. The device consists of three steel balls clamped together with a fourth ball held on top of the three in a rotating spindle, refer to Figure 3.4, for an equilateral triangle (three-point) contact. Chrome alloy steel ball (AISI E-52100) with a diameter of 12.7 mm and a 64-66 Rc hardness are used as test balls. Ball bearings are used as low cost, self-alignment samples given its geometry that provides multiple samples for surface analysis and before each experiment, all test balls are cleaned with toluene.

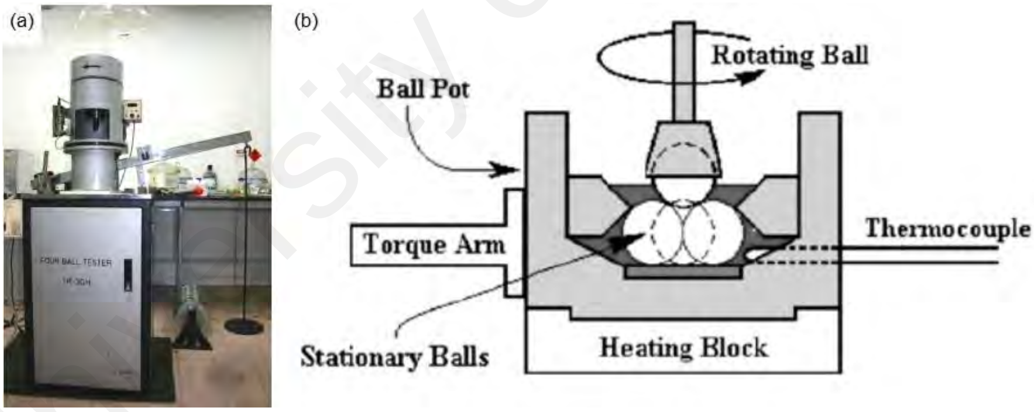

Figure 3.4: (a) Four-ball test machine and (b) Schematic diagram of four-ball arrangement (Golshokouh et al., 2014)

When load is applied, it is evenly distributed over three points of contact between the top rotating ball and the underlying three stationary balls. Temperature control of the sample chamber is provided by the heater block underneath the ball pot. About 10 mL lubricant volume is needed for each run. The primary measurement made with a four-ball machine is wear. Thus, a lubricant performance is assessed by comparing the wear scar diameters on the three stationary balls. The wear produced on the three stationary balls was measured using a calibrated optical microscope and reported as wear scar diameter (WSD).

3.9.2.1 Coefficient of friction (COF)

The friction coefficient (COF) is a dimensionless number that describes the ratio between the friction force between two bodies and the normal force pressing them together. COF determines the transmission efficiency where a lower COF denotes less friction and higher efficiency. COF was calculated from the frictional force that the instrument recorded automatically. COF was calculated following IP-239 standard:

$$\mu = \frac{T\sqrt{6}}{3Wr} \qquad [7]$$

where μ is the COF, T is the frictional force (Nm), W is the applied load (N), and r is the distance from the center of the contact surface on the lower balls to the axis of rotation, which was determined to be 3.67 mm.

3.9.2.2 Minimum film thickness, *h* and film thickness ratio, λ

It is believed that a thin lubricating film provides lubrication between the top rotating ball with the three stationery balls. According to the elastohydrodynamic lubrication (EHL) theory, the minimum film thickness for a circular point contact can be calculated. These calculated minimum film thickness, h and film thickness ratio, λ can be used to describe the lubrication regime and the relationship between λ and lubrication regime is given in Table 3.3.

Table 3.3: EHL Regime

λ	λ ≥ 3	3 < λ < 1	λ ≤ 1
Lubrication regime	Full fluid film	Mixed film	Boundary lubrication

The calculated minimum film thickness, h and film thickness ratio, λ can be obtained from the following equations (Hamrock & Dowson, 1981):

$$H_{min} = 3.63U^{0.68}\, G^{0.49}\, W^{-0.073}(1 - e^{-0.68k}) \qquad [8]$$

$$H_{min} = 3.63\left(\frac{u\eta_o}{E'R'}\right)^{0.68} (\alpha E')^{\,0.49}\, \left(\frac{F}{E'R'^2}\right)^{-0.073}(1 - e^{-0.68k}) \qquad [9]$$

The minimum film thickness H_{min} is dimensionless, *U* is the dimensionless speed parameter ($\frac{u\eta_o}{E'R'}$), *G* the dimensionless material parameter ($\alpha E'$) and *W* the dimensionless load parameter ($\frac{F}{E'R'^2}$). *R'* is the reduced radius ($\frac{1}{R^1} + \frac{1}{R^2})^{-1}$, *E'* the modulus of elasticity of the interacting solids $\left(\frac{1-v_1^2}{E_1} + \frac{1-v_2^2}{E_2}\right)^{-1}$, *F* is the applied load, *u* the mean speed of contact ($\frac{u_1+u_2}{2}$), η_o the dynamic viscosity, α the pressure-viscosity coefficient, *k* the ellipticity ratio ($\frac{R_y}{R_x}$) that is equal to one in point contact and σ_q the composite surface roughness.

$$h_{min} = H_{min}R' \qquad [10]$$

$$\lambda = \frac{h_{min}}{\sigma_q} \qquad [11]$$

3.9.2.3 Flash temperature parameter (FTP)

Flash temperature parameter (FTP) denotes a single number that is used to express the critical flash temperature at which a lubricant will fail under a given condition. A higher value of FTP is preferred because it indicates that a lubricating film is less likely to break down. In a four-ball test condition, the following equation is used (Lane, 1957).

$$FTP = \frac{W}{d^{1.4}} \quad [12]$$

where W is the load (kg) and d is the mean wear scar diameter (mm).

3.9.3 Wear scar morphology analysis

Beside wear scar diameter, test ball surface morphology and elemental composition were analyzed using a scanning electron microscope (SEM) with integrated Energy Dispersive Spectrometer (EDS) (ProX, Phenom).

3.9.4 Tribological test using the four ball wear tester

A four-ball wear test machine (Model: TR-30H, Ducom Instruments, USA) is used to evaluate the performance of MMO blend under the following conditions. MMO-10, 10% blending with PAO 170 (poly-alpha-olefin) was tested with PAO and a commercial full synthetic lubricant (FFL) grade 5W-40 served as control. Comparisons were also made against paraffin oil and pure corn oil as representatives of mineral oil and vegetable oil, respectively.

3.9.4.1 Wear prevention test

ASTM D4172-94 (Reapproved 2016) method is used to determine the relative wear preventive properties of lubricating fluids in sliding contact. Table 3.4 shows the testing condition of this method (S. M. Reddy et al., 2018). The lubricant's performance was assessed by comparing the wear scar diameters on the three stationary balls. The produced wear was measured using a calibrated microscope and reported as WSD (wear scar diameter).

Table 3.4: Testing conditions according to ASTM D4172-94 (reapproved 2016)

Parameter	Value
Temperature	75 °C
Speed	1200 rpm
Duration	1 h
Load	40 kg

3.9.4.2 Extreme pressure condition

ASTM D2783-03 (2014) is used to determine the load carrying-properties of lubricants. The test lubricant covered the lower three balls. Table 3.5 shows the testing condition for this method. A series of tests of 10s duration was conducted at increasing loads until welding occurred.

Table 3.5: Testing conditions according to ASTM D2783-03 (2014)

Parameter	Value
Temperature	18-35 °C
Speed	1760 ± 40 rpm
Duration	Series of 10 s
Load	Increasing until welding occur

Ten tests shall be conducted below the welding point, but in the event of less than 10 when the lower balls welded, no further test is necessary provided the scars at loads below seizure are within 5% of the compensation line. Bring the total up to 10 with the assumption that for loads below the last non-seizure load, the corresponding produced wear scars will be equal to that of the "compensation wear scar diameter" (Figure 3.5).

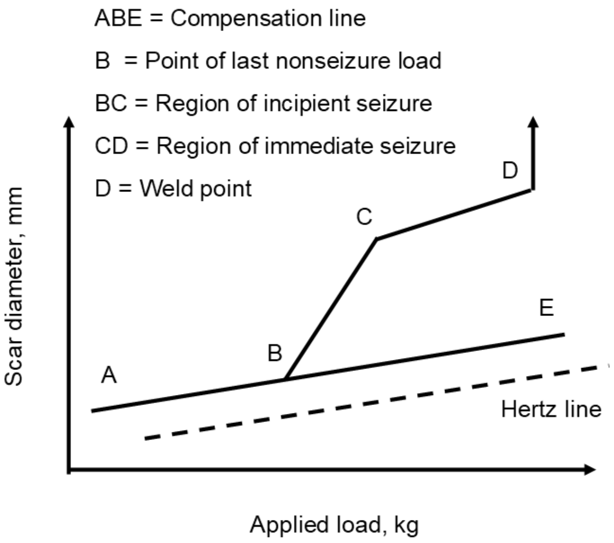

Figure 3.5: Wear load graph (reproduced from ASTM D2783)

By using the load-wear index, lubricating fluids having a low, medium and high level of extreme-pressure properties can be differentiated. Under this method, the test balls are subjected to different lubrication regimes when the load is increased, until welding occurs. The wear produced on the three stationary balls is measured using a calibrated microscope and reported as the wear scar diameter (WSD) or calculated volume.

3.9.4.3 Tribological characteristics of MMO-10 as additive in FFL

Five samples (FMO-1, FMO-2, FMO-5, and FMO-10) were prepared by blending FFL with 1, 2, 5 and 10 (v/v)% of MMO-10. A 100 % FFL served as control. FMO tribological performance was assessed using a four-ball tribotester (Model: TR-30H, Ducom Instruments, USA) by comparing the WSD on the three stationary balls and the average COF. The experimental conditions for FMO are shown in Table 3.6.

Table 3.6: Experimental conditions for FMO

Parameter	Value
Temperature	40, 75 °C
Speed	1200, 1400, 1600 rpm
Duration	60 min
Load	40 kg

3.9.4.4 Tribological characteristics of MMO as additive in diesel

Five samples (DMO-1, DMO-2, DMO-5, DMO-8, and DMO-10) were prepared by blending the normal diesel with 1, 2, 5, 8, and 10 (v/v)% of MMO. A pure 100 % diesel served as control. DMO tribological performance was assessed using a four-ball tribotester (Model: TR-30H, Ducom Instruments, USA) by comparing the WSD on the three stationary balls and the average COF. The experimental conditions for DMO are shown in Table 3.7.

Table 3.7: Experimental conditions for DMO

Parameter	Value
Temperature	Room temperature
Speed	1200 rpm
Duration	300 s
Load	40, 60, 80 and 100 kg

CHAPTER 4: RESULTS AND DISCUSSION

This chapter presents the results obtained from the research study and its comparisons with the work of others. The reasons for such observations and the findings of related past literature are deliberated to provide support to the drawn conclusions. As mentioned earlier, this study can be divided in to three parts, namely the feedstock prospecting, biolubricant production and finally, the tribological assessment.

Results pertaining to feedstock prospecting are covered in Section 4.1, 4.2, 4.3 and 4.4, which includes field sampling, growth study, microalgae oil structural effect on lubricity and the prediction of microalgae biolubricant's properties. Section 4.5 documented the findings and discussion about biolubricant production, which includes the extraction of crude oil from biomass up to the chemical modification of the crude oil via the transesterification reaction. Lastly, in Section 4.6, all the tribological assessments are included.

4.1 Field work sampling and isolates identification

Five different strains of freshwater microalgae were successfully isolated and cultured from Tasik Varsiti in University of Malaya, Kuala Lumpur, and Tasik Jaya, Selangor in Malaysia. Four of the isolates were from the green algae group and one from the cyanobacteria group (Figure 4.1).

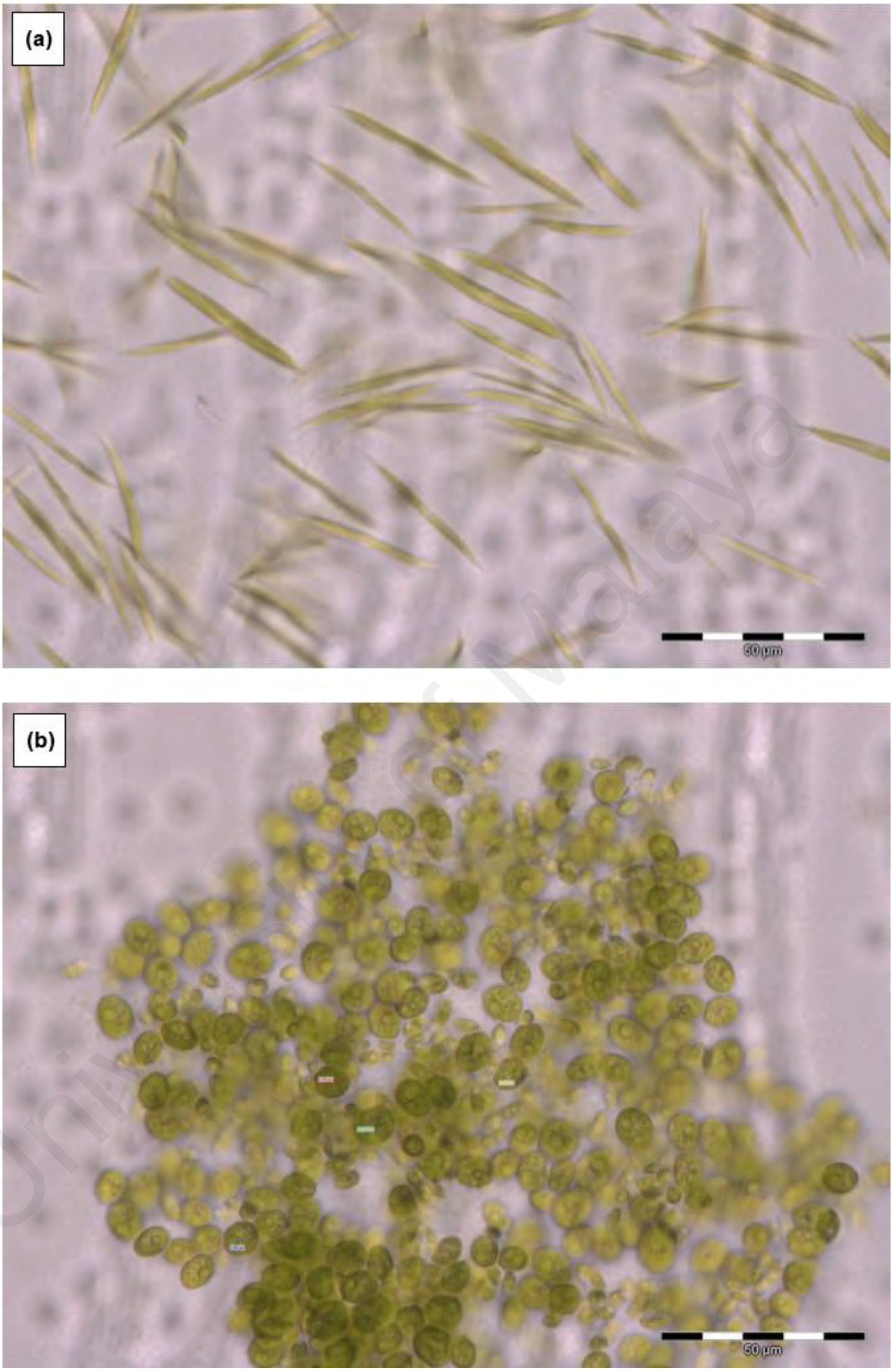

Figure 4.1: The isolated microalgae (a) *Ankistrodesmus* sp., (b) *Scenedesmus* sp. A, (c) *Scenedesmus* sp. B, (d) *Neochloris* sp. and (e) *Cyanosarcina* sp. under 600 X magnification

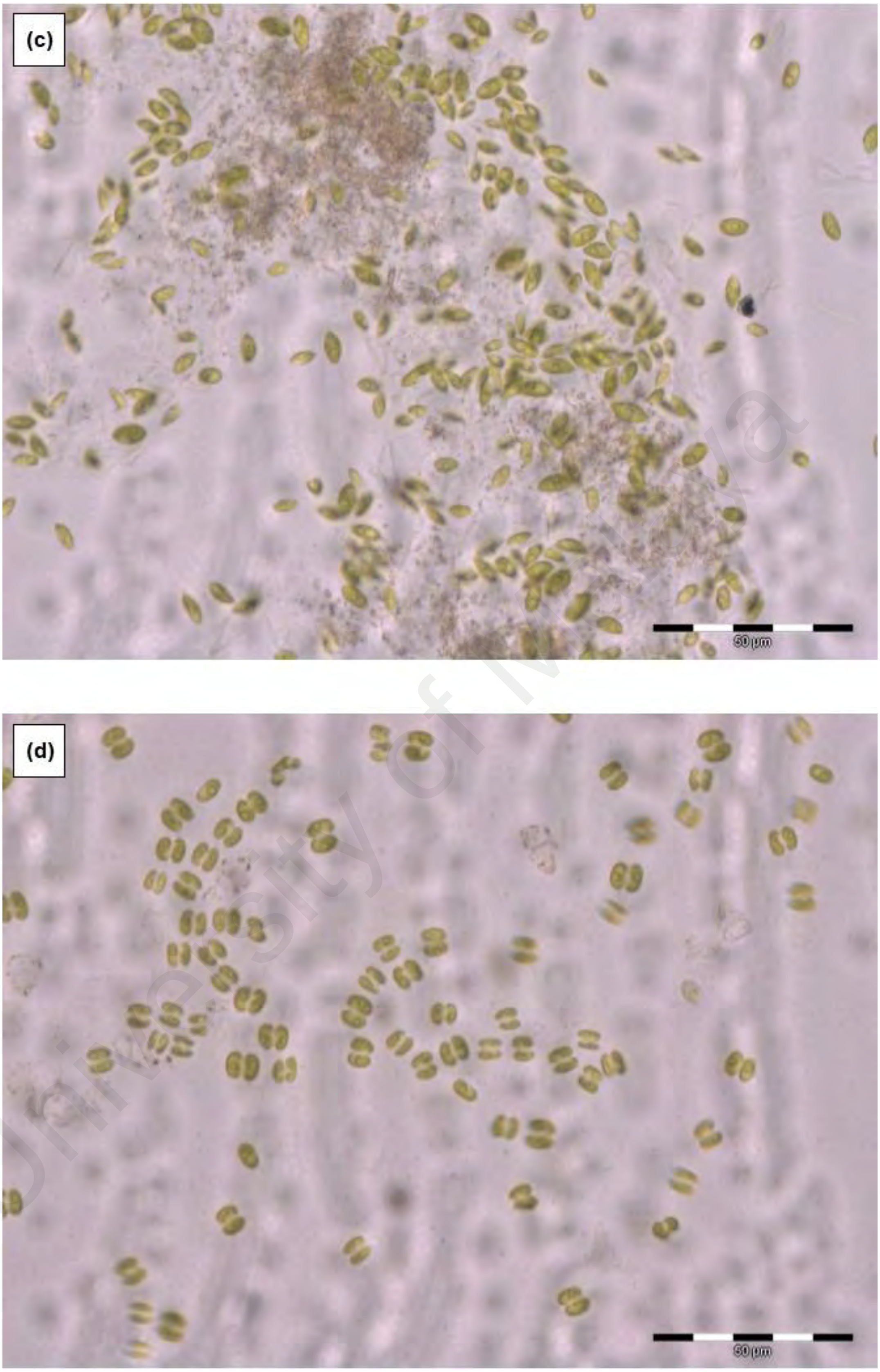

Figure 4.1, continued

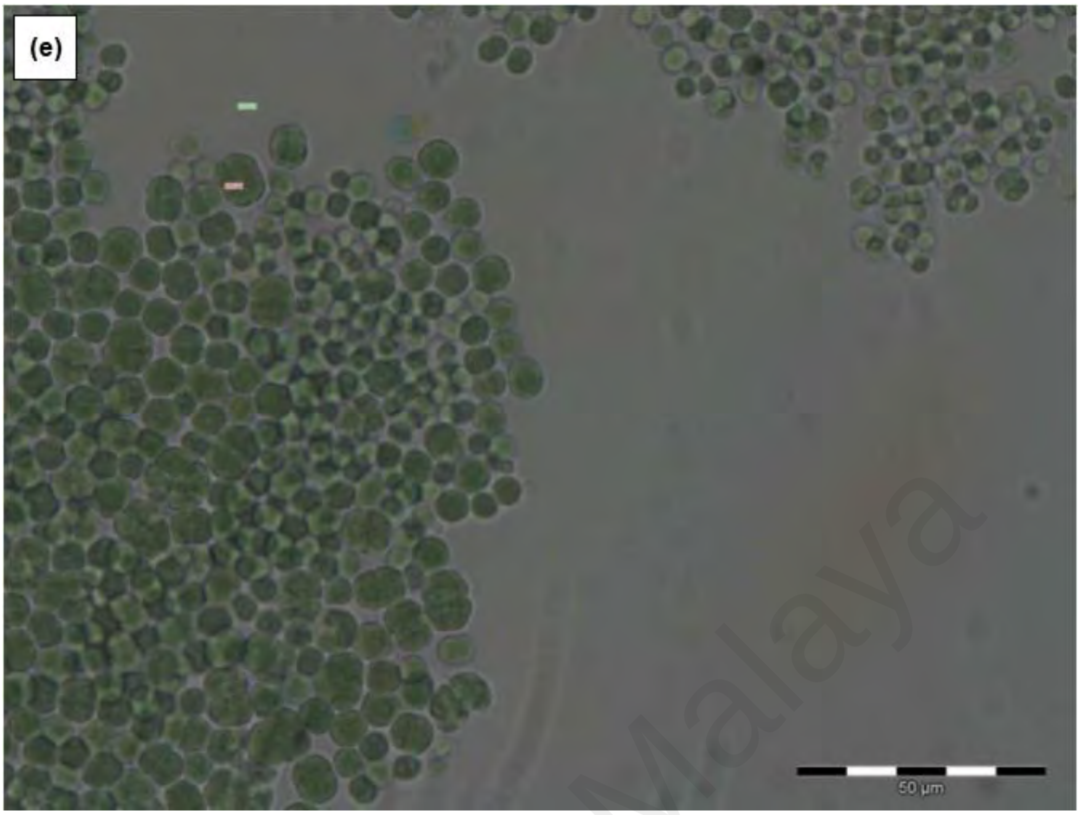

Figure 4.1, continued

Microscopy observations have shown that the four strains from the green algae group were from the Chlorophyta phylum and further identified as *Ankistrodesmus* sp., *Scenedesmus* sp. A and *Scenedesmus* sp. B and *Neochloris* sp. The final isolate was *Cyanosarcina* sp. from the Cyanophyta phylum (Table 4.1). Molecular identification and classification were also carried out using 18S rRNA gene. The obtained sequences were submitted to Genbank.

Table 4.1: Freshwater microalgae identification

Isolated Strains	Morphological Description	Group	Genbank Accession	18S rRNA gene
Ankistrodesmus sp.	Cells were long and spindle-shaped. Cells have lengths ranging from 41.35-43.83 µm and width of 3.49 ± 0.98 µm.	Green algae	KY819082	Full sequence
Scenedesmus sp. A	Cells were ellipsoidal in shape about 5.43-6.52 µm in length and 3.53 ± 0.18 µm in width. Terminal cells ornamented with short spines. The majority of the population were in two-cell form though four-cell coenobial colonies were also present.	Green algae	KY816918	Partial sequence
Scenesdesmus sp. B	Cells have pointed ends about 8.68-12.58 µm in length and 2.65 ± 0.28 µm in width. Terminal cells ornamented with chitinous hairs. The majority of the population were in single cell form.	Green algae	KY816917	Full sequence
Neochloris sp.	Cells were of spherical or oblong shapes. Cells' diameter varied, some may reach more than 15.00 µm while other may be much smaller of about 5.70 µm.	Green algae	KY816916	Full sequence
Cyanosarcina sp.	Colonies were of sarcinoid packet, with densely aggregated cells. Colonies varied in size from 4.28 µm to more than 8.00 µm, forming macroscopic mat.	Cyanobacteria	n.a.	n.a.

Note: n.a. = not applicable

4.1.1 Phylogeny analysis

Scenedesmus sp. A and *Scenedesmus* sp. B sequences were omitted from the phylogenetic analysis because of *Scenedesmus* sp. A sequence was only partially complete and *Scenedesmus* sp. B sequence failed to conform to the secondary structure screening prior to the phylogeny analysis, which was probably due to the presence of pseudogene. Therefore, only two SSU rDNA sequences were subjected to phylogenetic analysis, i.e. *Ankistrodesmus* sp. (Strain AB5_C1) and *Neochloris* sp. (BRC_C1). The SSU dataset yielded 1629 characters, with 368 parsimony informative characters. Generally, the phylogenetic trees revealed strongly supported monophyletic lineages for both *Ankistrodesmus* sp. and *Neochloris* sp. with their closest species (Figure 4.2). *Ankistrodesmus* sp. (AB5_C1) claded with *A. fusiformis* Corda with MP/ML/BI bootstrap and posterior probability of 99/100/1.00 while *Neochloris* sp. (BRC_C1) claded with *N. conjuncta* Archibald with 100 bootstrap in MP/ML and 1.00 posterior probability in BI. Based on the morphological observation and supporting evidence from molecular data, the identity of both AB5_C1 and BRC_C1 were *Ankistrodesmus* sp. and *Neochloris* sp.

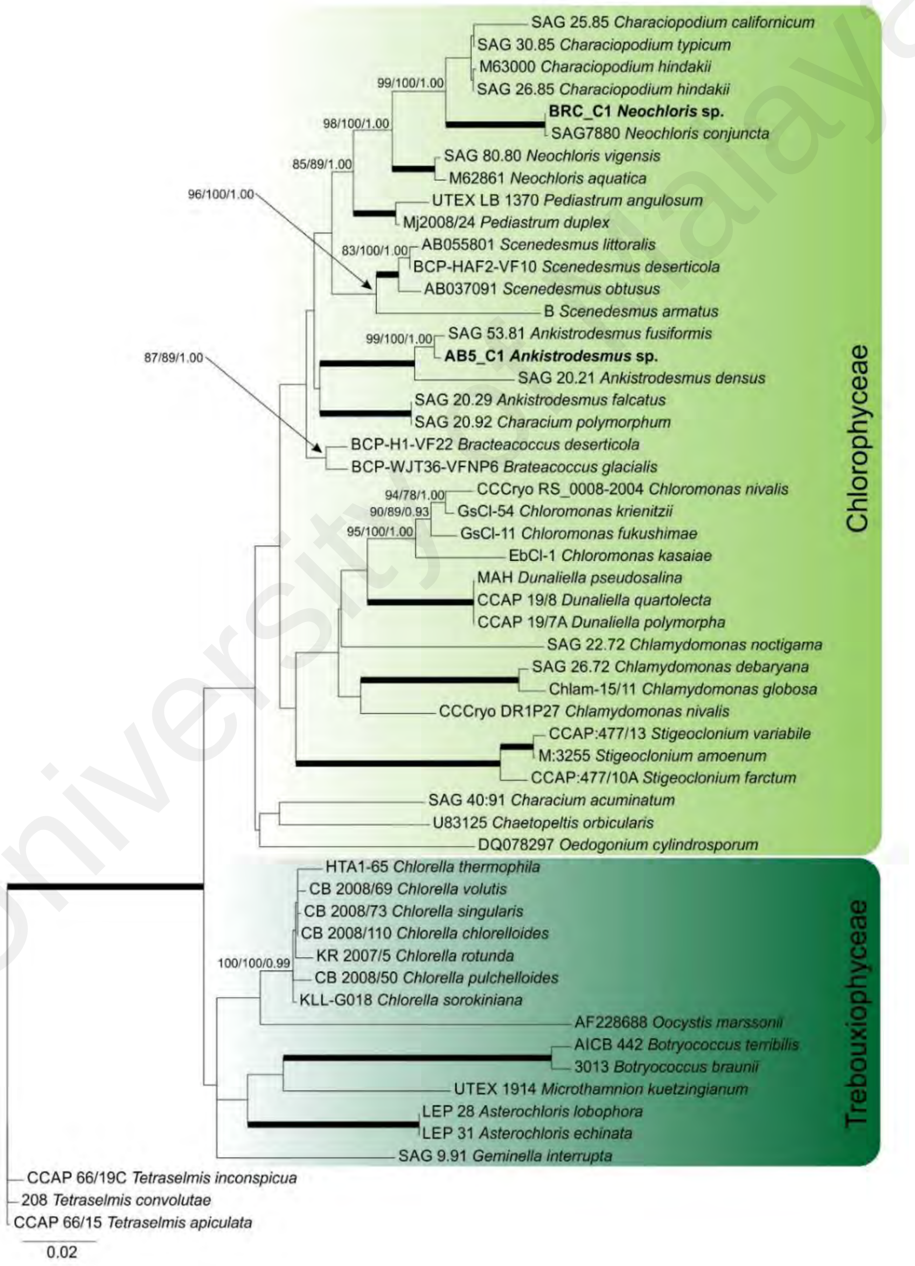

Figure 4.2: Phylogenetic tree inferred from MP/ML/BI based on 18S rDNA

4.2 Growth, biomass productivity, and oil yield

This section presents the results obtained from the growth, biomass productivity and oil yield investigation of the isolated microalgae and the two purchased species with the accompanying discussion. Figure 4.3 depicts the growth for the isolated strains *Ankistrodesmus* sp., *Neochloris* sp., *Scenedesmus* sp. A, *Scenedesmus* sp. B. and the two purchased strains *Chlorella* sp. and *Haematococcus* sp. Three of the isolated strains have shown a lag phase of about 8 to 10 days before entering into exponential growth except for *Neochloris* sp., which was at Day 14. In comparison, the two purchased strains were shown to have a longer lag phase where *Chlorella* sp. only entered exponential phase on Day 20, while for *Haematococcu*s sp., was even slower, only on Day 24.

Among all the microalgae (Table 4.2), *Chlorella* sp. has recorded the highest specific growth rate of 0.186 day^{-1} that was more than double the specific growth rate of *Scenedesmus* sp. A and *Neochloris* sp. *Ankistrodesmus* sp. was second highest at 0.185 day^{-1}. In comparison, the *Scenedesmus* sp. tested by Kim et al. (2017) exhibited a higher specific growth rate of 2.600 day^{-1} in effluent but only at 0.410 day^{-1} if cultured in BG11 media. These observations indicate that media manipulation is an important factor affecting the specific growth rate of microalgae. Further, among all the tested species, *Ankistrodesmus* sp. attained the highest maximum biomass productivity at 4.40 gL^{-1}day^{-1} followed by *Neochloris* sp. *Scenedesmus* sp. B, *Scenedesmus* sp. A., *Chlorella* sp. and, finally *Haematococcus* sp. The highest density attained among all the species was at 6.9 gL^{-1} by *Ankistrodesmus* sp. at Day 27, followed by *Chlorella* sp. at 6.8 gL^{-1} at Day 32 and among all the species, *Haematococcus* sp. was the lowest performer in term of biomass productivity.

Ankistrodesmus sp. also attained the highest lipid yield at 4 % (w/w) dry weight among all the species tested, *Chlorella* sp. was at the second place with 3.3% (w/w) dry weight.

However, the value attained was much lower than the *Ankistrodesmus* sp. reported in (Griffiths et al., 2012) that reached 12 % and 30 % (w/w) dry weight in nitrogen replete and limited states. This is because, under normal growth condition, microalgae will only accumulate a very small amount of neutral lipid but will start to accumulate lipid when subjected to environmental and nutrient stresses.

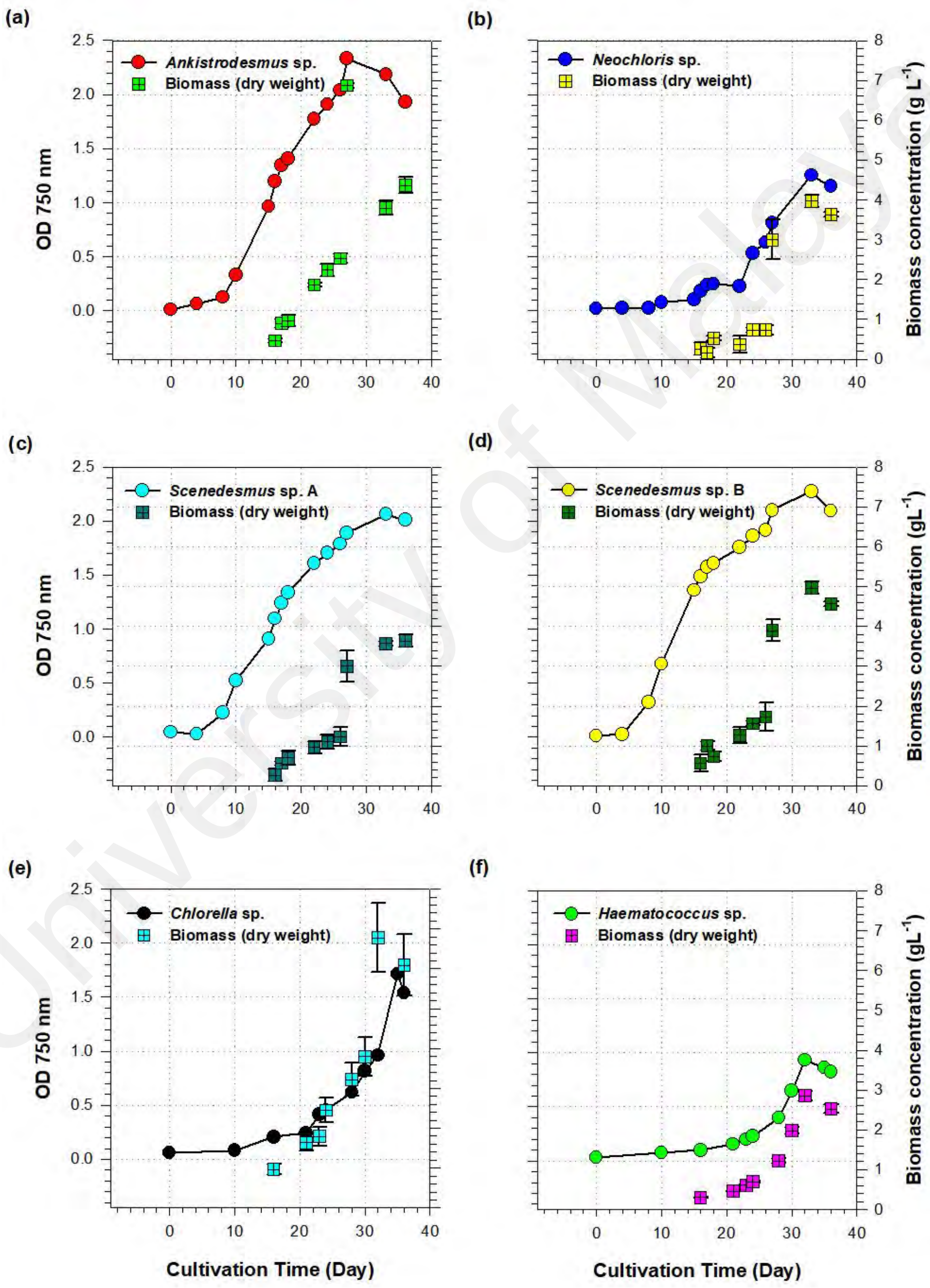

Figure 4.3: Growth and productivity of microalgae strains: (a) *Ankistrodesmus* sp., (b) *Neochloris* sp., (c) *Scenedesmus* sp. A, (d) *Scenedesmus* sp. B., (e) *Chlorella* sp. and (f) *Haematococcus* sp.

Overall, the lipid yield for all tested microalgae in this study (Table 4.2) was much lower than the maximum lipid yield of 75wt % as reported for the microalgae *Botryococcus braunii* (Chisti, 2007). Further, research has found that the lipid content between species is highly variable (Table 4.2) and can ranged between the 1.5 to 75% (D'Alessandro & Antoniosi Filho, 2016; Enamala et al., 2018). The same species from different locations (origin) may exhibit different lipid contents and different ability to adapt (tolerance level) to an environment (Teoh et al., 2013). Furthermore, in some of these experiments, some of the microalgae were subjected to environmental and nutrient manipulation to induce maximum growth and lipid accumulation (Abomohra et al., 2017; Griffiths et al., 2012; Ren et al., 2013). For example, the lipid content for the *Chlorella* sp. cultured under nitrate-deprived condition was 21.8% compared with under normal BG11 medium at 11.5% (Anto et al., 2019). In another study on *Scenedesmus* sp., the complete removal of nitrate has resulted in the highest lipid accumulation of 27.93% compared with under nitrate-limiting conditions, however, the microalgae's biomass content has also significantly reduced with the decrease in nitrate concentrations (Pancha et al., 2014). In another study by Poonam Singh et al. (2015), nitrogen stress has caused more than 50% drop of biomass productivity of *Ankistrodemus falcutus* (0.124 $gL^{-1}d^{-1}$) compared with the biomass productivity attained in BG11 (control) at 0.252 $gL^{-1}d^{-1}$.

Different types stress like salinity, temperature, and irradiance is used to induce lipid besides nutrient stress. For example, in a study of *Scenedesmus* sp., the cultivation in 400 nM of NaCl resulted in the highest lipid content of 33.13% compared with the control culture (BG11) at 18.98%, additionally, salinity stress at 400 nM also resulted in the increase of neutral lipid content reaching 76% of total lipid (Pancha et al., 2015). However, at the same time, the biomass productivity was significantly reduced. These observations show that lipid accumulation is induced at the expense of cell growth when stress is introduced. Cell growth is compromised when microalgae start to accumulate lipid as carbon and energy storage during nutrient starvation (Goh et al., 2019). The chloroplast will starts to disintegrate, causing a negative effect on photosynthesis, protein synthesis and cell divisions (Sun & Zerges, 2015). T. Li et al. (2015) revealed that starch and lipid accumulation in *Chlorella sorokiniana* is regulated by nitrogen levels and the exposure to prolonged nitrogen starvation will cause all available carbon and starch (from chlorophyll) to be converted into lipid and the space previously occupied by the plastid and chlorophyll will be used to store the new lipid bodies. Considering the damaging effect of nutrient starvation (for lipid accumulation) on biomass productivity, a two-phase cultivation regime has been proposed (Goh et al., 2019; Nagappan et al., 2019; Pancha et al., 2015), the first phase is implemented for maximum microalgae biomass cultivation and the second phase is to induce lipid accumulation, this could prevent the loss of biomass.

In this study*,* *Chlorella* sp. was selected over *Ankistrodesmus* sp. as feedstock for biolubricant production though both exhibited comparable growth rate and lipid yield that were higher than other tested species. *Chlorella* sp. was chosen based on its lipid composition and Section 4.3 will details the effect of lipid composition on a biolubricant's lubricity. On the other hand, another important variable to consider is the extraction solvent, which will be discussed in the next section.

Table 4.2: Comparison of growth rate, biomass productivity and lipid yield for microalgae cultivated in different type of cultivation media

Species	Specific growth rate, μ (day^{-1})	Biomass productivity, P (gL^{-1}day^{-1}, d.wt)	Biomass concentration (gL^{-1}, d.wt)	Culturing media	Extracted Lipid (w/w%, d.wt)	Extraction solvent	References
Ankistrodesmus sp.	0.185	4.4*	6.9**	BBM	4.0	Petroleum ether	This study
Neochloris sp.	0.085	2.3*	4.0**	BBM	1.4	Petroleum ether	This study
Scenedesmus sp. A	0.086	1.6*	3.6**	BBM	0.3	Petroleum ether	This study
Scenedesmus sp. B	0.104	2.2*	5.0**	BBM	1.3	Petroleum ether	This study
Chlorella sp.	0.186	1.49*	6.8**	BBM	3.3	Petroleum ether	This study
Haematococcus sp.	0.177	0.44*	2.9**	BBM	n.a.	n.a.	This study
Chlorella sp.	n.a.	n.a.	1.1	BBM	11.5	chloroform: methanol (2:1)	(Chi et al., 2019)
Chlorella vulgaris	0.30	0.0409	n.a.	Domestic waste water	32.7	chloroform: methanol (1:2)	(M. K. Lam et al., 2017)
Chlorella sp.	n.a.	0.046	n.a.	BG11	11.5	chloroform: methanol (2:1)	(Anto et al., 2019)
	n.a.	n.a.	n.a.	nitrate starvation	21.8		
	n.a.	n.a..	n.a.	phosphate starvation	13.9		
Chlorella sp.	n.a.	0.184 – 2.888	n.a.	Livestock waste compost 500-2680 mgL^{-1} COD	33.9 – 44.3	methanol: 10% DMSO: diethyl ether: hexane: water (1:1:1:1:1)	(Zhu et al., 2017)

Table 4.2, continued

Chlorella vulgaris UTEX	n.a.	0.078	1.167	Treated wastewater	25.7	Hydrolyzed with hydrochloric acid followed by Isopropanol: Hexane	(Fernández-Linares et al., 2017)
	n.a.	n.a.	2.250	Treated wastewater + fertilizer (high N)	8.73		
Chlorella vulgaris CICESE	n.a.	0.105	1.575	Treated wastewater	23.4	Hydrolyzed with hydrochloric acid followed by Isopropanol: Hexane	(Fernández-Linares et al., 2017)
	n.a.	n.a.	1.965	Treated wastewater + fertilizer (high N)	13.04		
Ankistrodesmus falcatus KJ671624	0.62	0.253	3.540	BG11	23.3	Microwave assisted chloroform: methanol (2:1)	(Poonam Singh et al., 2015)
	0.42	0.124	1.740	nitrogen starvation	59.6		
Ankistrodesmus falcatus	0.04	n.a.	n.a.	BBM	29.17	Ultrasonicated using chloroform: methanol (1:2)	(George et al., 2014)
	0.09	n.a.	n.a.	BG11	35		
	n.a.	n.a.	n.a.	CHU-10	~40		
	0.20	n.a.	n.a.	Zarrouk's Medium	67.15		
Neochloris aquatic SJ-1	n.a.	n.a.	n.a.	BG11	12	Ultrasonicated using chloroform: methanol (1:2)	(Jaiswar et al., 2017)
Scenedesmus sp. CCNM 1077	n.a.	n.a.	n.a.	BG11	n.a.	Ultrasonicated using chloroform: methanol (1:2)	(Pancha et al., 2014)
	n.a.	~0.550	n.a.	NO_3 rich (247 mg/L)	18.87		
	n.a.	0.333	n.a.	NO_3 starvation (0 mg/L)	27.93		

Table 4.2, continued

Scenedesmus sp. ESP 05	n.a.	0.187	2.61	BG11	30.35	Direct transesterification (FAME content)	(Tan et al., 2016)
	n.a.	0.170	1.36	BBM	35.29		
Scenedesmus sp. ESP 07	n.a.	0.187	2.43	BG11	23.41	Direct transesterification (FAME content)	(Tan et al., 2016)
	n.a.	0.154	0.92	BBM	16.93		

Note: * = Maximum biomass productivity, ** = Maximum biomass concentration, n.a. = not available.

4.2.1 Comparative study of extraction using different solvent

Figure 4.4 shows the lipid yield of using different extraction solvents. When 5g of *Ankistrodesmus* sp. was extracted with C: M (2:1), 68 % lipid yield was obtained compared with using petroleum ether where only 4 % yield was obtained. Studies have shown that under normal optimum growth condition, the amount of neutral lipid produced by microalgae is very little where generally polar lipid are bound in the chloroplast membrane as glycolipid (Goh et al., 2019). Since non-polar solvent can only extract non-polar compound, in this case, a low lipid yield was expected. Among all the tested solvent, hexane gave the least yield at 10 %. Based on our results, solvent selection is one of the important variables to consider for maximum lipid extraction where similar findings were also reported by other researchers (Wu et al., 2017; H.-Y. Yang et al., 2017). As most of the lipid in our study are glycolipid (polar lipid), thus a mixture of both polar and non-polar solvents will extract both polar and non-polar lipid more effectively.

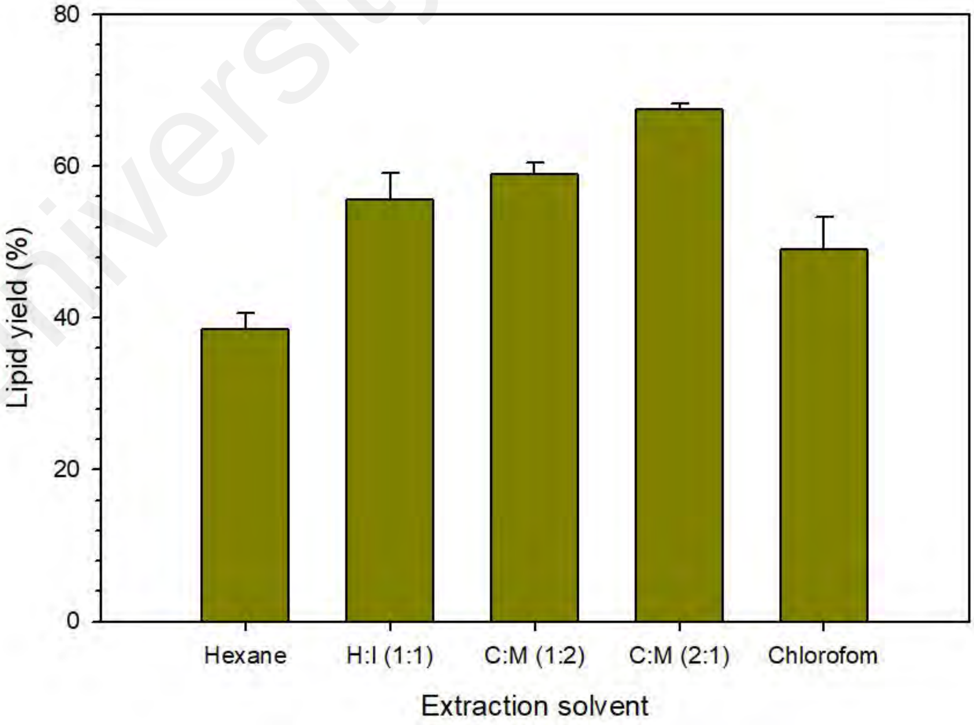

Figure 4.4: Lipid yield using different extraction solvent

4.3 Microalgae fatty acid composition and its effect on lubricity

Table 4.3 tabulates the fatty acid compositions of the microalgae, edible and nonedible vegetable oil. Results have revealed that all the tested microalgae contained high percentage of long chain fatty acids (13-21 carbons) reaching more than 80% of their total composition except for *Chlorella* sp.. Different microalgae species were dominated by a different type of fatty acids, for example, *Scenedesmus* sp. B has the highest amount of palmitoleic acid (C16:1) at 29%, *Heamatococcus* sp. with 29% of palmitic acid (C16:0) and *Neochloris* sp. with 39.2% of α-linolenic acid (18:3). On the other hand, linoleic acid (C18:2), was the major fatty acid found in *Cyanosarcina* sp. and *Ankistrodesmus* sp, at 19 and 33.1% respectively. Lastly, *Chorella* sp. has a high composition of fatty acids with four or more double bonds (collectively at 55.6%) like docosahexaenoic acid (C22:6n3, DHA) and arachidonic acid (C20:4n6, ARA). It is revealed that both DHA and ARA can independently fulfilled the dietary essential fatty acid requirements (Anez-Bustillos et al., 2018). Furthermore, the fatty acid compositions also revealed that unsaturated fatty acid, i.e. monounsaturated fatty acid (MUFA) and polyunsaturated fatty acid (PUFA) made up the dominant compounds (Figure 4.6) found in all the tested microalgae. The presence of high amount of MUFA and PUFA may negatively affect the oxidation stability of a biolubricant, yet it will provide good cold weather performance, therefore some properties trade-off are necessary.

Ester-based biolubricant's properties are affected by the physical and chemical structures of the compounds it constitute (Biresaw et al., 2003; Quinchia et al., 2012; Syahir et al., 2017), consequently by knowing what type of fatty acids an ester constitute, some critical parameters can be estimated. In addition, given that lubricity is affected by the fatty acids and microalgae-based biolubricant is also triglyceride-based, the same characteristics, namely, carbon chain length, chain branching, unsaturation, and polarity will also be applied and will be covered in Sections 4.3.1, 4.3.2 and 4.3.1.

Table 4.3: Fatty acids compositions of microalgae, edible and nonedible vegetable oil

Fatty acid	*Cyanosaarcina* sp. *	*Neochloris* sp. *	*Ankistrodesmus* sp. *	*Scenedesmus* sp. A *	*Scenedesmus* sp. B *	*Chlorella* sp. *	*Haematococcus* sp.^{a}	*Callophyllum*^{b}	Pongamia^{c}	Jatropha^{b}	Coconut^{d}	Sunflower^{e}	Soybean^{e}	Rapeseed^{f}	Palm^{g}	Corn^{h}	Olive^{h}	Safflower^{h}
C8:0	0.2	-	-	-	-	-	-	-	-	-	9.5	-	-	-	-	-	-	-
C10:0	0.3	0.2	-	-	-	-	-	-	-	-	4.5	-	-	-	-	-	-	-
C11:0	-	0.3	-	1.2	0.5	-	-	-	-	-	-	-	-	-	-	-	-	-
C12:0	5.5	-	0.2	0.2	0.1	-	0.1	-	-	-	51	-	-	-	0.5	-	-	-
C13:0	-	1.1	11.3	23.8	4.1	-	-	-	-	-	-	-	-	-	-	-	-	-
C14:0	7.1	0.8	1.7	0.7	1.4	1.7	0.5	-	-	1.4	18.5	-	-	-	1.2	-	-	0.1
C15:0	0.6	0.3	0.3	10.4	2.0	-	-	-	-	-	-	-	-	-	-	-	-	-
C16:0	0.7	5.9	7.7	0.6	2.9	1.3	29.0	17.9	10.6	15.6	7.5	6.2	11.3	4.8	47.9	12.2	13.7	6.5
C17:0	8.6	-	-	-	-	3.1	0.2	-	-	-	-	-	-	-	-	-	-	-
C18:0	5.7	0.1	0.3	-	0.3	1.0	2.1	18.5	6.8	9.7	3	2.2	2.7	1.8	4.2	2.2	2.5	2.4
C20:0	2.0	-	-	-	-	0.7	0.6	-	4.1	0.4	-	-	-	1.7	0.3	0.1	0.9	0.2
C21:0	1.7	-	-	-	-	-	-	-	-	-	-	-	-	-	-	-	-	-
C22:0	-	2.3	0.7	0.8	10.2	-	0.4	-	5.3	-	-	-	-	-	-	-	-	-
C24:0	-	0.1	1.4	-	0.5	4.5	0.2	2.6	2.4	-	-	-	-	-	-	-	-	-
C14:1	2.2	0.9	0.4	0.5	0.2	-	-	-	-	-	-	-	-	-	-	-	-	-
C15:1	1.2	0.6	0.4	0.7	0.3	12.4	-	-	-	-	-	-	-	-	-	-	-	-
C16:1	25.5	20.2	25.8	23.0	29.0	2.5	0.6	2.5	-	-	-	-	-	-	-	0.1	1.2	-
C17:1	4.8	3.5	0.9	0.4	5.8	2.6	1.3	-	-	-	-	-	-	-	-	-	-	-
C18:1	12.1	1.3	4.5	14.9	10.7	0.7	25.9	42.7	49.4	40.8	5	26.1	24.4	62.7	37	27.5	71.1	13.1
C20:1	0.4	0.8	1.1	0.6	0.7	-	0.3	-	2.4	-	-	-	-	-	-	-	-	-
C22:1	0.4	-	-	-	0.5	-	-	-	-	-	-	-	-	1	-	-	-	-

Table 4.3, continued

C24:1	-	-	-	-	-	0.8	-	-	-	-	-	-	-	-	-	-	-	-
C18:2	19.0	20.2	33.1	19.4	23.8	7.4	20.8	13.7	19	32.1	1	65.5	56.3	19.5	9.1	57	10	77.7
C20:2	0.2	-	-	-	1.6	-	1.2	-	-	-	-	-	-	-	-	-	-	-
C22:2	-	-	0.1	-	0.1	-	-	-	-	-	-	-	-	-	-	-	-	-
C18:3	0.5	39.2	5.2	2.3	2.7	2.3	12.8	2.1	-	-	-	-	5.3	8.6	0.3	0.9	0.6	-
C20:3n3	0.5	2.2	5.1	0.8	2.9	3.3	0.5	-	-	-	-	-	-	-	-	-	-	-
≥4 db	0.8	-	-	-	-	55.6	3.4	-	-	-	-	-	-	-	-	-	-	-

Note: "-" = not detected, "⩾ 4 db" = more or equal to 4 double bonds, * = in this study, [a] citing (Lorenz, 1999), [b] citing (Bringi, 1987), [c] citing (A. Kumar & Sharma, 2011), [d] citing (Jayadas & Nair, 2006), [e] citing (Quinchia et al., 2012), [f] citing (Gryglewicz et al., 2003), [g] citing (Crabbe et al., 2001), and [h] citing (Hasenhuettl, 2000).

4.3.1 Impact of carbon chain length

Carbon-chain length affects the adsorbed film thickness; and as mentioned in the previous section, longer chain contributes to better boundary friction coefficient due to the thicker molecular barrier that formed between the rubbing metals (A. Adhvaryu et al., 2004; Askwith et al., 1966; M. S. Reddy et al., 2016).

In this study, long chain length, with 13-21 carbons, is the main component in all tested microalgae (more than 80% of the total composition) with the exception of *Chlorella* sp. (Figure 4.5). Compared with other tested species, *Chlorella* sp. was composed of Very Long Chain Fatty Acid, VLCFA (> 21 carbons) and Long Chain Fatty Acid, LCFA (13-21 carbons) at 37 and 63% respectively. The high composition of very long and long chain fatty acids indicates that *Chlorella* sp.'s fatty acids are capable of forming a thicker and denser lubricating film compared with other tested species, suggesting better lubricity performance.

In addition, most of the common biolubricant feedstock is also comprised of long chain fatty acids as the dominant component of their compositions; refer to Table 4.3 (Cavalcanti et al., 2018; K. V. Fernandes et al., 2018). Moreover, G.W. Stachowiak& Batchelor (2005) proposed that for effective lubrication, the chain length must consists of a minimum of nine carbons.

In a lubricity study that involved of rice bran, sunflower and coconut oil, the coefficient of friction (COF) of rice bran and sunflower were found to be lower than that of coconut oil (Rani et al., 2015). The COF was reduced 28 and 41%, respectively. Based on the fatty acid composition analysis, rice bran and sunflower oil contained a high percentage of C18 carbon chain; whereas coconut oil was, consisted of shorter chains of C8-C16, with C12 as the dominant component. Consequently, the lubricating film formed by the coconut oil (from shorter carbon chains) would be thinner that the lubricating film formed by the rice bran and sunflower oil, evidenced by the higher COF observed for coconut oil compared with the two other. Accordingly, from the chain length factor, it can be deduced that microalgae oil in this study is capable of imparting good lubricity.

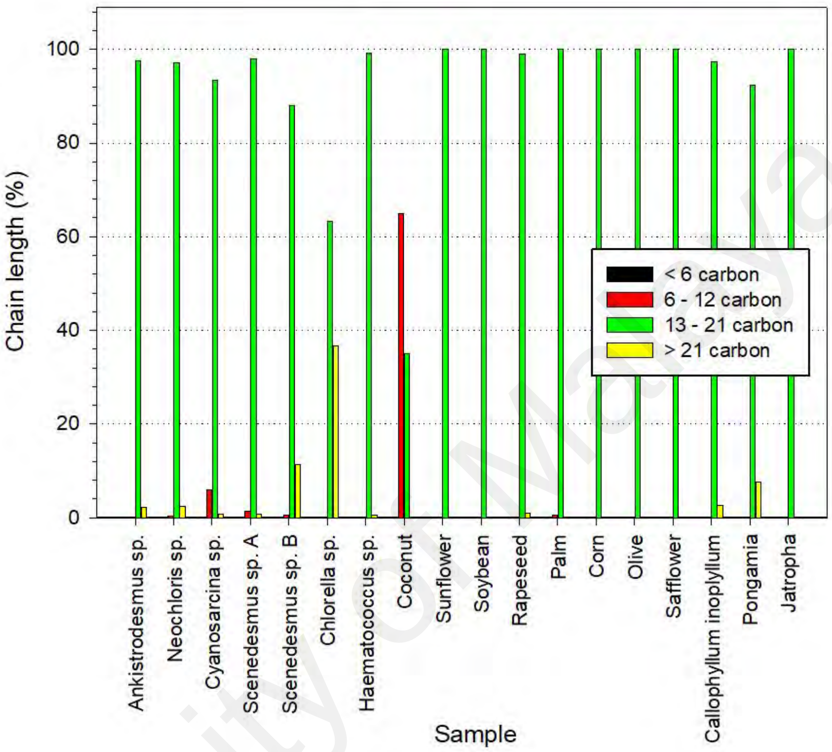

Figure 4.5: Chain length distributions of microalgae, edible and nonedible vegetable oil

4.3.2 Impact of unsaturation

In section 2.6.2, the degree of unsaturation has been identified as one of the factors affecting biolubricant lubricity. The fatty acid unsaturation, due to the forming of isomers have prevented the close packing of fatty acids in a lubricating film, and that, weaken the formed molecular barrier (Fox et al., 2004). In this study, the unsaturated fatty acids, i.e. monounsaturated fatty acid (MUFA) and polyunsaturated fatty acid (PUFA) were the dominant compounds found in the microalgae. This may suggest that the lubricating film formed will be less sturdy than species with a higher percentage of straight saturated fatty acids.

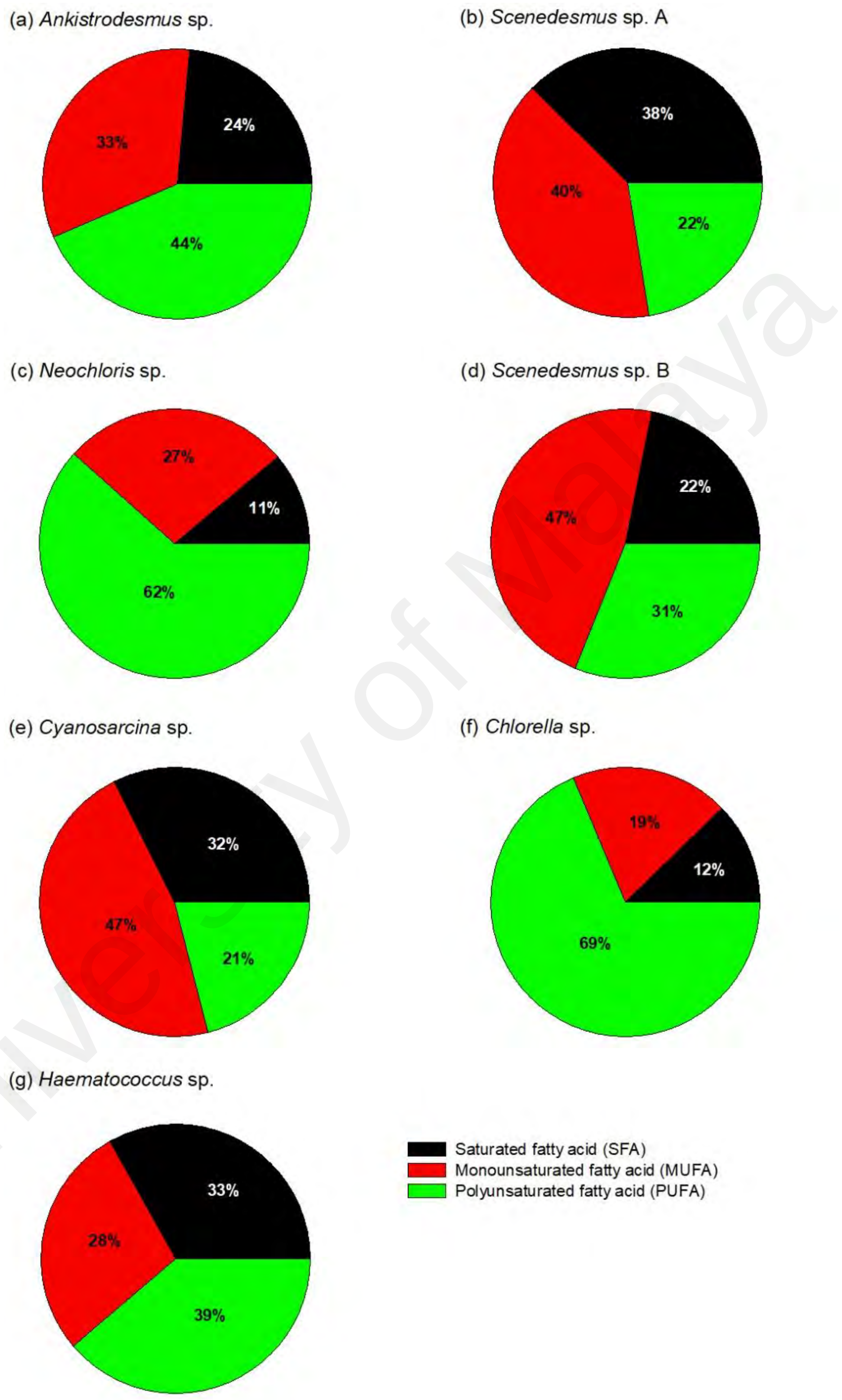

Figure 4.6: Microalgae fatty acid composition distributions

For biolubricant application, chemical modification can be employed to counter the limitation caused by the high degree of unsaturation. These molecules can be chemically modified to reduce the unsaturation in cases where the excessive unsaturation are causing the deterioration of oxidation stability that shortened the lubricant shelf life. For example, partial hydrogenation has been applied to improve the oxidation stability of biodiesel (McNutt & He, 2016; Sukjit et al., 2019) without sacrificing too much on properties attributed to unsaturation. This is because unsaturation contributes to the low-temperature performance of a biolubricant, while a high percentage of saturated fatty acid will lead to poor cloud point (CP), pour point (PP) and cold filter plugging point (CFPP), parameters associated with low temperature usability. Sukjit et al. (2019) reported that partial hydrogenation improved the oxidation of palm biodiesel when the amount of polyunsaturated fatty acids were reduced. Furthermore, the transformation of *cis* mono-unsaturated fatty acid (C18-1 *cis*) into *trans* mono-unsaturated fatty acid (C18:1 *trans*) enhances the lubricity of the biodiesel because the configuration of *trans* isomer enabled the formation of a denser and stable tribofilm compared with the *cis* isomer, which was indicated by the reduction of wear. Nonetheless, in the health supplement industry, microalgae are highly priced for their PUFA compounds.

4.3.3 Impact of chain branching and polarity

Next, chain branching can be a double-edged sword. Excessive branching disrupts the adhesion of the molecule on the sliding surfaces that leads to the increase of direct metal-to-metal contact (G. Stachowiak & Batchelor, 2013). But at the same time, steric hindrance inhibits the stacking of molecules that prevents the crystallization of molecules at low temperature, therefore improving the low-temperature performance of a biolubricant (Erhan et al., 2006). Further, branching also found to enhance the load carrying capacity of a biolubricant . For microalgae oil, most esters are comprised of straight fatty acids, therefore, just like its vegetable oil counterparts, chemical modifications can be used to improve its quality.

Similar to other vegetable oil based biolubricant, microalgae ester polarity is contributed by the carboxyl group ($-COO^-$) and a non-polar hydrocarbon tail. Stronger lubricating film may be obtained with chemical modifications like epoxidation (Abdullah & Salimon, 2010) and transesterification (McNutt & He, 2016), by substituting some of the functional groups with higher polar species like polyhydric alcohols (pentaerythritol, trimethylolpropane and neopentyl glycol), which contain more than one hydroxyl group (Aziz et al., 2016; Kania et al., 2015). The higher polarity causes the esters to adsorb strongly onto the metal surfaces (which are positively charged) and are less likely to disengage. The subsequent formation of the lubricating film (from the lineup of molecules on the metal surfaces) will prevent direct metal-to-metal contact, contributing to the lubricity of a biolubricant.

4.4 Physicochemical properties of microalgae

The derived physicochemical properties generally used for biodiesel prospecting are used in this study to provide an approximation of the relevant biolubricant properties. Given the good lubricity of biodiesel, it has been proposed to be utilized as an additive to improve the lubricity of petroleum fuel (Ball et al., 1999; Hazrat et al., 2015). Many researchers have found that biodiesel is more effective in imparting lubricity than the neat vegetable oil (Mohd Noor et al., 2018; Van Gerpen et al., 1999). Table 4.4 tabulates the critical biolubricant properties and the corresponding related biodiesel properties. These properties are mostly influenced by the degree of unsaturation of the biolubricant feedstock.

Table 4.4: Critical biolubricant properties and the related biodiesel properties

Biolubricant properties	Related biodiesel properties	Importance and implication	Reference
Viscosity and viscosity index	Kinematic viscosity (KV)	Generally, biodiesel possesses higher viscosity than diesel fuel. The high viscosity leads to poor atomization, incomplete combustion and power loss if used directly in the engine. The different viscosity-temperature characteristics projected by biodiesel could result in higher fuel injection pressures at low engine operating temperatures.	(Knothe et al., 2015; Knothe & Steidley, 2005)
Oxidation stability	Iodine value (IV)	Iodine value (IV) is a measure of total unsaturation that is expressed in grams of iodine added to the double bonds, in 100g of the sample. A higher IV denotes a higher number of double bonds, higher unsaturation. According to EN 14124, the max limit for IV is 120 g I_2/ 100g. Some commercially produced biodiesel such as camelia, soy, and sunflower have exceeded this limit.	(N. Kumar, 2017; Serrano et al., 2013)
Low-temperature performance	Cold filter plugging point (CFPP)	CFPP is the temperature at which the filter starts to plug and begins to crystallize but each temperate country has its own limit due to differences in longitude. It is one of the parameters denoting low-temperature usability beside pour point (PP) and cloud point (CP).	(Smith et al., 2010; Yuan et al., 2017)

In comparison with other edible and nonedible vegetable oil, (Figure 4.7), *Neochloris* sp. and *Chlorella* sp. fatty acid compositions were similar to that of sunflower, soybean, and corn. Meanwhile for *Scenedesmus* sp. B, its lipid composition resembled that of Jatropha. For *Scenedesmus* sp. A and *Cyanosarcina* sp., the fatty acid compositions resembled that of *Calophyllum* and *Pongamia*, respectively.

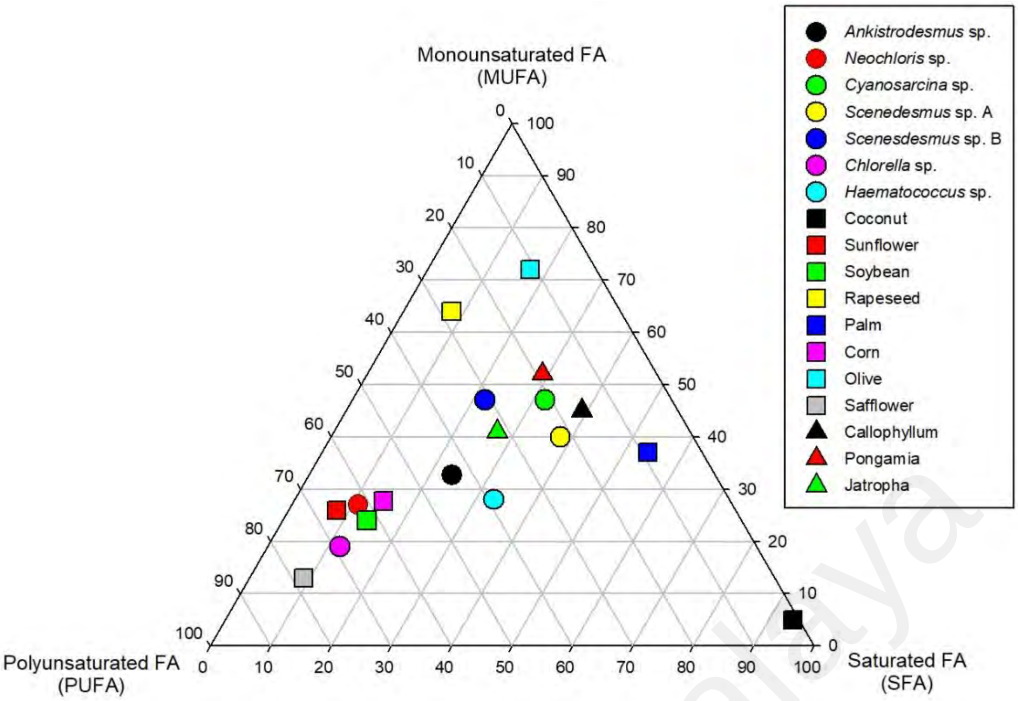

Figure 4.7: Fatty acid composition comparison between microalgae, edible and nonedible vegetable oil

Table 4.5 shows the derived physicochemical properties of microalgae biodiesel in comparison to edible and nonedible biodiesel. The KV for all the tested microalgae fell within the accepted values stipulated for ASTM D6751. The predicted CFPP for all the microalgae, apart from *Haematococcus* sp., were below zero degree Celsius, which is desirable for low-temperature operation. Additionally, the high IV reflected the high unsaturation of *Chlorella* sp. and *Neochloris* sp. Generally, when we compared the properties between microalgae and their nearest biodiesel neighbors (based solely on the fatty acid composition), we found that their KV and IV values were quite similar. However, exceptions were evidenced with *Chlorella* sp. and *Neochloris* sp., as these two species have an exceptionally high percentage of double bonds. Meanwhile, the CFPP values provide a general idea about the low-temperature usability of microalgae biodiesel in comparison with their nearest vegetable oil based neighbors.

Table 4.5: Physicochemical properties of microalgae, edible and nonedible biodiesel

Properties	KV (mm^2/s)	IV ($gI_2/100g$)	CFPP (°C)	Reference
Limit	1.9-6.0	120.0 max	-	ASTM D6751
Callophyllum	5.21	80.5	0	(Silitonga et al., 2016)
Pongamia	4.23	82.5	-2	(Sarin et al., 2009)
Jatropha	4.30	99.0	1	(Sarin et al., 2009)
Coconut	3.12	n.a.	-1	(I. Monirul et al., 2015)
Sunflower	4.20	132.0	-3	(Ramos et al., 2009)
Soybean	4.12	110.9	-5	(de Sousa et al., 2014)
Rapeseed	4.40	109.0	-10	(Ramos et al., 2009)
Palm	4.18	51.22	4	(Silitonga et al., 2016)
Corn	4.14	126.6	−8	(El Boulifi et al., 2010)
Olive	4.50	84.0	-6	(Ramos et al., 2009)
Safflower	4.23	145.0	-9	(Mihaela et al., 2013)
Cyanosarcina sp.	4.2	81.8	-7	In this study
Neochloris sp.	3.66	167.7	-5	In this study
Ankistrodesmus sp.	3.85	113.6	-4	In this study
Scenesdesmus sp. A	3.82	77.7	-8	In this study
Scenedesmus sp. B	4.41	100.7	-6	In this study
Chlorella sp.	3.76	261.9	-7	In this study
Haematococcus sp.	4.43	103.3	7	In this study

Note: n.a. = not available

4.5 Microalgae biolubricant

After evaluating the growth, biomass productivity and lipid yield of all the tested species, *Chlorella* sp. was selected for further testing. This section presents the results and discussion on the oil extraction from *Chlorella* sp. dry biomass and the chemical conversion of crude microalgae oil (CMO) into modified microalgae oil (MMO). The physicochemical properties of CMO and MMO were also investigated.

4.5.1 Crude microalgae oil (CMO) and modified microalgae oil (MMO)

The physicochemical properties of crude microalgae oil (CMO) and modified microalgae oil (MMO) are presented in Table 4.6. CMO was extracted from the selected microalgae *Chlorella* sp. dry biomass. MMO was derived from CMO after acid-catalyzed esterification and alkaline-catalyzed transesterification.

Table 4.6: Physicochemical properties of the CMO and MMO

Properties	Unit	CMO	MMO
Acid value	mg KOH/g	49.688	19.703
Heating value	MJ/kg	27.078	32.939
Total ester content	(m/m)%	n.a.	48.48

Note: n.a. = not available

The CMO yield (CMO extracted from the dry biomass of *Chlorella* sp.) is 70% whereas the MMO yield is 83%, indicating the yield is significantly increased after chemical modification. The physical appearance of the CMO and MMO is almost grease-like. Based on the GC-MS analysis, the MMO is composed of esters, sterols, ketones, peroxides, and ether, as shown in Table 4.7. Cellulose residues such as furan derivatives are also present. Y. Xu, Zheng, et al. (2014) also found that furan derivatives and amino acids were present in the bio oil derived from *Spirulina* sp.. Phytol (which is diterpene alcohol from chlorophyll), as well as plant sterols such as stigmasterol and β-sitosterol, were also present. Phytol is widely used in the cosmetics and food industries because of its aromatic properties. Stigmasterol and β-sitosterol are lucrative secondary metabolites that are marketed as dietary supplements in the nutraceutical industry, owing to their antioxidant and anti-inflammatory properties (Bin Sayeed et al., 2016; Gabay et al., 2010). These oxygen-containing compounds and polyaromatics are natural lubricity enhancers, as indicated by the results of previous studies (Danping & Spikes, 1986; Hughes et al., 2003).

Table 4.7: Main compounds present in the MMO identified from GC-MS analysis

No.	Compound	Molecular formula	Chemical structure	Retention time (min)	% Area
1	Tetrahydrofuran, 2,2-dimethyl-	$C_6H_{12}O$	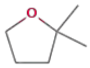	3.771	3.433
2	4-Butoxy-2-butanone	$C_8H_{16}O_2$	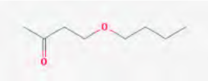	4.069	9.328
3	Hydroperoxide, 1-methylhexyl	$C_7H_{16}O_2$	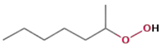	4.341	0.219
4	Hydroperoxide, 1-ethylbutyl	$C_6H_{14}O_2$	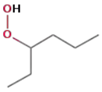	4.446	2.465
5	Hydroperoxide, 1-methylpenthyl	$C_6H_{14}O_2$	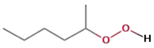	4.612	3.385
6	Cyclopentane, 1-acetyl-1,2-epoxy-	$C_7H_{10}O_2$		4.843	11.873
7	Cyclopropane, 1,1,2,3-tetramethyl-	C_7H_{14}		5.300	0.573
8	Cyclopropane, 1,1,2,2-tetramethyl-	C_7H_{14}		5.482	0.173
9	7,10-Hexadecadienoic acid, methyl ester	$C_{19}H_{34}O_2$	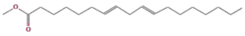	17.969	0.406
10	Hexadecanoic acid, methyl ester	$C_{17}H_{34}O_2$	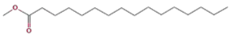	18.348	0.742
11	1-Docosanol, methyl ether	$C_{23}H_{48}O$	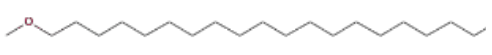	19.702	0.168
12	9,12-Octadecadienoic acid, methyl ester	$C_{19}H_{34}O_2$		20.693	1.094
13	Phytol	$C_{20}H_{40}O$	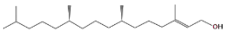	20.951	0.167
14	Heneicosanoic acid, methyl ester	$C_{22}H_{44}O_2$	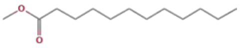	25.586	0.078
15	Stigmasterol	$C_{29}H_{48}O$	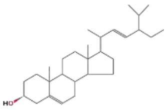	26.793	1.083
16	β-sitosterol	$C_{29}H_{50}O$	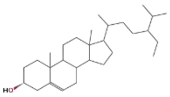	32.147	4.619

The FAME content of MMO determined from GC-FID analysis is presented in Table 4.8. The total ester content of the MMO is 48.48 (m/m)%. The total ester content is primarily composed of polyunsaturated fatty acid methyl esters (68.7%), whereas monounsaturated and saturated fatty acid methyl esters constitute 19.1 and 12.2%, respectively. Geller& Goodrum (2004) found that lubricity is improved as unsaturation increases. In this study, for MMO the total unsaturated fatty acid methyl esters were 87.8%.

Table 4.8: FAME content of the MMO

FAME	Carbon structure	(m/m)%
Methyl myristate	C14:0	0.80
Methyl palmitate	C16:0	0.63
Methyl heptadecanoate	C17:0	1.50
Methyl stearate	C18:0	0.49
Methyl arachidate	C20:0	0.34
Methyl lignocerate	C24:0	2.18
cis-10-Pentadecenoic acid methyl ester	C15:1	6.03
Methyl palmitoleate	C16:1	1.23
cis-10-Heptadecenoic acid methyl ester	C17:1	1.27
cis-9-Octadecenoic acid methyl ester	C18:1n9c	0.34
Methyl nervonate	C24:1	0.37
Linolelaidic acid methyl ester	C18:2n6t	3.60
γ-Linolenic acid methyl ester	C18:3n6c	1.12
cis-8,11,14-Eicosatrienoic acid methyl ester	C20:3n6	0.85
cis-11,14,17-Eicosatrienoic acid methyl ester	C20:3n3	0.75
cis-5,8,11,14-Eicosatetraenoic acid methyl ester	C20:4n6	11.77
cis-4,7,10,13,16,19-Docosahexaenoic acid methyl ester	C22:6n3	15.20

It can be seen from Table 4.6 that the CMO has a very high acid value (49.688 mg KOH/g). However, the acid value is significantly reduced to 19.703 mg KOH/g after acid-catalyzed esterification and alkaline-catalyzed transesterification, which corresponds to a reduction of more than 50%. This indicates that catalytic modification has successfully reduced the acidity of CMO by converting free fatty acids into esters. The acid value reading is still quite high, a buffer solution containing a weak base and its conjugate acid can be applied to further reduce the acidity. The high acid value is not desirable as it causes severe corrosion to engine parts (Fazal et al., 2018) besides affecting the storage stability of ester-based lubricant. The chemical composition of ester changes upon exposure to water and air, and acidic condition that will accelerate the initiation of oxidation (N. Kumar, 2017). Therefore, by lowering the acid value, lubricant storage stability is indirectly prolonged.

In addition, the heating value of the MMO (32.939 MJ/kg) is higher than that for the CMO (27.078 MJ/kg), which indicates that the MMO has higher energy content. Hong et al. (2015) found that the heating value for fatty acid alkyl esters increases with the increase of molecular weight but decreases when the number of double bonds increases. In this study, the lubricant's molecular weight may have increased when a hydrogen (H) from carboxylic acid was replaced with a methyl group (CH_3) during acid-catalyzed esterification.

Figure 4.8 shows the FTIR spectra of the CMO and MMO. The broad peak at 3550–3200 cm^{-1} is ascribed to the alcohol hydroxyl group (O–H), which is present in both CMO and MMO. It can be observed from the FTIR spectra that the broad carboxylic acid O–H stretch at 3300-2500 cm^{-1} has reduced in intensity after the chemical modification. At the same time, the peak at 1059 cm^{-1} (CMO) assigns to C−O stretching has shifted to 1025 cm^{-1} (MMO) after the chemical reaction. The peak intensity has increased from 0.20A to 0.34A. This is due to the increase of C−O bond from the R group during esterification when H from the carboxylic acid group (–COOH) is substituted with carbon from CH_3, forming ester (-COOR).

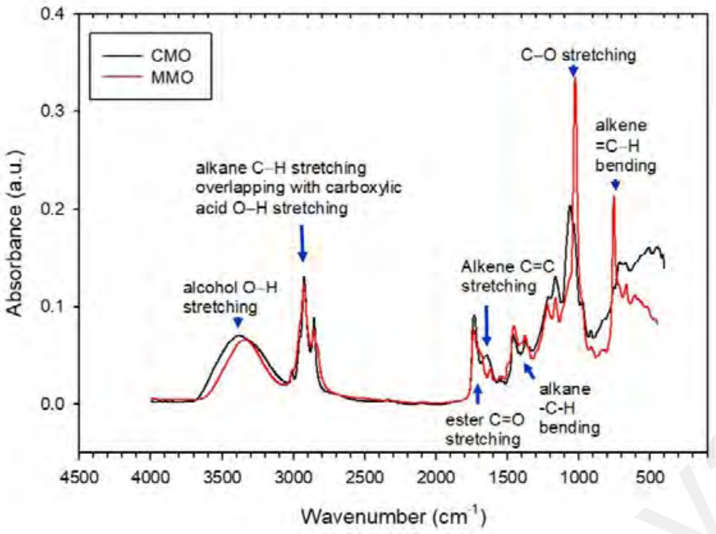

Figure 4.8: FTIR spectra of the CMO and MMO

Further, the prominent peak at 1732 cm^{-1} (conjugated ester C=O stretch) for the CMO has shifted to 1734 cm^{-1} due to the steric effect of alkyl group after chemical reaction (Y. Xu, Zheng, et al., 2014). In addition, a strong peak at 754 cm^{-1} ascribed to the =C−H bending has appeared after the acid-catalyzed esterification and alkaline-catalyzed transesterification. All of these observations demonstrate that free fatty acids have been converted successfully into FAMEs and increase in lubricity is expected when more of the free fatty acids are converted into esters providing more functional groups for the formation of the lubricating film.

4.6 Tribological performance of MMO

Following the properties prediction of MMO as potential biolubricant and coupled with the understanding that natural triglycerides (vegetable oil and animal fats) enhances lubricity by providing an effective boundary layer through the adsorption of polar constituent on metal surfaces that separates the rubbing surfaces (Biresaw et al., 2003;

Habibullah et al., 2015; Hazrat et al., 2015; Zulkifli et al., 2016). This section investigates the actual tribological performance of MMO, both as a biolubricant and as an additive in diesel and a commercial full synthetic lubricant. Figure 4.9 illustrates the overview of all the tribological analysis conducted on MMO.

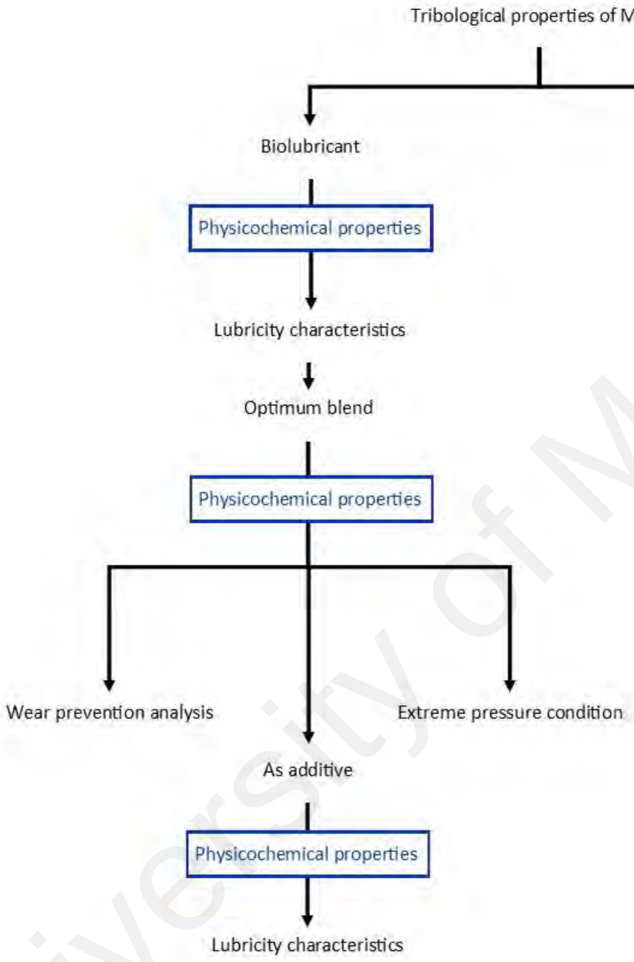

Figure 4.9: Tribological analysis conducted in this study

4.6.1 Lubricity of MMO as biolubricant

This section investigates the performance of MMO as a biolubricant along with the corresponding physicochemical properties.

4.6.1.1 Physicochemical properties MMO blends, PAO and commercial full synthetic lubricant (FFL)

The physicochemical properties of the PAO, FFL, and MMO blends are presented in Table 4.9. The density of MMO blends and FFL are almost similar but the dynamic viscosity and kinematic viscosity of MMO blends are generally lower than FFL. Meanwhile, the acid value increases with an increase in the percentage of MMO in the blend. A buffer solution containing a weak base and its conjugate acid can be applied to further reduce the acidity since high acidity is not desirable due to its effect on storage duration (Saber et al., 2016).

Table 4.9: Physicochemical properties of the PAO, FFL, and MMO blends

Lubricant	Dynamic viscosity (mPa.s)	Kinematic viscosity (mm^2/s)	Density at 15 °C (g/cm^3)	Acid value (mg KOH/g)
PAO	54.224	66.185	0.835	0.1794
MMO-1	54.123	66.039	0.835	0.9379
MMO-2	59.687	72.757	0.836	1.0824
MMO-5	58.996	71.495	0.841	3.6244
MMO-10	57.869	69.355	0.850	5.0191
MMO-20	66.156	78.645	0.857	13.6883
FFL	64.216	76.749	0.852	0.2583

4.6.1.2 Friction characteristics

Figure 4.10 shows the average coefficient of friction (COF) of the PAO, FFL, and MMO blends over a test duration of 60 min. Generally, all MMO blends exhibited better COF than pure PAO and FFL. The COF is lower by 2.2–10.1% for blends containing up to 10 (v/v)% of MMO relative to that for PAO. The COF decreased as the MMO percentage increased to up to 10%. Similar observations were also reported by other ester-based lubricants where it is believed that the absorption of the fatty acid hydrocarbon chains through the polar glycerol heads on the rubbing surfaces serves as a lubricating film during sliding motion, which inhibits direct metal-to-metal contact (A. Adhvaryu et al., 2004; Amiril et al., 2018; Zulkifli et al., 2016). The increase of ester content will provides more polar functional groups for the establishment of a stronger and denser lubricating film due to the presence of a higher amount of fatty acids available for close packing against each other. It can be seen in Figure 4.11 that the intensity of the C=O peak increases with an increase in the concentration of esters in the MMO blends. This observation is in agreement with many studies that wear and friction decreases with the increase of biodiesel concentration (Habibullah et al., 2015). On contrary, H. Xiao et al. (2019) found that the impact of soybean biodiesel's concentrations on COF was less remarkable, their results revealed that the COF of steel-steel contacts between biodiesel blends and pure diesel were very similar, at approximate 0.12.

In this study, it can be seen from Figure 4.10 that there is no further improvement in the COF when the amount of MMO in the blend is increased to 20 (v/v)%, which is likely due to tribocorrosion. This may overrides the effectiveness of the lubricating film, considering that MMO-20 has the highest acid value (13.688 mg KOH/g) among all of the lubricants investigated in this study. Tribocorrosion can be described as the surface damage that occurred due to the interaction of mechanical loading and chemical/electrochemical reactions between the various elements of a tribosystem in a corrosive environment (Sankara narayanan, 2012). Surface pitting was visible on MMO-20-lubricated surface (Figure 4.14d). Interestingly, the average COF is similar for PAO and FFL; however, the COF values are higher for these synthetic lubricants compared with those for the MMO blends.

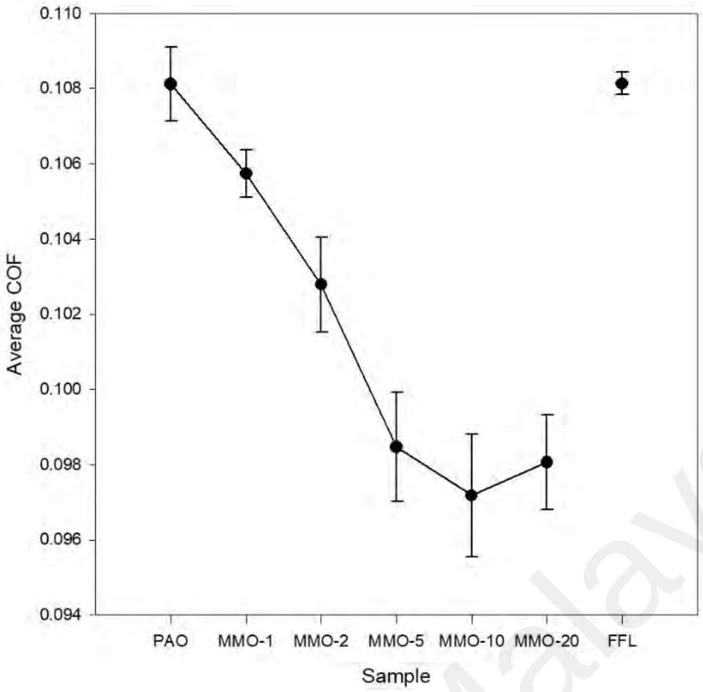

Figure 4.10: Average COF of PAO, FFL, and MMO blends

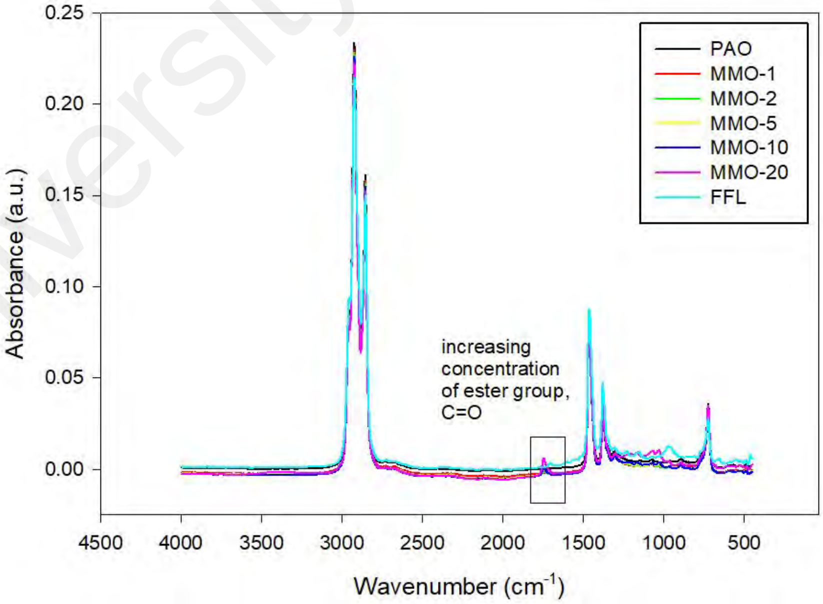

Figure 4.11: FTIR spectra of the MMO blends

Figure 4.12 shows the variation of COF with respect to time for the PAO, FFL, and MMO blends during the tribological test. It can be observed that the COF stabilizes 6-8 min after the start of the tribological test (i.e., run-in phase). The duration of the run-in phase is dependent on the physical, chemical, and geometrical characteristics of the contact surfaces as well as the ability of the lubricant to provide wear protection. Mosarof et al. (2016) also observed a run-in phase with *Calophyllum inophyllum* and palm biodiesel blends in their experiments. They found that the scratchy contact surface contributed to the run-in period and after the removal of the prominent asperities from the contact surfaces, the test ball could rotates smoothly, resulted in stabilized frictions.

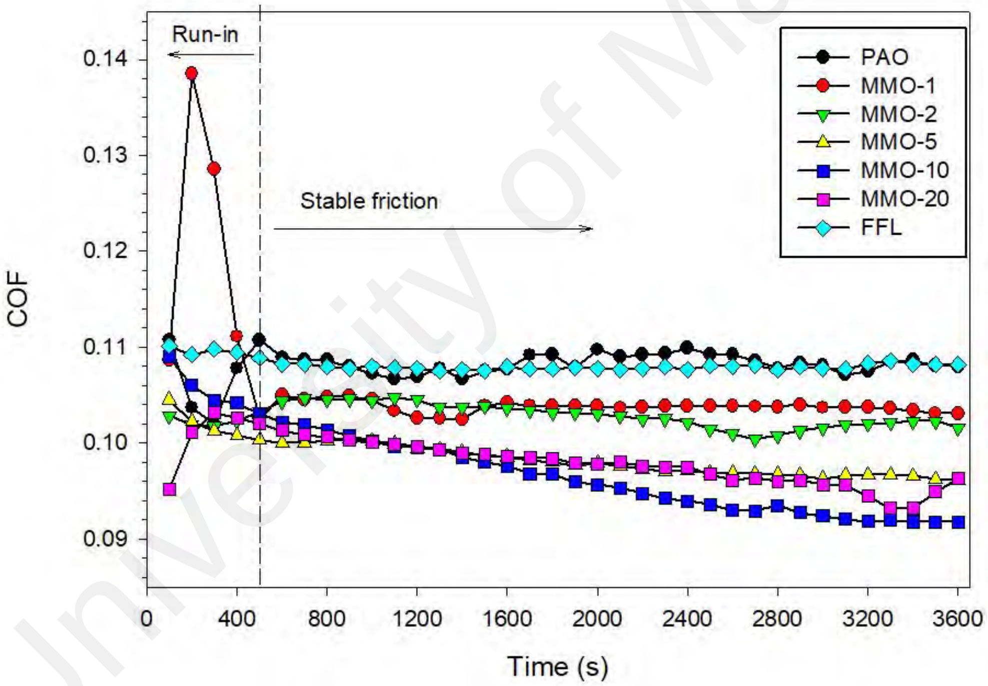

Figure 4.12: Variation of the COF with respect to time for the PAO, FFL, and MMO blends during the tribological test

In this study, it is evident that the FFL demonstrates stable friction characteristics from the start of the tribological test, which is expected because FFLs are typically formulated with friction improvers and dispersant in order to improve dispersion of the lubricants on the contact surfaces. During the stable friction phase, the COF is lower for all MMO blends compared with those for PAO and FFL. According to Habibullah et al. (2015), the presence of more esters provides better scuffing protection on the sliding surfaces. In addition, it can be seen that the COF decreases with respect to time for the MMO-5, MMO-10, and MMO-20 blends. This is expected due to the presence of more functional groups, which improves lubricity.

I. M. Monirul et al. (2016) also reported that the COF decreases gradually with respect to time for all of the tested biodiesel blends except for the pure *Calophyllum inophyllum* blend (CIB100), where the COF only begins to decrease after a certain period. A delay reaction from the fatty acids present in the biodiesel in developing a thin protective film may be have caused it (N. W. M. Zulkifli et al., 2013). Conversely, the results obtained in this study indicate that all of the fatty acids in the MMO blends are readily available to form a lubricating film.

4.6.1.3 Wear characteristics

Figure 4.13 shows the SEM images of wear scar on the rubbed surfaces. It is apparent that there is severe scratching on the PAO-lubricated surface with a series of deep grooves parallel to the sliding direction, which is indicative of abrasive wear. The materials are transferred by ploughing (Figure 4.13b). Additionally, PAO also recorded the highest wear loss and surface roughness among all tested samples (Figure 4.14). The copper color of the wear scar indicates the formation of iron oxide at the rubbing interface. This natural oxide layer that forms when metals are exposed to air is the simplest form of wear protection but they are easily removed, even under light loading (Errichello & Cardis, 2014). Based on the results of the EDS elemental analysis (Table 4.10), the PAO-lubricated surface has the highest oxygen content among all of the tested surfaces.

In contrast, the wear scar width is reduced significantly on the FFL-lubricated surface (Figure 4.13a). The FFL-lubricated surface has a few large pits compared with the PAO-lubricated surface, which has many small pits, considering that the COF is similar for both lubricants. This may be due to anti-wear properties of the FFL, which is a commercial full synthetic lubricant. Typically, anti-wear additive is added to prevent wear by forming a low shear strength tribofilm on the metal surfaces when non-metals such as sulfur and phosphorus react with the exposed metal surfaces (Errichello & Cardis, 2014). Anti-wear additive is designed to be sacrificed first before wear reached the actual metal surfaces (Machinery Lubrication, 2018). Based on the results of the EDS elemental analysis (Table 4.10), phosphorus is detected on the FFL-lubricated surface, indicating that the FFL contains an anti-wear additive. When we compared the wear loss and surface roughness among the entire tested samples, FFL actually recorded the lowest for both (Figure 4.14). This supported the above observation; the formed tribofilm was the first to be worn (sacrificed) prior to the actual metal surfaces, indicated by the reduced wear loss.

Wear is also significantly reduced on the MMO-1-lubricated surface (Figure 4.13c). The wear scar width is 0.23 mm, which is significantly lower compared with that for the PAO-lubricated surface (1.76 mm). Even at higher magnification (500×), it can be observed that only pits are visible and there are no grooves on the surface. Wear is further reduced for the surfaces lubricated with MMO blends containing higher concentrations of MMO where further reductions in wear loss and surface roughness were also recorded, refer Figure 4.14. For instance, only shallow pits are visible on the MMO-5-lubricated surface (Figure 4.13e) and these pits are less apparent on the MMO-10-lubricated surface (Figure 4.13f). Based on the results of the EDS elemental analysis (Table 4.10), the MMO-10-lubricated surface has the lowest oxygen content but the highest carbon content among all of the tested surfaces, indicating that there is a large number of fatty acid chains present to form a lubricating film as well as lower oxidation rate. Adhesive wear is found to be the main mode of wear for the MMO-lubricated surfaces. According to Bhushan (2013), adhesion may have occurred at the asperities which serve as contact sites, which initiates friction or plastic deformation. This will induce pressure and energy at the contact zone. When the pressure and heat increase within the deformed area, greater adhesion will occur between the surfaces causing material transfer, lump built-up and formation of protrusions above the original surface. When these protrusions are sheared by the continual sliding, the sheared fragments detached from one surface and reattached to another surface, the continual cycle will result in galling wear.

On the other hand, the deep pits on the MMO-20-lubricated surface (Figure 4.13g) are likely caused by tribocorrosion, considering that the MMO-20 blend has the highest acid value among all of the lubricants tested in this study. Further, the COF is slightly higher for MMO-20 compared with that for MMO-10, though the COF is similar to that for MMO-5.

Table 4.10 shows elemental composition of the lubricated surfaces after the tribological test. The presence of carbon and oxygen on the MMO blend-lubricated surfaces indicate that the polar long chain fatty acid compounds are physically adsorbed onto the oxide layers on the metal surfaces, forming a lubricating film that reduces friction and wear. Carbon is not detected on the PAO-lubricated surface, which suggests that there are no polar heads for metal surface attachment.

	Magnification: 20x	Magnification: 500x	Magnification: 3500x
(a) FFL			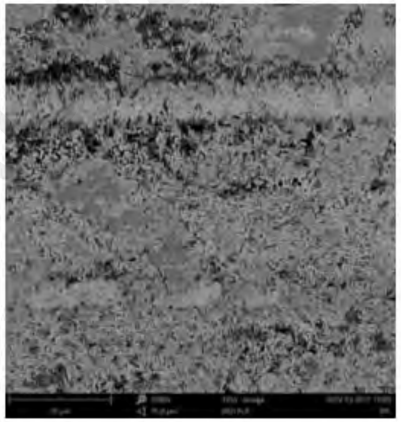
(b) PAO	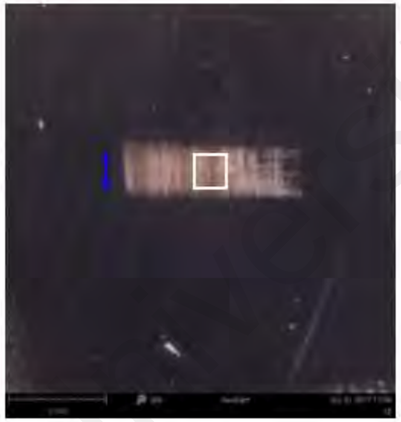	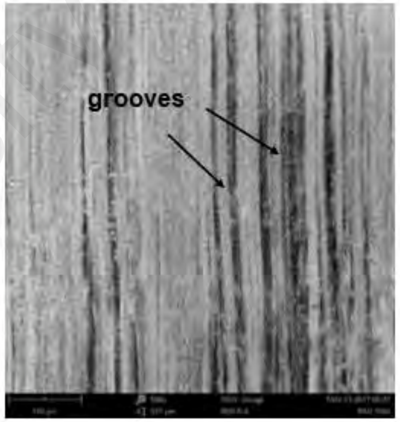	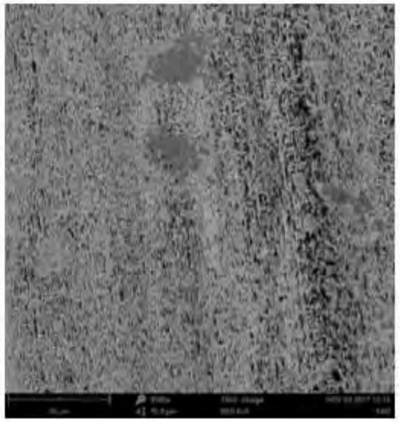

Figure 4.13: SEM images (magnification: 20×, 500×, and 3500×) of the carbon steel plate surfaces lubricated with (a) PAO, (b) FFL, (c) MMO-1, (d) MMO-2, (e) MMO-5, (f) MMO-10, and (g) MMO-20

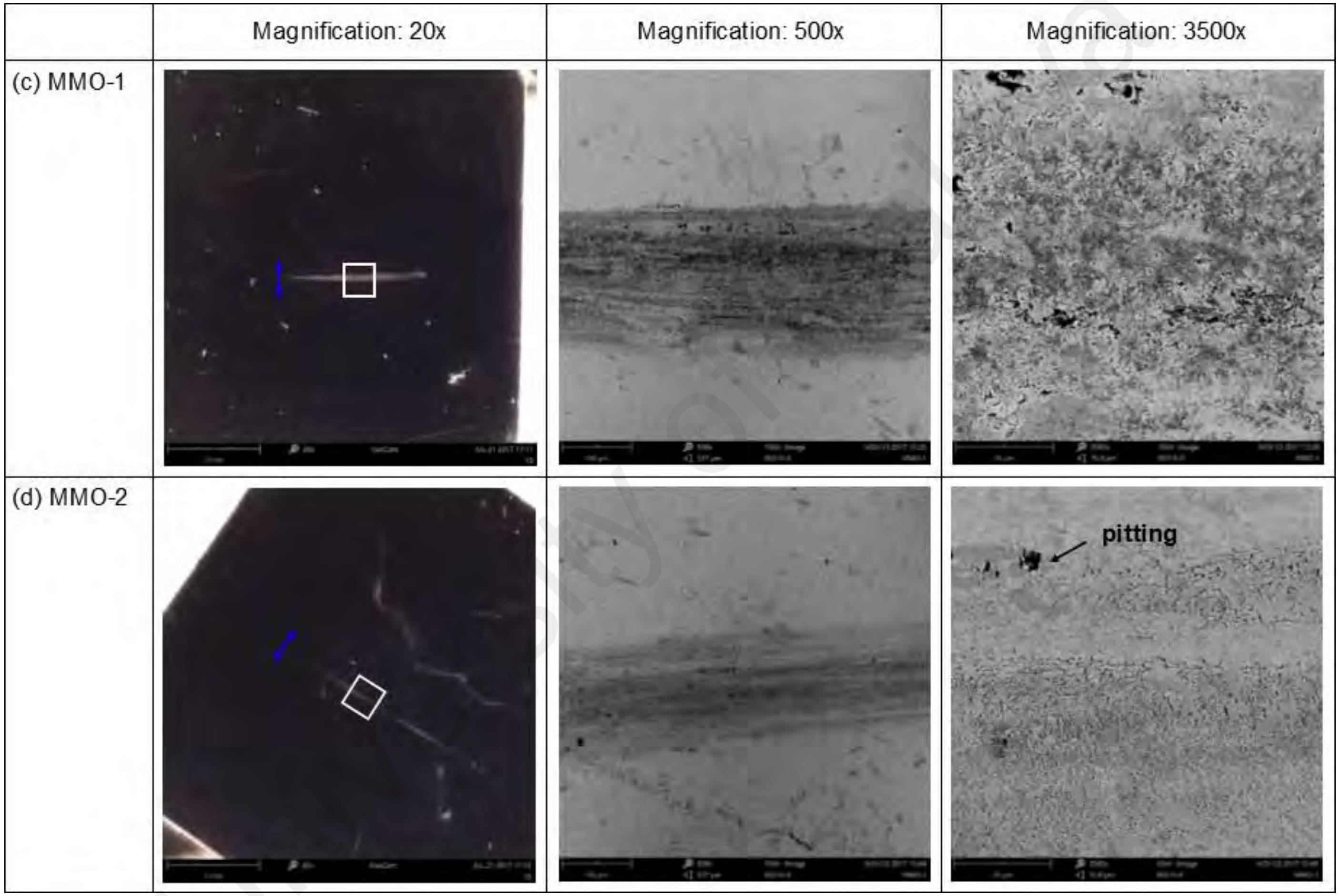

Figure 4.13, continued

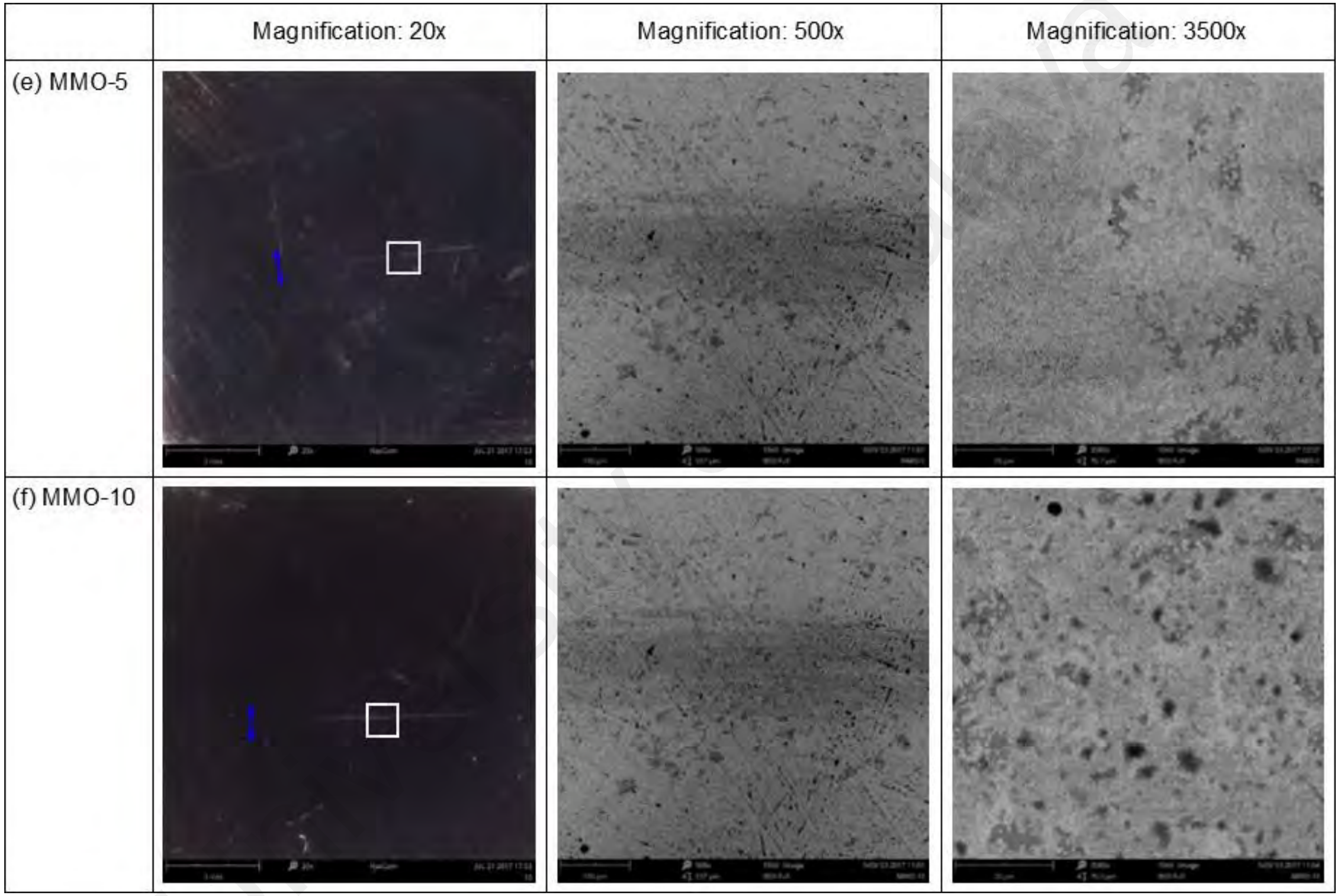

Figure 4.13, continued

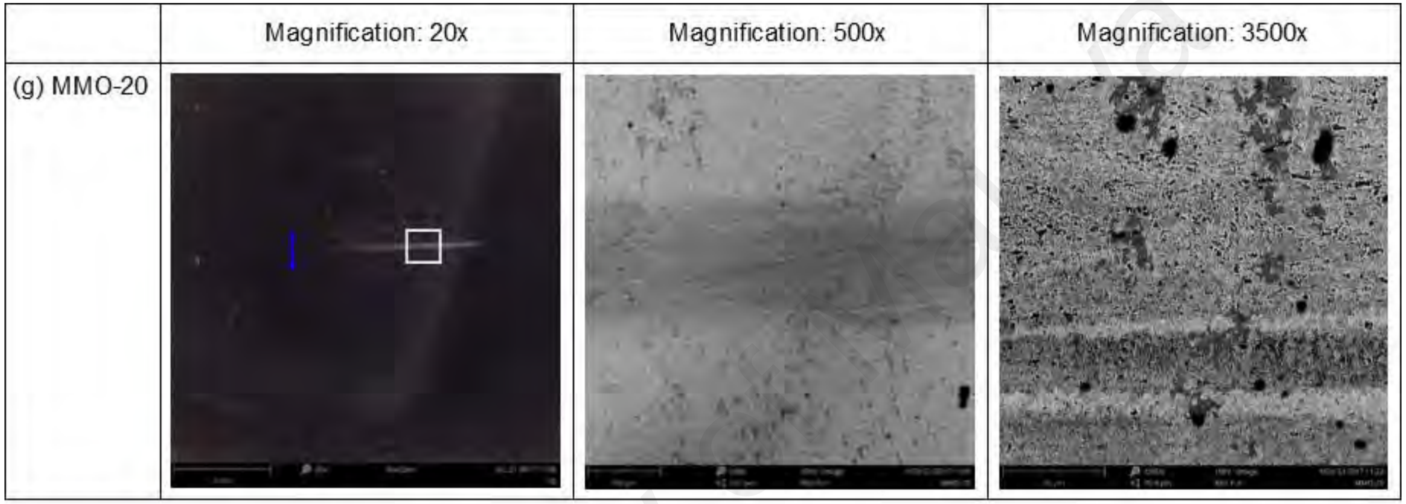

Note: ↕ = sliding direction

Figure 4.13, continued

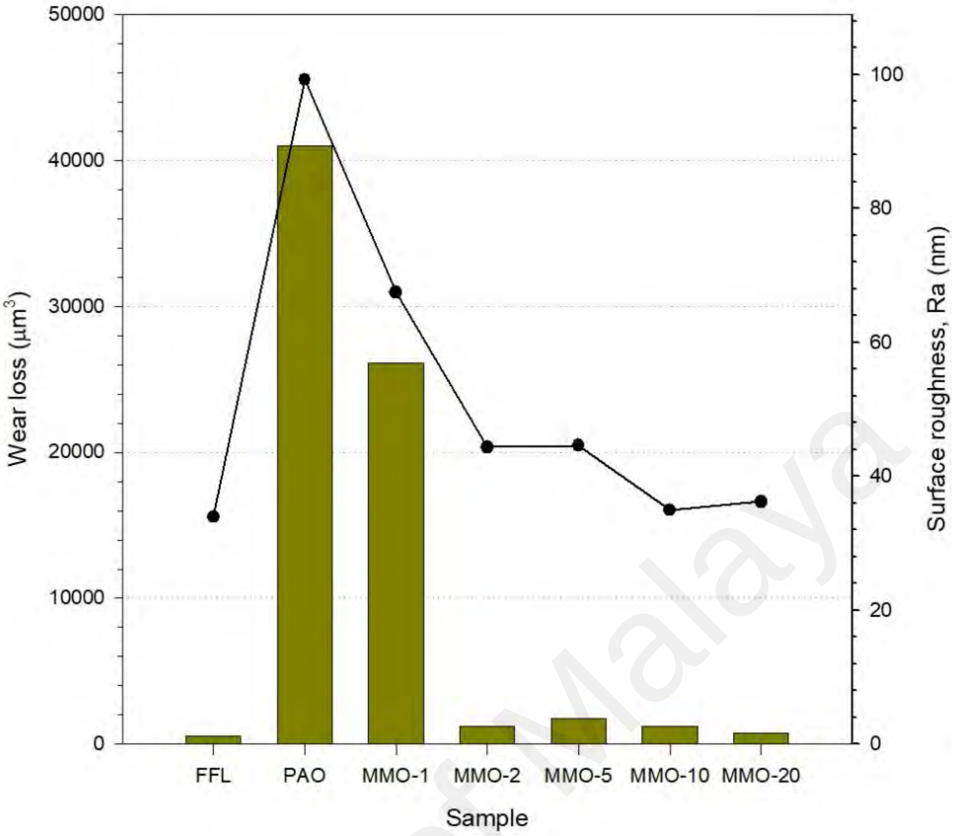

Figure 4.14: Wear loss and surface roughness of the worn surfaces

Table 4.10: EDS elemental analysis of the carbon steel plate surfaces after tribological test

Specimen	Element (Atomic %)								
	Fe	O	Cr	C	Co	N	Zn	P	Si
PAO	60.30	25.33	12.93						1.44
FFL	41.03	16.10	9.83	7.45	15.47	6.68	2.79	0.65	
MMO-1	58.53	20.86	14.10	6.51					
MMO-2	43.31	15.47	8.36	7.62	15.58	9.66			
MMO-5	56.42	16.71	11.85	7.13		7.89			
MMO-10	40.63	13.83	9.99	13.44	14.73	7.38			
MMO-20	51.91	18.55	12.06	9.40		8.09			

Note: Fe: Iron; O: Oxygen; Cr: Chromium; C: Carbon; Co: Cobalt; N: Nitrogen; Zn: Zinc; P: Phosphorus; Si: Silicon

Figure 4.15 shows the FTIR carbonyl C=O peaks of the PAO and MMO blends before and after tribological tests. It can be seen from the FTIR spectra of the MMO blends that there is a slight shift of the C=O peak and the peak intensity increases after the tribological test, which indicates that chemical reaction has occurred to the carbonyl group during the sliding process. It is believed that the following may have occurred: (1) a tribo-induced esterification indicated by the increase in peak intensity, implying an increase of ester contents (Peng et al., 2017) and (2) the formation of the ester lubricating film on the metal surfaces. According to Errichello& Cardis (2014), for lubricating films formed through physical adsorption on metal surfaces are only effective in low-load and low-temperature conditions, that their effectiveness will be loss at temperature above 150 °C.

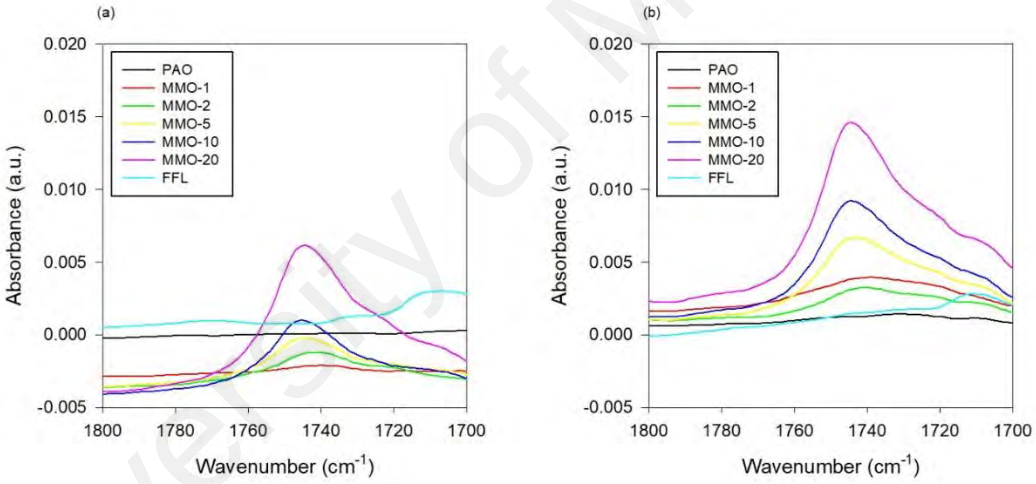

Figure 4.15: FTIR ester C=O peaks of the PAO and MMO blends (a) before and (b) after tribological tests

Nowadays, it is essential for lubricants to provide thermal protection against the heat generated during sliding motion, apart from providing wear protection. Figure 4.16 shows the average temperature measured during the stable friction phase. The programmed test temperature was 75 °C and the results indicate that the MMO offers a certain degree of thermal protection. The average temperature of the MMO blends is lower by 0.19– 0.37

°C compared with the average temperature for PAO. The average temperature of the MMO blends is lower by 0.14–0.32 °C compared with that for FFL. The results indicate that MMO improves heat dissipation of the lubricant, which is likely one of the reasons for the reduced wear on the MMO blend-lubricated surfaces. It is believed that the progression of adhesive wear is reduced at lower temperatures (Fazal et al., 2011). However, a more comprehensive study is needed to verify this observation.

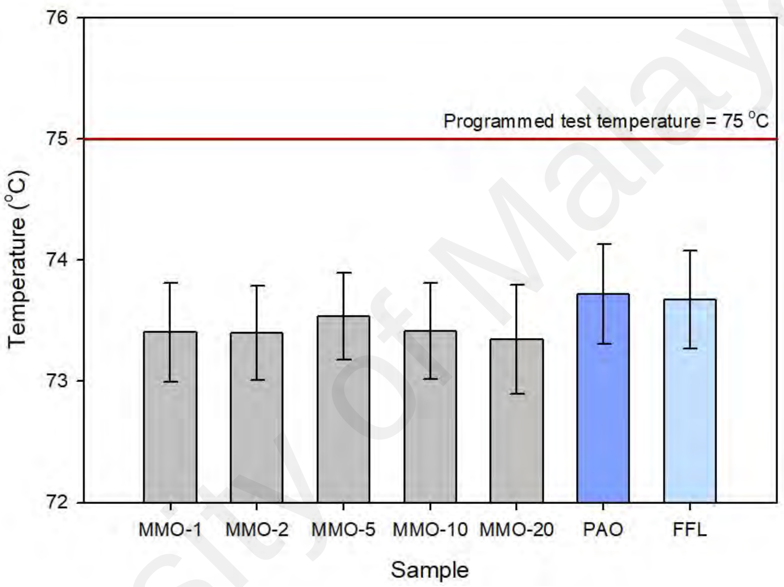

Figure 4.16: Average temperature measured during the stable friction phase

4.6.2 Tribological performance of MMO-10

This section provides a more in-depth investigation of MMO-10's performance as a biolubricant. MMO-10 was selected because it is the best performing MMO blending percentage from the lubricity test conducted using the HFRR (Section 4.6.1). Evaluation on MMO-10 wear prevention ability and performance under extreme pressure condition were detailed in Section 4.6.2.2 and Section 4.6.2.3. Comparisons were made against pure PAO, pure Paraffin, pure FFL and pure Corn oil, refer to Table 4.11.

Table 4.11: Lubricant samples investigated

Sample	Description	Note
MMO-10	10% MMO blending with PAO 170	Microalgae oil blend
PAO	100% PAO 170 (poly-alpha-olefin)	Synthetic base oil
FFL	100% full synthetic lubricant	Commercial lubricant
Corn	100% corn oil	Vegetable oil
Paraffin	100% paraffin	Mineral base oil

4.6.2.1 Physicochemical properties of lubricant

Table 4.12 shows the physicochemical properties of the lubricant samples. FFL was the most viscous followed by MMO-10, PAO, Corn, and Paraffin. MMO-10 possessed the highest AV many folds higher than PAO, FFL and Corn.

Table 4.12: Physicochemical properties of lubricant

Sample	Kinematic viscosity (mm^2/s)		Viscosity index	Density at 15 °C (g/cm^3)	Acid value (mg KOH/g)
	40 °C	100 °C			
PAO	64.581	9.799	134.7	0.835	0.1794
MMO-10	79.395	10.656	119.6	0.851	5.0191
FFL	81.471	13.474	168.8	0.853	0.2583
Paraffin	13.935	3.306	106.2	0.838	n.a.
Corn	33.750	7.885	217.3	0.922	0.2230[a]

Note: n.a. = not available, [a] citing Kardash& Tur'yan (2005)

4.6.2.2 Wear prevention test ASTM D4172-94 (reapproved 2016)

This method is used to determine the relative wear preventive properties of lubricating fluids in sliding contact.

(a) ***Friction characteristics***

A low COF does not necessarily translate into better wear (Bhushan, 2013; H. Xiao et al., 2019), as in this study, Corn has the lowest COF but its wear was the third highest among all tested samples (Figure 4.17), on the contrary, FFL recorded the highest COF but its wear is the second lowest. Additionally, MMO-10 recorded the lowest wear and Paraffin has the highest wear. Aravind et al. (2015) also reported similar findings in their experiment with rubber seed oil, coconut oil, sunflower oil, and SAE20W40 commercial lubricant; they found that sunflower oil has exhibited the lowest COF but also recorded the highest WSD among all the tested lubricant.

MMO-10 lubricated run has a significant wear reduction of 36.5% in comparison to PAO lubricated run, while FFL recorded reduced wear of 30.1% when compared with PAO. Generally, all samples recorded some reductions in wear compared with PAO with the exception of Paraffin. Paraffin recorded higher WSD than PAO. These results indicate that ester-containing lubricants display a better friction performance compared with the non-ester containing samples. Likewise, the average COF of olive oil was 26.05% lower than that of a commercial SAE15W40 lubricant as reported by Kalam et al. (2017). Similarly, according to Zulkifli et al. (2016), improved wear was observed for TMP palm ester and PE palm ester in comparison to pure paraffin oil. In their study, polyol esters that possess higher polarity than methyl ester were used.

The above observation can be explained using the friction behavior based on the Stribeck diagram (Figure 4.18). Oil film thickness is influenced by $\eta V/W$, where η is the oil viscosity, V the average sliding velocity and W the normal load (Bayer, 1994; Hutchings, 1992). In this testing, V/W was considered constant due to the same testing conditions, thus, the variation of oil film thickness is affected by the sample's viscosity. FFL was more viscous than PAO and MMO-10 (Table 4.12), thereby; FFL would have a better ability to separate the rubbing surfaces owing to a thicker fluid film. Contrary, Paraffin was the least viscous compared with the others and consequently, the wear scar diameter (WSD) recorded was also the highest.

Based on the calculated film thickness, *h*, at the testing load of 40 kg (392N) and temperature of 75 °C, Paraffin has the lowest film thickness (at 0.0063 µm) among all the samples, supporting the above observations (Table 4.13). According to (Rudnick, 2009), a higher viscosity will also cause fluid drag, the friction produced by the fluid on the sliding surfaces and this, in turn, may explain the higher COF recorded by FFL.

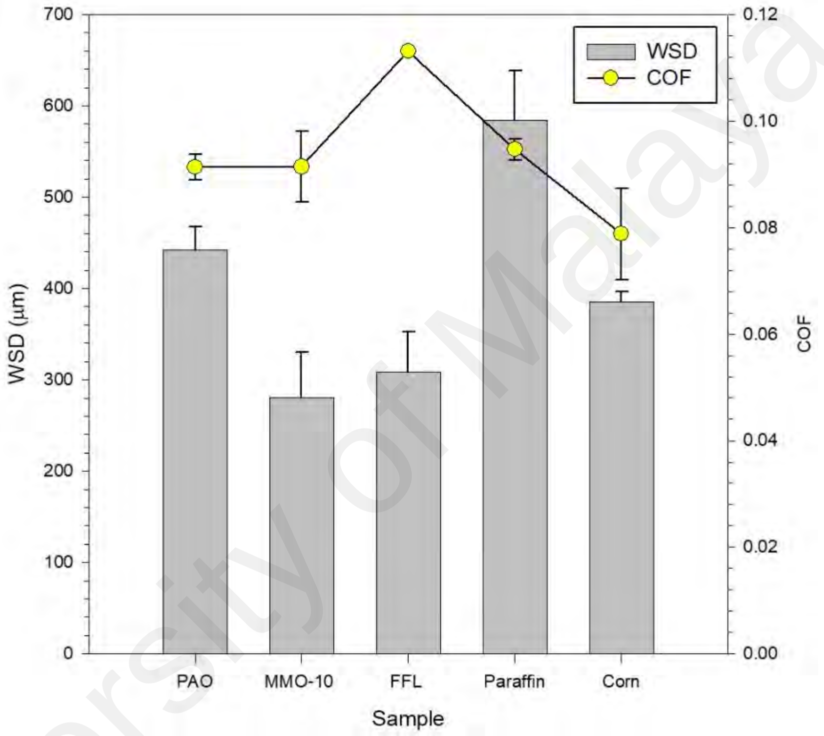

Figure 4.17: WSD and average COF

Table 4.13: Calculated minimum film thickness at 392 N (40kg)

Sample	At 40 °C			At 75 °C		
	Min film thickness, h (µm)	Film thickness ratio, λ	Lubrication regime	Min film thickness, h (µm)	Film thickness ratio, λ	Lubrication regime
PAO	0.0305	1.08	Mixed	0.0124	0.44	Boundary
MMO-10	0.0319	1.13	Mixed	0.0124	0.44	Boundary
FFL	0.0342	1.21	Mixed	0.0152	0.54	Boundary
Paraffin	0.0133	0.47	Boundary	0.0063	0.22	Boundary

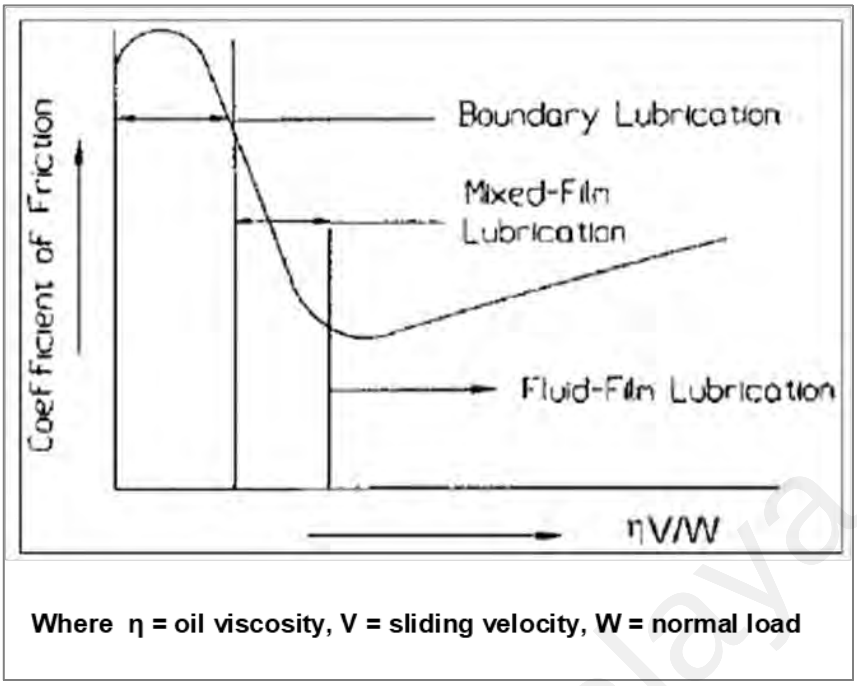

Where η = oil viscosity, V = sliding velocity, W = normal load

Figure 4.18: Stribeck diagram (reproduced from (Bayer, 1994))

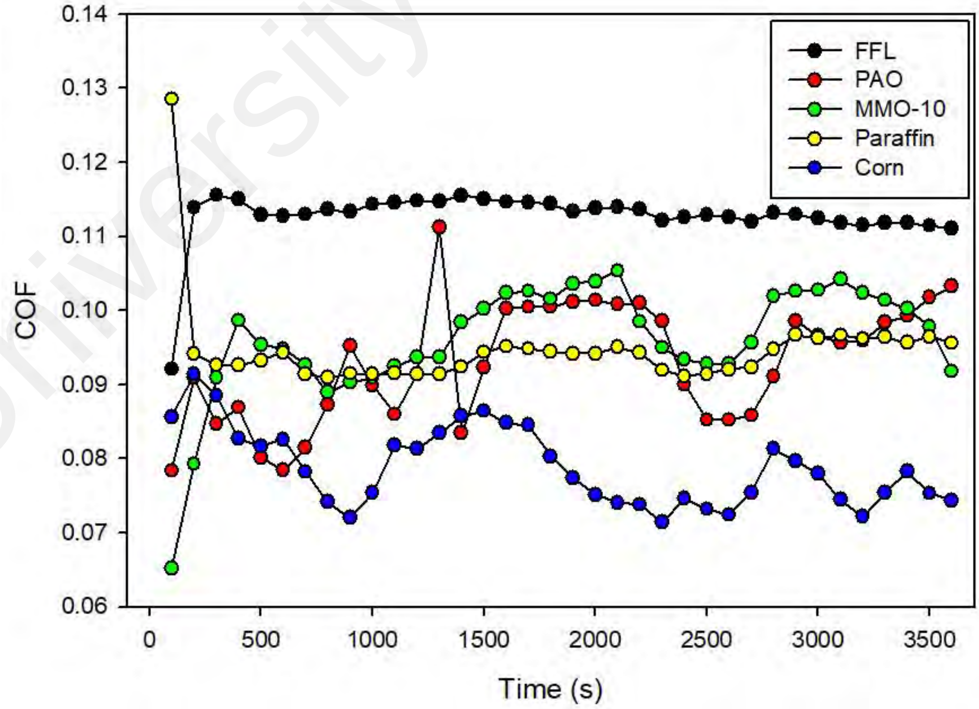

Figure 4.19: Relationship of COF with time

Considering the variations of COF against time (Figure 4.19), the commercial FFL exhibited very stable friction throughout the whole testing duration. Better fluid dispersion with the help of dispersant and surfactant on the contact surfaces and anti-wear additives may be the reasons behind these observations besides a higher film thickness. Similarly, Gulzar et al. (2015) have found that 1wt% of oleic acid as surfactant has enable uniform dispersion of nanoparticles that improved wear protection of chemically modified palm oil (CMPO). Their results revealed the addition of oleic acid with or without the addition of nanoparticles resulted in a reduction of COF compared with pure CMPO with no surfactant added.

MMO-10 and PAO exhibited fluctuating COFs that may indicate that the thickness of the fluid film is not sufficient in separating the two rubbing surfaces, resulting in boundary lubrication regime. Furthermore, all tested samples were in boundary lubrication regime with $\lambda < 1$. This lubricating mode occurred when the solid surfaces are so close together that surface interaction between the solid asperities dominates the contact (Bhushan, 2013; Maru et al., 2013). In the absence of boundary lubricant, failure and seizure are caused by adhesive and chemical (corrosive) wear (Upadhyay & Kumar, 2019).

(b) *Wear characteristics*

Figure 4.20 shows the surface morphology and EDS analysis of the wear scars. Lubrication film between the mating surfaces became thinner at higher temperature causing adhesion at the highest asperities contact sites. The tribological testing temperature was at 75 °C. Plastic deformation will begin with cracks initiation that propagates further to cause deformation while materials transfer occurred when fragments detached and reattached on the interacting sites. The continual cycle would lead to scuffing, galling and smearing. Further, the test result indicates that MMO-10 has good anti-wear properties that are comparable to a commercial FFL.

Generally, PAO lubricated surface was rougher with a series of deeper grooves indicating abrasive wear while MMO-10 surface has fewer grooves, though there were a few deeper ones present. The presence of esters and other oxygen-containing compounds in MMO-10 has offered some wear protection to the rubbing surfaces (Figure 4.20b). The lowest oxygen and highest carbon concentrations detected on its surface in comparisons to other samples have indicated a lower oxidation rate and the presence of an ester-based lubricating layer on MMO-10-lubricated surface.

On the contrary, wear scar on FFL-lubricated surface was smoother though signs of galling are present at some sites. The anti-wear properties helps prevent scuffing in FFL as indicated by presences of zinc and phosphorus compounds from EDS results (Figure 4.20c). These anti-wear compounds have formed a sacrificial tribofilm on the matting surfaces and were the first to be worn off during the tribology processes to protect the metal surfaces, this has led to the shallower grooves found on FFL-lubricated surfaces.

On the other hand, no carbon was detected on Paraffin-lubricated surface because paraffin composed of only hydrocarbons. With the absence of polar molecules for surface attachment for lubricating film formation, higher wear is expected. The WSD of paraffin is the highest among all tested lubricant samples with the sign of delamination. Since Corn oil contains esters and esters forms a lubricating film on the surface, the WSD recorded for corn were below that of PAO and Paraffin.

<table>
<tr><th>Sample</th><th>Magnification: 500x</th><th>EDS analysis</th></tr>
<tr><td>(a) PAO</td><td>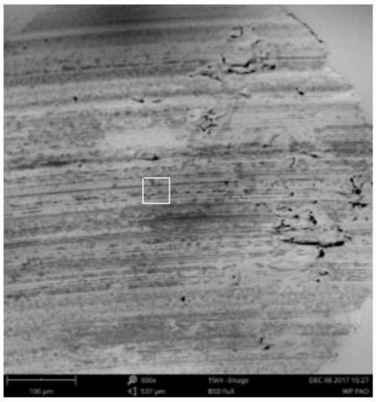</td><td>
<table>
<tr><th>Element Symbol</th><th>Atomic Conc.</th><th>Weight Conc.</th></tr>
<tr><td>Fe</td><td>51.85</td><td>80.99</td></tr>
<tr><td>C</td><td>29.62</td><td>9.95</td></tr>
<tr><td>O</td><td>17.76</td><td>7.95</td></tr>
<tr><td>Cr</td><td>0.76</td><td>1.11</td></tr>
</table>
</td></tr>
<tr><td>(b) MMO-10</td><td>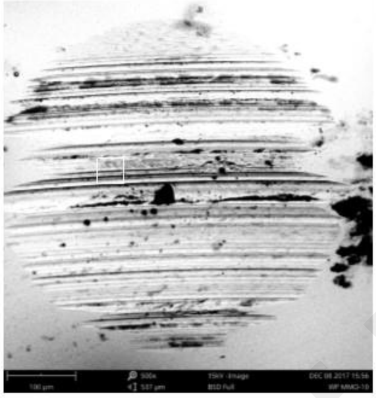</td><td>
<table>
<tr><th>Element Symbol</th><th>Atomic Conc.</th><th>Weight Conc.</th></tr>
<tr><td>Fe</td><td>49.69</td><td>79.84</td></tr>
<tr><td>C</td><td>34.74</td><td>12.01</td></tr>
<tr><td>O</td><td>14.62</td><td>6.73</td></tr>
<tr><td>Cr</td><td>0.95</td><td>1.41</td></tr>
</table>
</td></tr>
<tr><td>(c) FFL</td><td>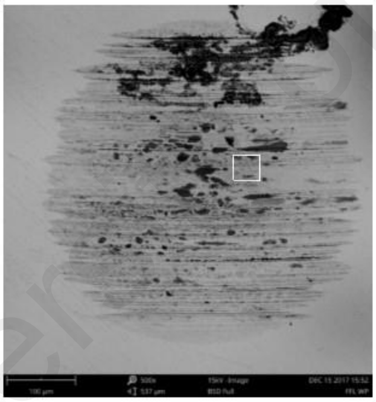</td><td>
<table>
<tr><th>Element Symbol</th><th>Atomic Conc.</th><th>Weight Conc.</th></tr>
<tr><td>Fe</td><td>44.64</td><td>67.61</td></tr>
<tr><td>O</td><td>19.83</td><td>8.61</td></tr>
<tr><td>C</td><td>25.22</td><td>8.22</td></tr>
<tr><td>Zn</td><td>2.00</td><td>3.54</td></tr>
<tr><td>S</td><td>3.12</td><td>2.71</td></tr>
<tr><td>P</td><td>2.70</td><td>2.27</td></tr>
<tr><td>Ca</td><td>0.96</td><td>1.04</td></tr>
</table>
</td></tr>
<tr><td>(d) Paraffin</td><td>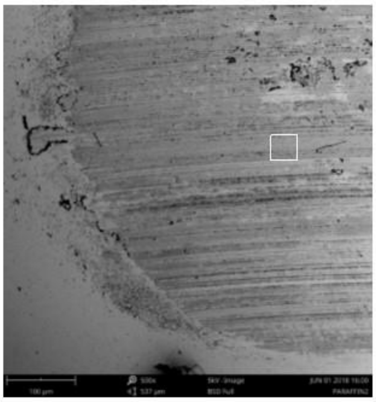</td><td>
<table>
<tr><th>Element Symbol</th><th>Atomic Conc.</th><th>Weight Conc.</th></tr>
<tr><td>Fe</td><td>82.15</td><td>94.14</td></tr>
<tr><td>O</td><td>17.85</td><td>5.86</td></tr>
</table>
</td></tr>
</table>

Figure 4.20: Surface morphology and EDS at constant load of 392 N at 1200 rpm at 75°C for 1h

<table>
<tr><th>Sample</th><th>Magnification: 500x</th><th>EDS analysis</th></tr>
<tr><td>(e) Corn</td><td>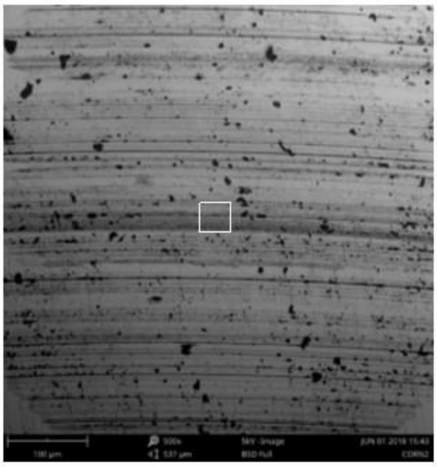 </td><td><table>
<tr><th>Element Symbol</th><th>Atomic Conc.</th><th>Weight Conc.</th></tr>
<tr><td>Fe</td><td>48.12</td><td>66.64</td></tr>
<tr><td>Co</td><td>8.71</td><td>12.72</td></tr>
<tr><td>Cr</td><td>5.67</td><td>7.31</td></tr>
<tr><td>O</td><td>17.88</td><td>7.09</td></tr>
<tr><td>C</td><td>11.85</td><td>3.53</td></tr>
<tr><td>N</td><td>7.77</td><td>2.70</td></tr>
</table></td></tr>
</table>

Figure 4.20, continued

(c) *Multi element oil analysis*

Multi element oil (MOA) analysis provide a lot of information about the wear of parts in a mechanical system, particularly at the location where visual inspection is difficult. By looking at the changes in the element, the component where wear has occurred may be predicted since different part may be built with a different type of materials. The element that all the samples have were Fe, Cr, Al, Cu, Pb, Ni, Mn, Ti and Ag (Figure 4.21). FFL and MMO-10 contained the most elements at 13 and 15 respectively. Some elements were added to enhance a lubricant’s properties, for example, Zn and B were present in a high percentage in FFL, probably as an anti-wear additive, detergent, and anti-foaming agent. Meanwhile, MMO-10 has high concentration of Mg where magnesium made up the central atom of the porphyrin ring found in the chlorophyll pigment of plant.

Furthermore, elements that only exist or increases after the tribological test may indicate wear whereas if the elements’ concentration reduces, then a chemical reaction might have occurred with the compounds found in the lubricant or the surrounding bodies like the metal surfaces. In this study, the increase of elements from before to after the tribological test were most prominent in PAO followed by Paraffin and on a lesser degree, Corn oil, which indicate that wear have occurred. Likewise, this observation also supported the findings that ester-containing lubricant (Corn oil) offered better wear protection than non-ester containing samples (PAO and Paraffin), evidenced by the reduced WSD from the previous section.

On the other hand, for MMO-10 and FFL, some elements have reduced after the tribological test. For example, Zn concentration in the FFL has reduced after the tribological test. This may indicate that Zn (from the anti-wear additive) was used to form a tribofilm to protect the interacting surfaces. According to Errichello& Cardis (2014), anti-wear tribofilm is formed by chemical bonding to the oxide layers of the metal surfaces and these layers are effective at moderate loads and temperatures of up to about 200°C. Significant reduction of Na concentration was detected on MMO-10 lubricant after the tribological test and Na in MMO-10 might have originated from the chloroplast or from residue contamination from the oil extraction process. However, the presence of Na may have affected MMO-10 in a positive way. This is because detergents that are added in commercial lubricant, used to neutralize strong acid, to remove neutralized products, and for film formation on surface to prevent high temperature deposition of sludge and varnish are, generally produced from alkaline and alkaline earth elements like calcium (Ca), magnesium (Mg), sodium (Na) or Ba (barium) (Kopeliovich, 2012). However, further research is needed to determine the actual effect of Na on MMO-10's lubricity.

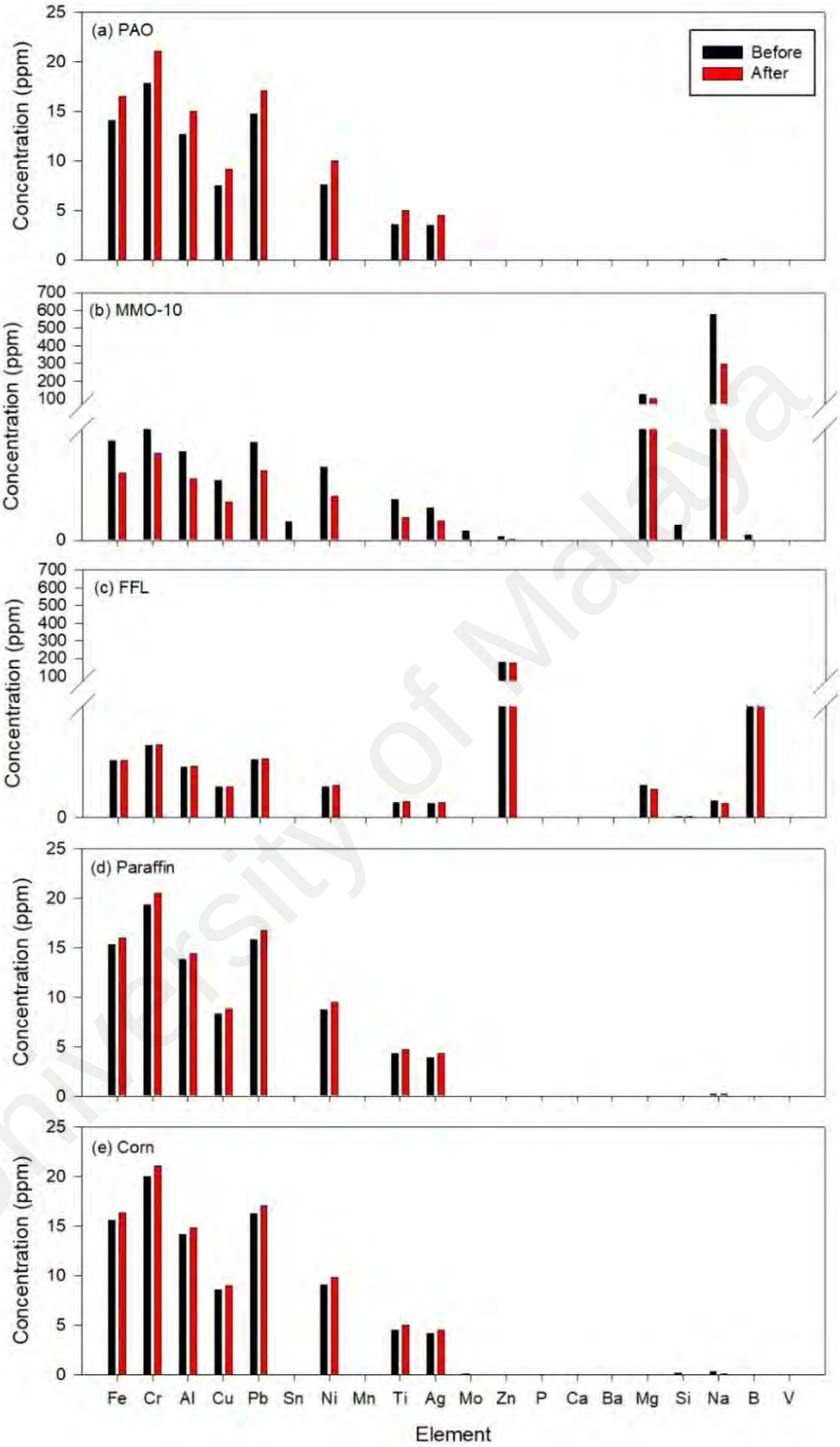

Figure 4.21: Multi element oil analysis of sample before and after tribological test

(d) *Flash Temperature Parameter (FTP)*

Flash temperature parameter (FTP) denotes a single number that is used to express the critical flash temperature at which a lubricant will fail under a given condition. Table 4.14 tabulates the FTP of the tested samples. Since a higher FTP is desirable, therefore MMO-10 would display better lubricity than the lower value samples (i.e. MMO-10 > FFL > Corn > PAO > Paraffin). Studies have found that lower FTP results in the breakdown of the lubrication films (Habibullah et al., 2015; Mosarof et al., 2016).

Table 4.14: Flash temperature parameter

Sample	Flash parameter temperature (FTP)
PAO	0.00793
MMO-10	0.01495
FFL	0.01309
Paraffin	0.00536
Corn	0.00961

4.6.2.3 Extreme pressure condition (ASTM D2783-03 (2014)

This test is used to determine the load carrying-properties of lubricants. This parameter is crucial for operation in slow, highly loaded and geared applications. In industrial application, extreme pressure (EP) additive is added to provide protection to components when the lubricating film thickness can no longer separate the interacting surfaces, in what is called boundary condition (Wright, 2008). Therefore, EP additive is designed to prevent adhesive wear under such condition (Bhaumik et al., 2018; Rastogi & Yadav, 2003; Yan et al., 2017).

(a) *Friction characteristics under EP*

This session discussed the extreme pressure test, in reference to the wear load graph (Figure 3.5). Figure 4.22 depicts the relationship between the applied load and wear scar diameter (WSD). The non-seizure load's region is perceived as undergoing the elastohydrodynamic lubrication regime, a regime in between mixed and hydrodynamic lubrication. The recorded corresponding COFs were also at low magnitudes that are less than 0.10 (Figure 4.23). These were due to the presence of a minimum fluid film that helps to separate the two rubbing surfaces. In this lubrication condition, the oil film supports the load at low friction making surface characteristics and asperities less significant due to the minimum contact between the interacting surfaces (Hunter & Zienkiewicz, 1960), where, on the contrary, fluid properties like viscosity, density, thermal and oxidative stability become important. In this lubrication condition, the oil film supports the load at low friction making surface characteristics and asperities less significant due to the minimum contact between the interacting surfaces though research has found that surface texturing can helps improve the COF (H. Wang et al., 2019).

Generally, when the load increased, the film thickness decreases, change of lubrication regime from mixed lubrication to boundary conditions. But at high contact loading, localized plastic deformation will occur when the produced stress intensified followed by crack initiation and propagation and where lastly spall will form (Al-Bukhaiti et al., 2011; Zulkifli et al., 2016). Results have shown that the last non-seizure load for PAO was 30 kg compared with MMO-10 and FFL at 80 kg, this indicates that an addition of 10 % MMO has successfully sustained another 50 kg of applied-load to maintain the lubricating fluid film in this regime. Corn also recorded a last non-seizure load at 30 kg, and the worst performer was Paraffin where its last non-seizure load was at 20 kg. Corn was able to sustain a higher load due to the presence of esters, but for Paraffin that composed of only hydrocarbon chains (without the polar functional groups) was unable to form a strong molecular barrier because it cannot be adsorbed strongly onto the metal surfaces (Bhaumik et al., 2018; Masjuki et al., 1999). Furthermore, studies have revealed that higher polarity esters (such as polyol ester) offer better lubrication compared with their lower polarity counterparts (Humood et al., 2019; Kania et al., 2015) due to the better absorption and the resulting stronger film.

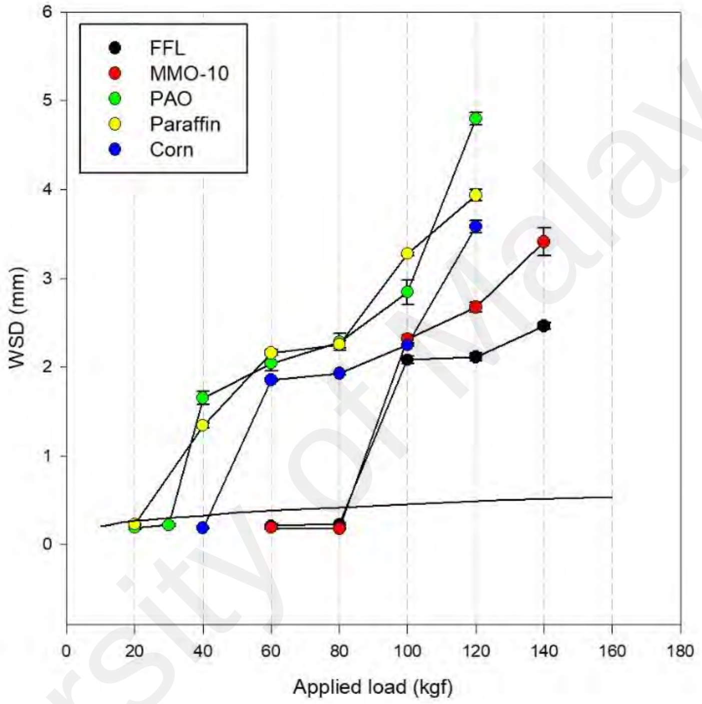

Figure 4.22: Relationship between load and WSD

When the load is further increased, as in the incipient and immediate seizure regions, a sudden rise of WSD marked the beginning of the mixed-lubrication mode. This is a transition from elastohydrodynamic to boundary lubrication. Depending on thermal effect and the location of asperities, momentary breakdown of the lubricating film causes intermittent contact between the rubbing surfaces (N.W.M. Zulkifli et al., 2013), leading to scuffing at these sites. The solid contacts between the interacting surfaces could lead to a cycle of adhesion, metal transfer, wear-particle formation and eventual seizure

(Bhushan, 2013). Correspondingly, fluctuating COFs with higher magnitude were recorded in this region (Figure 4.24). On the contrary, FFL's COF stabilized after the run-in phase, owing to the anti-wear additive, dispersant and surfactant it contained (Zainal et al., 2018). Dispersant and surfactant will prevent agglomeration and assist in uniform deposition of lubricant on to the interacting surfaces (Chan et al., 2018).

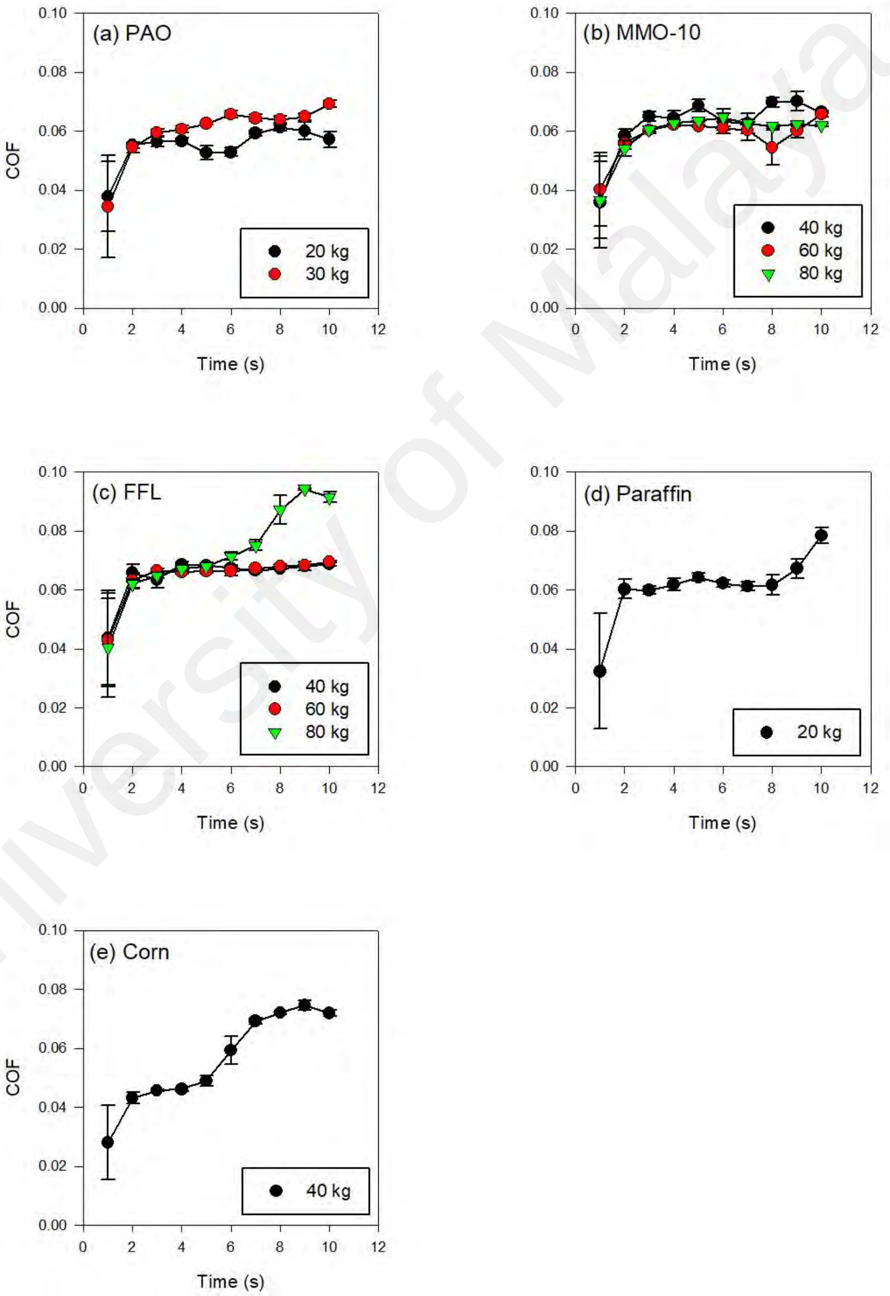

Figure 4.23: Evolution of COF against time in the non-seizure region for (a) PAO, (b) MMO-10, (c) FFL, (d) Paraffin and (e) Corn

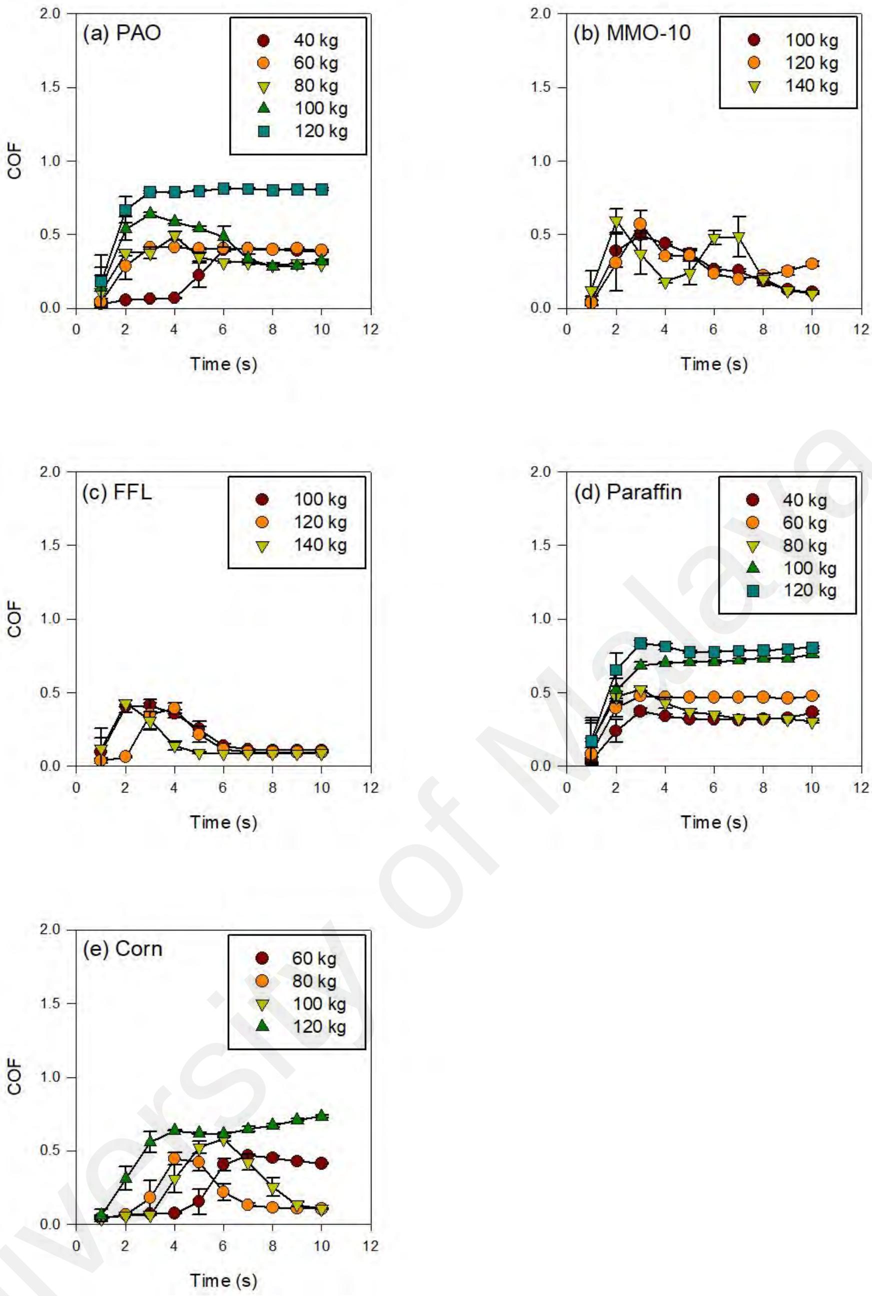

Figure 4.24: Evolution of COF against time in the incipient and immediate seizure region for (a) PAO, (b) MMO-10, (c) FFL, (d) Paraffin and (e) Corn

Table 4.15 tabulates initial seizure load (ISL), weld point (WP) and load-wear index for all the tested lubricants. The initial seizure (ISL) and weld loads (WL) recorded for MMO-10 and FFL were 100 kg and 160 kg respectively. When compared with PAO, the ability of MMO-10 lubricating film to sustain the increasing applied-load was on a par with FFL.

Table 4.15: Extreme pressure conditions

Sample	Initial seizure load, ISL (kg)	Weld point, WP (kg)	COF at 140 kg	WSD at 140 kg	Load-Wear Index
PAO	40	140	–	–	15.3
MMO-10	100	160	0.27220	3.41	47.9
FFL	100	160	0.21537	2.46	44.7
Paraffin	40	140	–	–	17.3
Corn	60	140	–	–	22.2

The presence of polar functional group has facilitated the absorption of fatty acid hydrocarbon chain on metal surfaces by forming lubricating layers that inhibit direct metal-to-metal contact (A. Adhvaryu et al., 2004; Jamshaid et al., 2019). Moreover, the ability of these layers to hold, even at the weld load where PAO rotating ball welded to the three stationary balls, has demonstrated that MMO-10 has good load carrying properties. This addition of 10% MMO has extended the extreme pressure level of PAO-force by 40 kg. This finding is supported by the ASTM D2783-03 load-wear index obtained by MMO-10, at 47.9. It was more than three folds the index of PAO and was slightly better than FFL.

Moreover, past studies have shown that the increase of polarity in esters and oxygen-containing functional groups increases the wear protection on the sliding surfaces (Imran et al., 2013; Sripada et al., 2013; Yao, 2009). Higher polarity esters are believed to impart higher affinity toward metal surfaces than their lower polarity counterpart, resulting in stronger adsorption of polar molecules on the interaction surfaces, hence creating stronger lubricating film (Kamalakar et al., 2013). N.W.M. Zulkifli et al. (2013) has reported a weld load of 220 kg obtained using TMP palm, a polyol ester with higher polarity.

(b) *Wear characteristics under EP*

At initial seizure load ISL, the lubricating film can no longer withstand the pressure load and failure is imminent. Adhesive wear became severe, leading to plastic deformation. Figure 4.25 shows the SEM images of different lubricated surfaces at the initial seizure load. Severe deformation was prominent for PAO at its ISL, in comparison for MMO-10, the ISL has been extended to 100 kg without severe wear thought galling were noticeable at some sites. As a control, at FFL surfaces at ISL, some shallow deformations and galling were noticeable. For Corn (the representative of pure vegetable oil) has a higher ISL than Paraffin and PAO, though serious delamination with fragment detachment was observed at ISL. This observation agrees with the findings that esters provide better lubricity than mineral and synthetic base oil (Biresaw et al., 2003; Madankar et al., 2013; Zulkifli et al., 2016). Paraffin, however, showed the lesser degree of delamination than PAO though both having the same ISL, at 40 kg. This observation agreed with the load-wear index where Paraffin has a higher load-wear index than PAO, at 17.3 and 15.3 respectively, indicating Paraffin could carry load better than PAO.

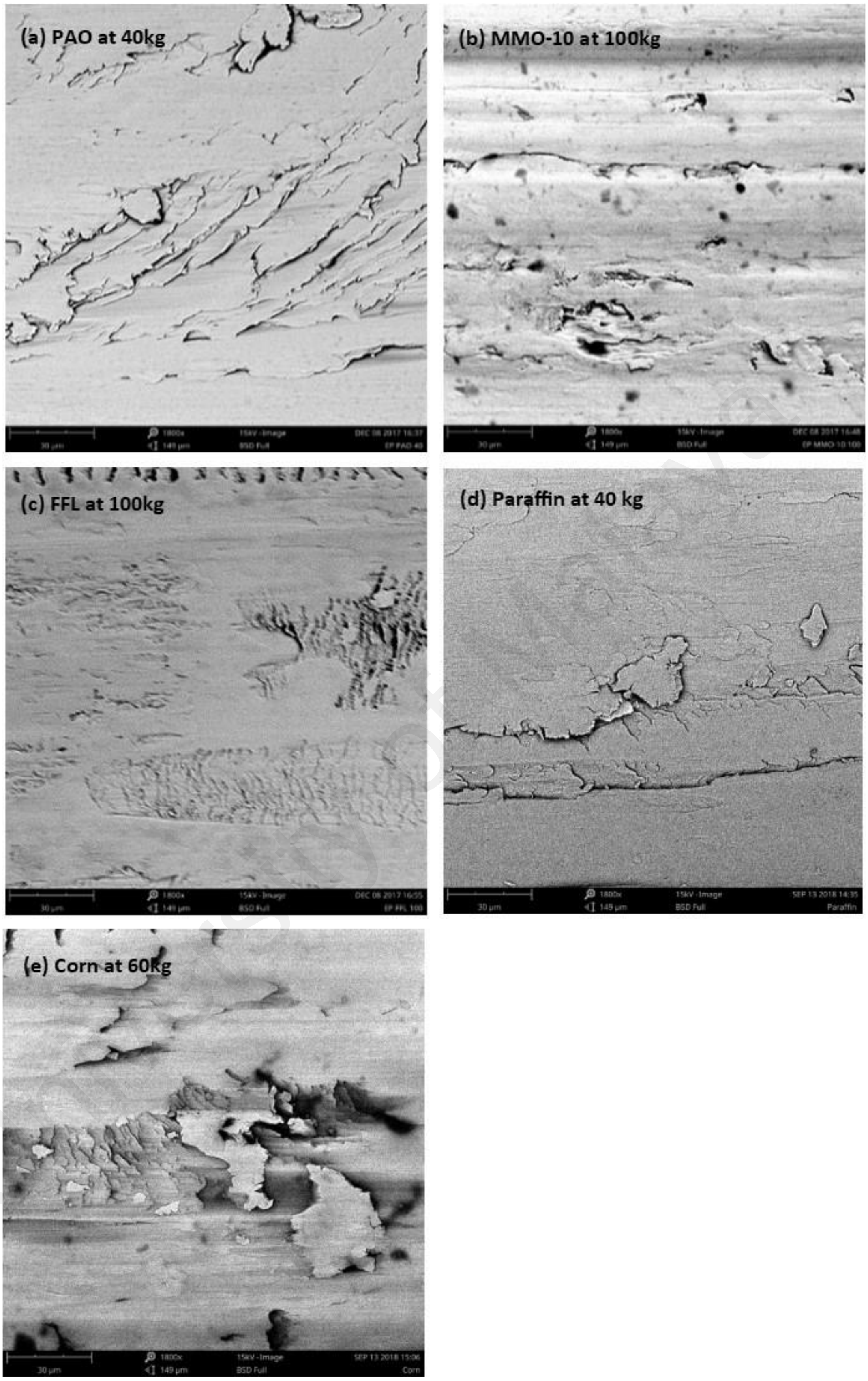

Figure 4.25: Surface morphology at ISL of different samples

4.6.2.4 Thermal and oxidative stability

Thermal and oxidative stability are important parameters facing biolubricant commercialization because they directly affect the operating temperature and shelf life of a product. The following subsection discussed each parameter in detailed.

(a) ***Oxidation stability***

Vegetable oil is known for its poor oxidation stability compared with synthetic esters due to the presence of polyunsaturated fatty acids (Rudnick, 2013; van der Westhuizen & Focke, 2018) and the easily-cleavage β-CH group found in glycerol (Adu-Mensah et al., 2019; Wagner et al., 2001), both are factors contributing to poor oxidation performance. As such, it is believed that, when an ester and non-ester samples were investigated together, the ester sample will most likely exhibit poorer oxidation characteristics. Therefore, in this study, the oxidative stability of MMO-10, the best performing MMO blending percentage determined from the tribological evaluation was compared with pure PAO (synthetic base oil), pure Paraffin (mineral base oil), pure FFL (commercial fully formulated synthetic lubricant) and pure corn oil (vegetable oil).

For all the samples except for Corn oil, the oxidation stability was determined by the relative changes (in percentage) of the samples' kinematic viscosity between 48 and 144 h (subjected to aging at 95 °C and under constant aeration), higher percentage denotes poorer oxidation behavior and vice versa (Figure 4.26). Corn oil has solidified before the experiment ended, hence the oxidation stability of Corn (6.15 h) was determined according to EN 14112 method. It was found that the oxidation stability of all samples was in the following order: Corn < PAO < Paraffin < MMO-10 < FFL.

Generally, in industrial applications, the antioxidant is added to prevent aging caused by auto-oxidation and to increase a lubricant lifespan. It is designed to delay, inhibits auto-oxidation and to reduce the unwanted by-product (Varatharajan & Pushparani, 2018). Further examination on the oxidation stability of MMO-10 using the DSC method (ASTM D3895-14) has revealed that MMO-10 could significantly extend the oxidative induction time (OIT) of pure PAO to more than 24 folds. OIT is the time between melting and the onset of decomposition in isothermal conditions and it provides information about the oxidative stability of materials. The presence of natural antioxidants such as stigmasterol and β-sitosterol may be responsible for such observation. The OIT results indicate that MMO-10 could make a good oxidation stability enhancer (Figure 4.27). In many studies, the use of antioxidant has proven to extend the oxidative stability of biodiesels. However, limited research has used natural antioxidant for fuel applications; perhaps it is too costly for overall biodiesel feasibility since antioxidant for the health supplement market is more lucrative (Varatharajan & Pushparani, 2018). Studies have found that soy methyl ester with caffeic acid addition met the EN14214 requirement of minimum 6h even after three months of storage and has outperformed tert-butylhydroquinone (TBHQ), a common synthetic antioxidant (Damasceno et al., 2013). D. M. Fernandes et al. (2015) has found that the addition of M. oleifera leaves extract successfully increased the induction period of soybean biodiesel from 3.8 to 10.3 h. The use of ginger extract was investigated as an antioxidant to *Pongamia pinnata* biodiesel, it is found that the increase of ginger extract concentration in biodiesel increases the induction period (Devi et al., 2017b).

Therefore, if the additive itself could serve another role rather than just as an antioxidant, it might be a viable option worth exploring. Considering that commercially available synthetic antioxidant like tert-Butylhydroquinone (TBHQ) (a type of phenol) is found to be harmful for human health and can be carcinogenic especially for prolonged exposure to high-doses (Gharavi & El-Kadi, 2005). Therefore, MMO-10 could make an attractive alternative besides serving as a friction modifier.

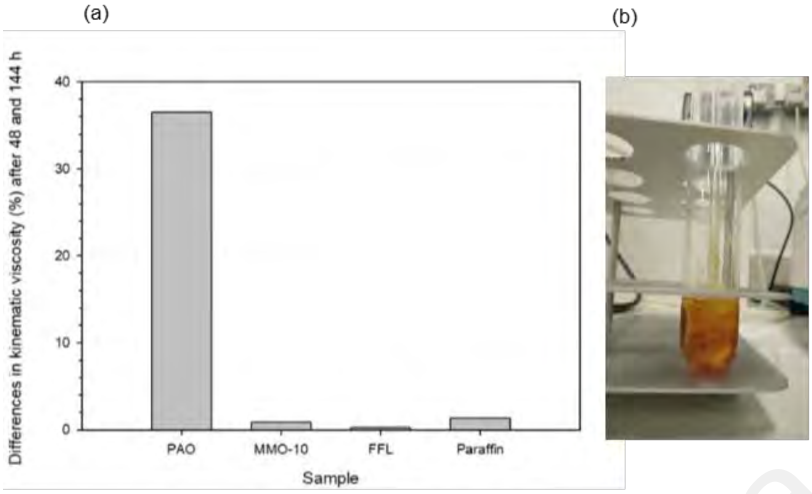

Figure 4.26: (a) Oxidation stability of different sample after 48 and 144 h and (b) corn oil has solidified before the experiment ended

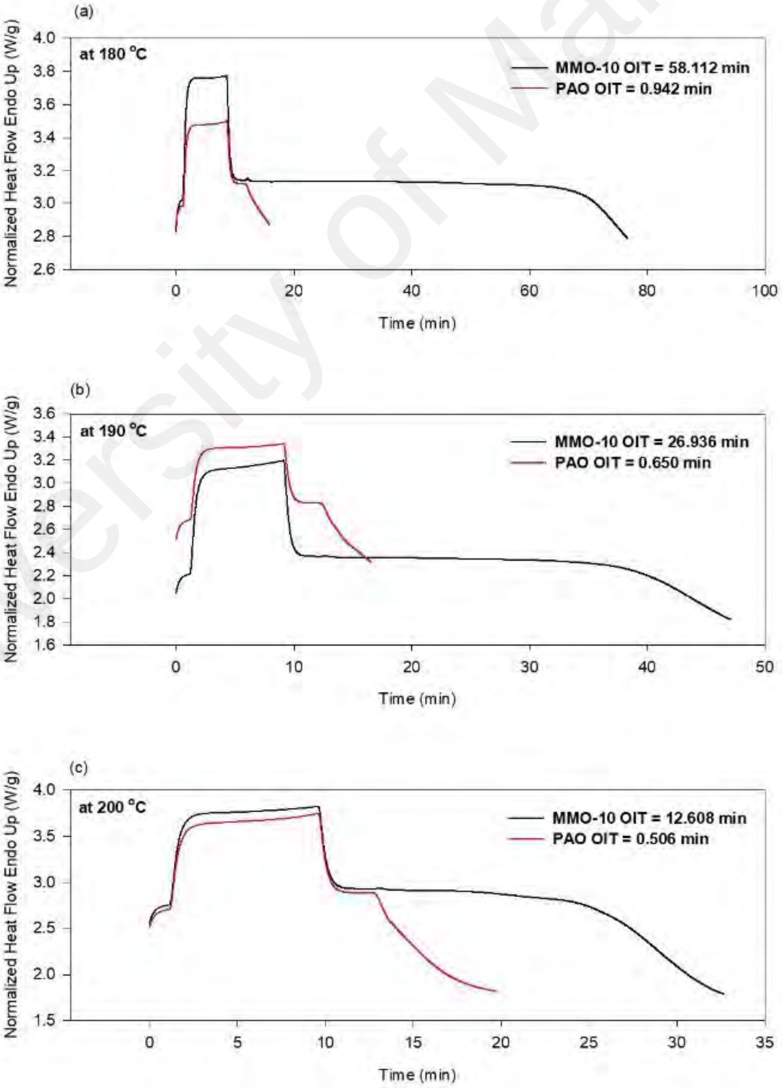

Figure 4.27: Oxidation Induction Time, OIT

(b) *Thermal stability*

Thermal stability is crucial for vegetable oil-based biolubricant application at high temperature condition (Kalam et al., 2017) and the onset temperature is used to define the temperature at which a lubricant starts to decomposed. Figure 4.28 shows the thermal curves of PAO, MMO-10 and FFL. The thermal stability of vegetable oil is predominantly affected by the chemical structure of its fatty acid composition. Therefore, the fatty acid's properties like carbon chain length, branching, and degree of unsaturation will directly influence the thermal stability of the vegetable oil.

Results revealed that MMO-10 was quite stable thermally; its decomposition temperature was just 4 °C lower than pure PAO. It showed better combustion than PAO, attributed to its oxygen content (from ester and other oxygen-containing moieties). A high decomposition temperature not only indicates that a lubricant is thermally stable, but it also shows that the lubricant can function at a higher operating temperature. Our results indicate that MMO-10 can function at a slightly higher temperature than FFL. Similarly, Kalam et al. (2017) also found that olive oil showed better thermal stability than a SAE15W40 commercial lubricant where the decomposition temperature of olive oil and the commercial lubricant were at 395.15 and 249.20 °C respectively. Furthermore, the thermal curve have shown that there were other compounds added to FFL (Figure 4.28), probably as additives.

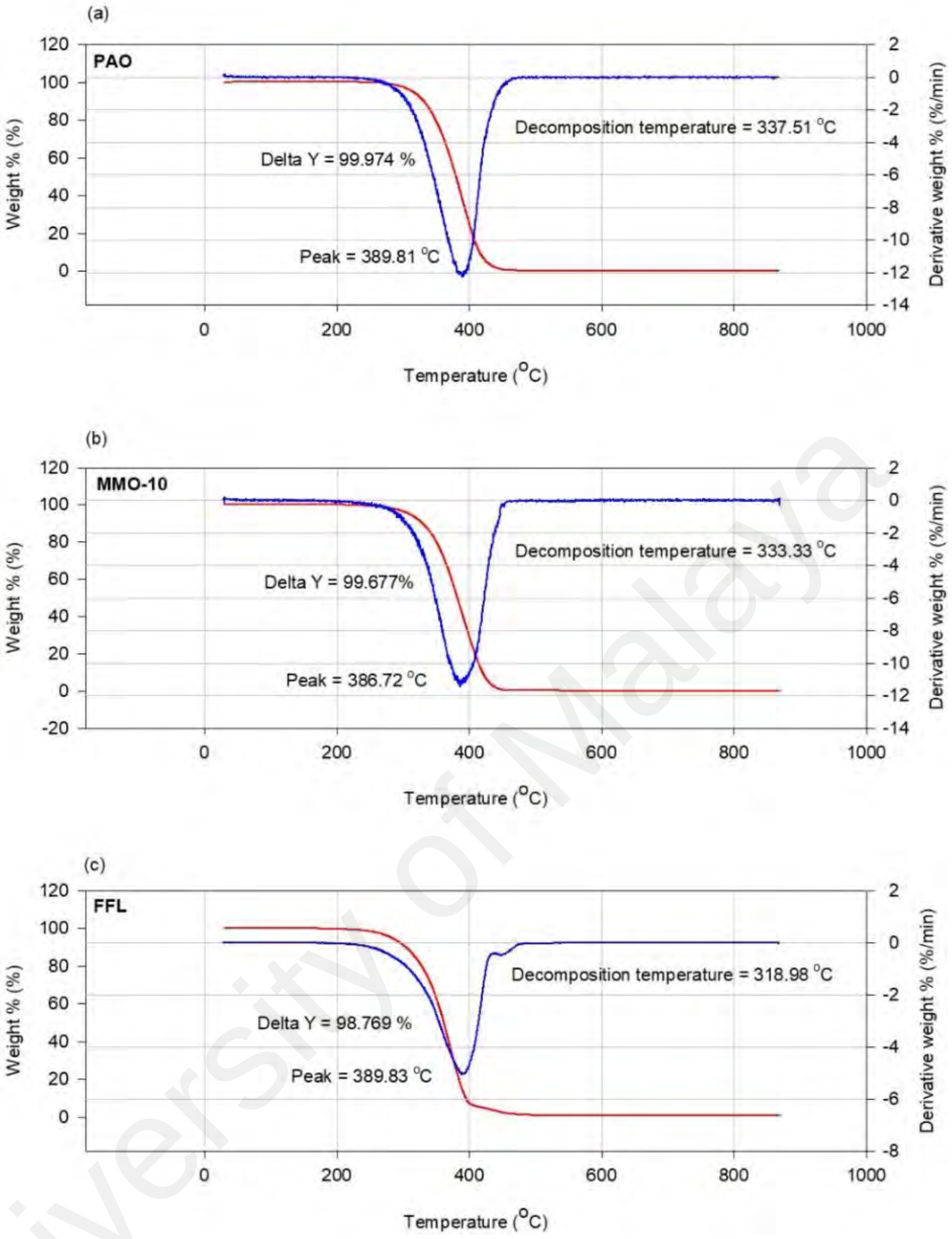

Figure 4.28: TGA analysis of lubricant

4.6.3 MMO-10 as additive in FFL

This section investigates the effect of MMO-10 as an additive in FFL. Additives are used to enhance existing lubricant properties, to suppress undesirable properties and/ or to introduce new properties to a lubricant, therefore it is important for the additives to be compatible and synergized with the existing compounds found in the lubricant. The positive lubricity results of MMO-10 forms the motivation of this investigation. Series of tribological experiment using the four-ball tester was carried out to provide an indication regarding MMO-10 application as an environmentally friendly additive to a commercial full synthetic lubricant. The amount of MMO-10 additive added into the FFL was varied from 1-10%. FFL 100% is indicated as FMO-0.

4.6.3.1 Physicochemical properties

Table 4.16 tabulates the physicochemical properties of FFL-MMO-10 (FMO) blends. There are no distinctive trends observed when MMO-10 blending percentage is increased. This may be due to the complex chemical interactions within the lubricant as FFL contained many additives.

Table 4.16: Physicochemical properties of FMO blends

Sample	Kinematic viscosity (mm^2/s)		Viscosity index	Density at 15° C (g/cm^3)
	40 °C	100 °C		
FMO-0	81.471	13.474	168.8	0.8528
FMO-1	84.401	14.128	173.5	0.8542
FMO-2	84.109	14.066	173.1	0.8542
FMO-5	83.389	13.909	172.1	0.8538
FMO-10	81.618	13.527	169.4	0.8531

(a) ***Oxidation stability***

Studies have found that when vegetable oil-based esters oxidizes, its viscosity will increase and changes to other properties such as iodine value, acid value, and peroxide value will occur due to the chemical interactions within the materials (Acharya et al., 2019; Zuleta et al., 2012). Collectively, these changes will affect the quality and storage of the product (N. Kumar, 2017). In this study, the changes of viscosity was used as an indication of relative oxidation performance, the negative percentage may indicate that the addition of very low percentage of MMO-10 (in this case 1%) into FFL helps in lowering the viscosity of FFL and may assist in improving the oxidative stability of FFL (Figure 4.29).

In the lubricant industry, oxidation is the major cause of oil thickening and the formation of sludge and varnish. Generally, commercial lubricants contain antioxidant additives used to extend the shelf life of the products where it is designed to disrupt the oxidation process that is initiated by the formation of reactive free radicals and peroxides (Lubeletter, 2016). Since FFL is a commercial lubricant, usually antioxidant is present to extend the shelf life of the lubricant. Our results revealed that the addition of a higher percentage of MMO-10 might not be useful in improving the oxidation stability and kinematic viscosity of FFL, which demonstrates that more does not mean better. However, some experiments involving biodiesel have shown that the increase of antioxidant composition increases the oxidation stability of the fuel, as concluded by Devi et al. (2017a), the increased of ginger extract, increases the stability of *Pongamia pinnata* biodiesel compared with no antioxidant added. Conversely, past research also demonstrate that the effectiveness of different types of antioxidant varies in different types of biodiesel (Borugadda et al., 2018; Varatharajan & Pushparani, 2018; Zhou et al., 2017), where some antioxidant may be less reactive in certain type of biodiesel (Orives et al., 2014) while some facing solubility issues (Ni et al., 2020). It is important to note that commercial FFL contains many different types of additives; therefore, the interactions between the MMO-10 and the compounds found inside FFL would be much more complex.

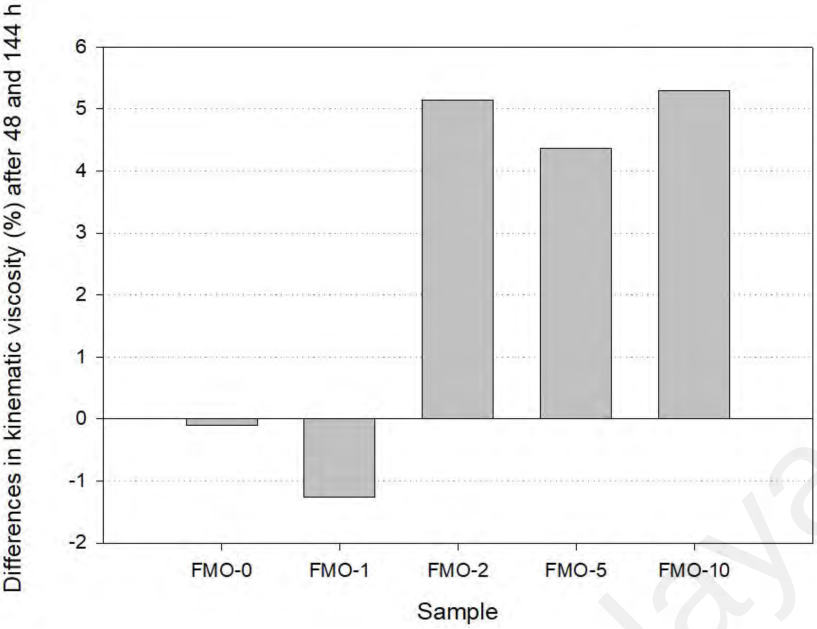

Figure 4.29: Oxidative stability of FMO blends

4.6.3.2 Friction and wear characteristics

Speed increases the COF and wear (Figure 4.30), this agrees with the observation of Fazal et al. (2013). At a lower speed of 1200 rpm, the COF recorded is found to be much lower compared with at 1600 rpm. For example, the COF of FMO-1 has increased from 0.059 at 1200 rpm, to 0.077 at 1400 rpm, and reaching 0.104 at 1600 rpm. Meanwhile, the same trend was also observed for wear, the WSD of FMO-1 were found to have increased from 191.76 to 248.45 μm when the speed were increased from 1200 to 1600 rpm. The heat produced during the high-speed rotation raises the temperature, which in turn decreases the viscosity of a lubricant. When the viscosity is lowered, the capacity to sustain the lubricating film will also be reduced, and the reduced film thickness causes more asperities to contact thus leading to the increased wear.

Temperature increases the wear; the effect of temperature on the tribological characteristics of FMO can be explained as before. The increase in temperature has made a lubricant less viscous, thinning the lubricating film, thus increases the wear. The WSD in this study also increases when the temperature was raised from 40 to 75 °C. The recorded WSD for FMO-5 at 40 °C was 208.56 µm but had increased to 220.45 µm when temperature was raised to 75 °C. The same conclusion was drawn by Haseeb et al. (2010) in an experiment using palm biodiesel, they also found that biodiesel gets oxidized easily at a higher temperature.

Generally, the addition of MMO-10 into FFL improves the wear, but only at a low percentage, i.e. up to 2% (FMO-2). On the contrary, there is no distinct trend on COF improvement. For an additive to be effective, its molecules need to be compatible with the lubricant it is supposed to enhance. In this study, at a low percentage, MMO-10 seems to synergize with the lubricant in reducing wear, but at a level higher than 2%, its benefits seem to diminish. The WDS recorded was increasing with the increase of MMO-10 added, and in some instances, the WDS have exceeded that of the FMO-0. A higher concentration of MMO-10 may have interfered with FFL's anti-wear additive such as Zinc dialkyldithiophosphates (ZDDP) where the polar components in MMO-10 compete with polar ZDDP molecules for surface attachment, reducing the additive's anti-wear performance (Machinery Lubrication, 2018; Shanta et al., 2011). When competition occurred, the anti-wear additive might not be able to lineup systematically on the limited metal surface to form a dense tribofilm structure and, this compromises the strength of the formed tribofilm, evidenced by the increased wear.

(a) 1200 rpm

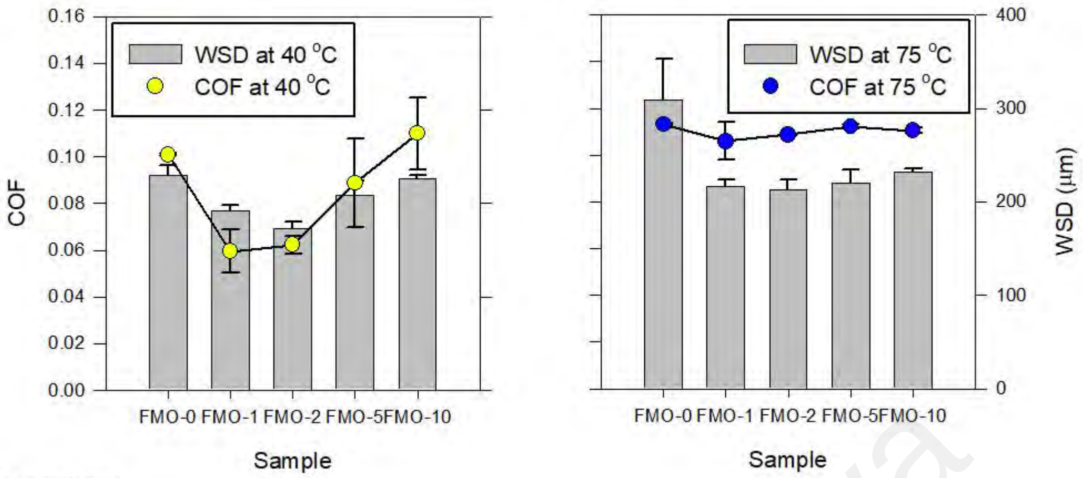

(b) 1400 rpm

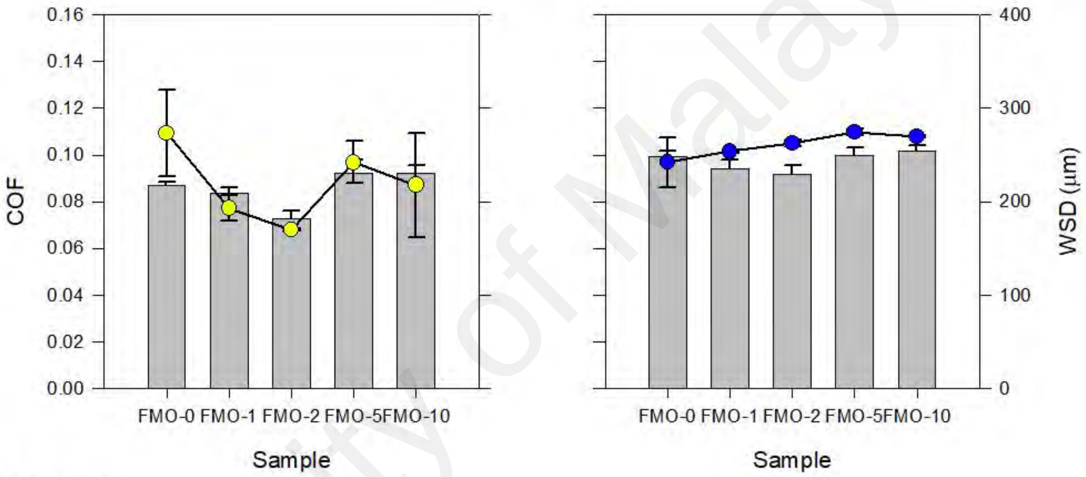

(c) 1600 rpm

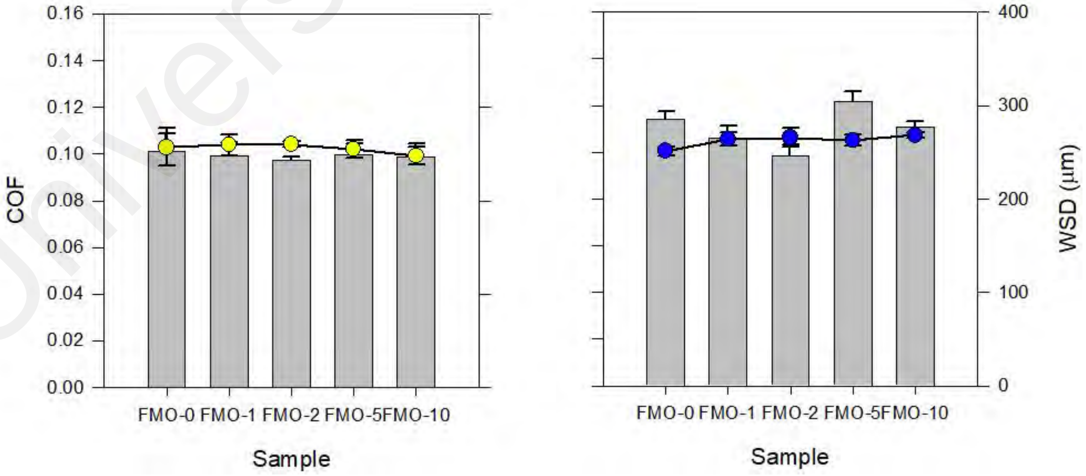

Figure 4.30: COF and WSD of different FMO blends

4.6.4 MMO as additive in diesel

This section investigates the effect of MMO as an additive in diesel. Biodiesel has better lubricity than diesel and past research has found that friction and wear decreases when the percentage of biodiesel blending increases. Hence, in this section, a series of tribological experiment using the four-ball tester with varying loads were carried out, prospecting for MMO as diesel additive. The amount of MMO blended into diesel was varied from 1-10%. Diesel 100% is indicated as DMO-0.

4.6.4.1 Physicochemical properties

The physicochemical properties of the Diesel-MMO (DMO) blends are shown in Table 4.17. The increase of MMO percentage increases the viscosity and density of the diesel. Due to the high acidity of MMO, the resulting DMO blends also possess high AV. The chlorophyll content of MMO increases the reflective index. Additionally, a small percentage of MMO seems to improve the oxidation stability of diesel, but at a higher percentage (more than 2%), the oxidation stability was drastically reduced. It may be due to the high acidity of higher blends. Since high acidity is not desirable for additive application, future works will focus on reducing the acidity of MMO.

Table 4.17: Physicochemical properties of DMO blends

Properties	DMO-0	DMO-1	DMO-2	DMO-5	DMO-8	DMO-10	Limit
Dynamic viscosity (mPas)	2.559	2.627	2.690	3.042	3.460	3.694	
Kinematic viscosity, KV (mm^2/s)	3.087	3.163	3.233	3.631	4.099	4.358	1.9-6.0
Density at 15° C (g/cm^3)	0.845	0.846	0.848	0.854	0.860	0.863	
Acid value, AV (mgKOH/g)	0.862	2.248	3.994	5.321	7.510	11.452	0.5 max
Calorific value (MJ/kg)	44.31	42.4	42.7	42.58	42.54	42.57	
Reflective index	1.4661	1.4665	1.4667	1.4681	1.4695	1.4702	
Oxidation stability, 110 °C (h)	67.85	109.08	110.86	0.10	0.17	0.23	6 h min

4.6.4.2 Friction and wear characteristics

Generally, COF and wear increase with the increase in load (Figure 4.31). It is evident that WSD for the lowest load, at 40 kg, was less than 50% of the WSD recorded at 60 kg. Moreover, at 100 kg load, the recorded WSD and the corresponding COF were the highest. The observation is in agreement with most published work on biodiesel. In a study by Mosarof et al. (2016), they found that even though Palm biodiesel exhibited a higher COF than that of *C. inophyllum* biodiesel blends but the COF demonstrated by both biodiesels were still lower than that of diesel.

Biodiesel is able to impart better lubricity by displaying better COF due to the methyl ester it contained (Hazrat et al., 2015). The lubricating barrier formed from the adsorption the carboxyl groups from ester strongly on to the metal surfaces has separated the mating surfaces, hence offering some scuffing protection compared with diesel that consists of only nonpolar hydrocarbons. Further, it is found that, the increase of MMO percentage reduces the wear and COF, but for MMO above 8% (DMO-8), the wear reduction benefit diminished though the wear recorded were still lowered than that of pure diesel (DMO-

0). Similarly, Jamshaid et al. (2019) also revealed that the increase of cottonseed biodiesel concentration reduces the COF. Conversely, H. Xiao et al. (2019) has found that the change in soybean biodiesel blending percentage, has no significant effect on the COF where the recorded COFs for the biodiesel blends and diesel remained approximately the same, at about 0.12. However, a slight increase of COF was observed for B80 (80% biodiesel blend).

In this study, WSD was successfully reduced 3-13% by adding 1% of MMO into diesel (DMO-1), except for the lowest load and were most prominent at the highest tested load of 100 kg. This indicates that MMO is better at preventing adhesive wear at higher load, agreeing to the finding from the biolubricant EP test. Moreover, reductions in WSD of between 20 – 35% (compared with WSD of DMO-0) were recorded when DMO-8 was used at different loads. Habibullah et al. (2015) also found that pure *Calophyllum inophyllum* biodiesel offered better wear protection than pure diesel where a wear scar diameter (WSD) reduction of 40% was obtained. Furthermore, Jamshaid et al. (2019) reported that when the cotton seed biodiesel concentration was increased, the corresponding WSD decreases where the lubricity was provided by the stearic acid that COME contained. While Fazal et al. (2013) further revealed that for palm biodiesel, the reduction of WSD were most significant at the blending range of 10-20%. From these observations, it can be deduced that MMO has demonstrated good potential as a friction improver and anti-wear additive for diesel just like its vegetable oil-based counterparts due to the creation of a lubricating film between the rubbing surfaces.

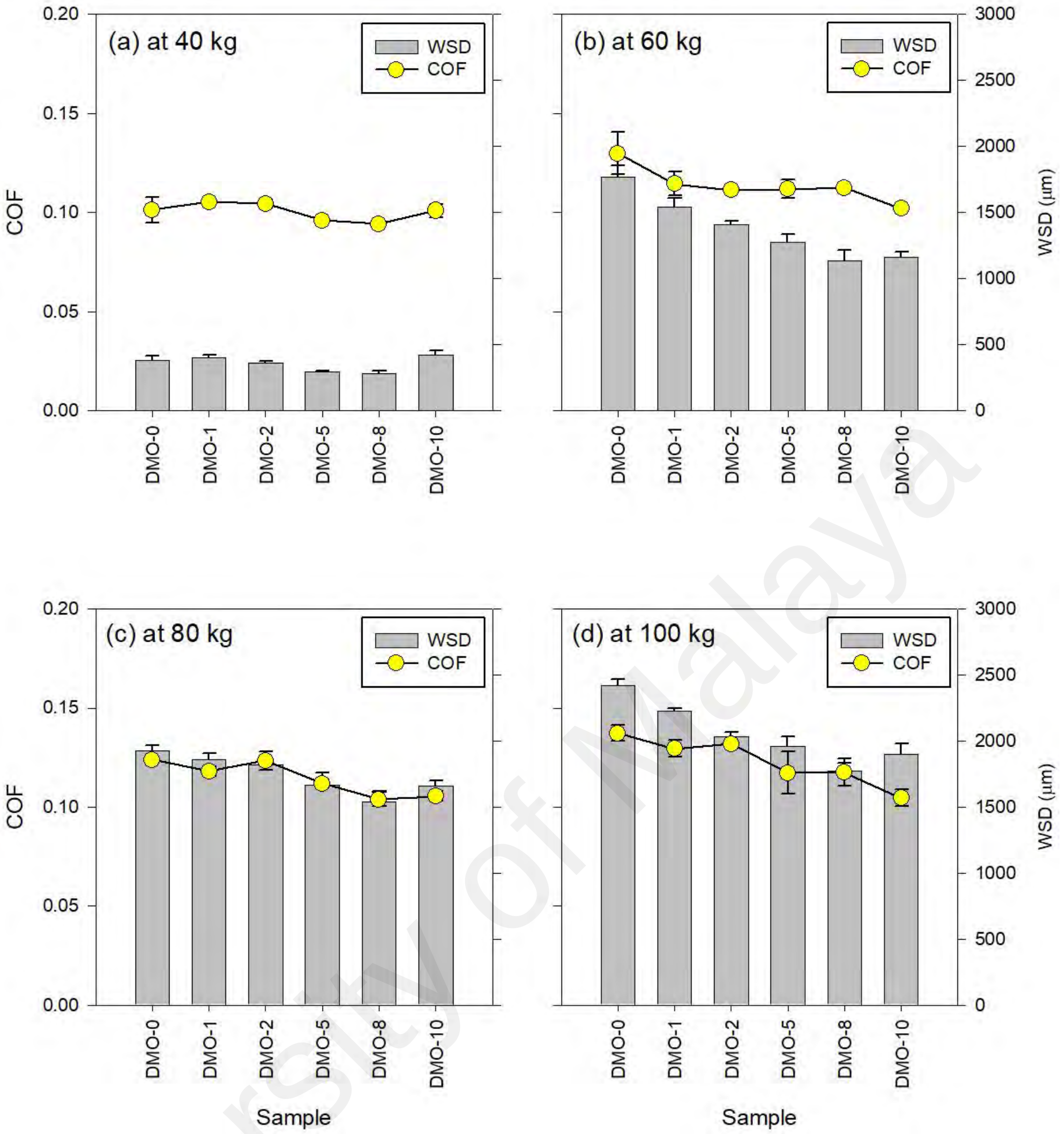

Figure 4.31: COF and WSD of different DMO blends

CHAPTER 5: CONCLUSION

The pressing demand for a green lubricant has led to the intense exploration of biolubricant. Generally, biolubricant is formulated from vegetable oil, which is triglyceride based and since microalgae contain triglyceride; therefore, it could become a possible candidate. The main aim of this research was to assess the potential of using microalgae oil for biolubricant application and the following are the conclusions drawn from this study:

Five local microalgae species have been successfully isolated and cultured. Among all the tested species, which include the two species purchased from a local vendor, *Chlorella* sp. has the best growth and biomass productivity; it was followed by *Ankistrodesmus* sp. (one of the isolates). In terms of for lipid yield, *Ankistrodesmus* sp. was slightly better than *Chlorella* sp. Even though both microalgae exhibited comparable growth rate and lipid yield (higher than the other tested species), *Chlorella* sp. was selected for further testing over *Ankistrodesmus* sp. due to its lipid composition as this species contained higher amount of long carbon chain fatty acids and unsaturation. Higher amount of long carbon chain fatty acids and unsaturation are found to produce thicker lubricating film and exhibit better cold weather performance. The lipid yields for all the tested species were low because, under optimum growth condition, microalgae produce very small amount of neutral lipid. We found that by changing the extraction solvent to Chloroform: Methanol (2:1), lipid yield was successfully increase to 68% for *Ankistrodesmus* sp. compared with using petroleum ether. The combination of non-polar and polar solvents have extracted both neutral and polar lipid (glycolipid in the chloroplast).

The physicochemical properties of an ester-based lubricant are directly affected by the lipid composition of the feedstock. Generally, microalgae oil are mostly made up of straight chain fatty acid esters and polarity are impart by the carboxyl functional group. In this study, long chain fatty acid (consist of 13-21 carbons) and unsaturated fatty acid dominated the compositions of all the tested microalgae. The physicochemical properties (KV and CFPP) derived from the fatty acid compositions of the microalgae-oil were found to be within the acceptable range for biodiesel except for IV. The high IVs were attributed by the high content of polyunsaturated fatty acid (PUFA) the microalgae contained. Apart from the high IV, it can be deduced that the microalgae tested in this study were capable of imparting good lubricity due to the high concentration of long chain fatty acid, minimum chain branching and good polarity.

After evaluating the growth, biomass productivity and lipid yield of all the tested species, *Chlorella* sp. was selected for further testing. We found that the two-step chemical modification of esterification followed by transesterification can significantly reduced the acidity of the extracted crude microalgae oil (CMO) as free fatty acids were converted into esters. The GCMS analysis has revealed that besides esters, other compounds like sterols and ketones were also present in the modified microalgae oil (MMO). Additionally, MMO-10 is also thermally stable in the pyrolysis process where its decomposition temperature was just 4 °C lower than pure PAO but shows better combustion ability than PAO. This is mainly due to its oxygen content. Moreover, MMO-10 has significantly extended the oxidative induction time (OIT) of pure PAO, improving PAO's oxidation stability to more than 24 folds that is probably attributed to the presence of natural antioxidant such as stigmasterol and β-sitosterol in MMO-10.

In the biolubricant application, MMO addition was found to improve the friction and wear of PAO (base oil). The formation of a lubricating film due to the adsorption of the ester groups on the rubbing surfaces reduces the friction and minimizes the wear by preventing direct metal-to-metal contact. Moreover, the increase of MMO blending percentage increases these abilities, however at a higher blending percentage of above 10% of MMO (MMO-10) no further improvement was found. The same trend was also observed for MMO-diesel blends (DMO). For blending above 8% of MMO (DMO-8), the anti-wear advantage ceased though the recorded wear is still lower than that of pure diesel. Furthermore, MMO-10 also demonstrated that it is a good anti-wear and extreme pressure additive where our results further revealed that MMO-10 exhibited a load carrying capacity (an important parameter for EP) that was comparable to that of a commercial FFL. Additionally, wear reduction was also observed when MMO-10 was used as an additive in FFL, but only at a very low blending percentage (FMO-2).

Collectively, modified microalgae oil (MMO) has shown great potential to be exploited for engine and machinery applications particularly MMO-10. Yet the only drawback, for the time being, is the production cost. However, if the cultivation of microalgae can become part of an integrated water remediation system, the production cost can be reduced where the biomass attained from the system can be used as feedstock.

5.1 Future study

In order to make microalgae oil based biolubricant viable, the following are proposed for future studies:

(a) Growth rate and lipid accumulation - As the microalgae used in this study were not optimized for growth rate and lipid accumulation, therefore for future work; the focus would be on enhancing these features. Past research has indicate that nutrient manipulation of the growth media can achieve these objectives.

(b) Further chemical modifications to improve MMO quality - The upgraded MMO in this study have very high acidity. Past research has shown that high acidity has an adverse effect on oxidation stability and enhances corrosion. In order to be a potential biolubricant, further chemical modifications may need to be employed to improve the overall quality of MMO, particularly the acidity.

(c) Chlorophyll removal - Chlorophyll is a priced commodity. It would be ideal, if chlorophyll can be removed and recovered as a high-value by-product of microalgae oil based biolubricant.

(d) More in-depth tribological testing - Further investigation is important to better understand the behavior of the MMO. To answer questions like how compatible MMO is with the surrounding environment. Alternatively, how long MMO biolubricant will last before the next oil change is needed in a closed system application.

REFERENCES

Abdullah, B. M., and Salimon, J. (2010). Epoxidation of vegetable oils and fatty acids: catalysts, methods and advantages. *Journal of Applied Sciences, 10*(15), 1545-1553.

Abinandan, S., Subashchandrabose, S. R., Panneerselvan, L., Venkateswarlu, K., and Megharaj, M. (2019). Potential of acid-tolerant microalgae, Desmodesmus sp. MAS1 and Heterochlorella sp. MAS3, in heavy metal removal and biodiesel production at acidic pH. *Bioresource Technology, 278*, 9-16.

Abomohra, A. E.-F., El-Sheekh, M., and Hanelt, D. (2017). Screening of marine microalgae isolated from the hypersaline Bardawil lagoon for biodiesel feedstock. *Renewable Energy, 101*, 1266-1272.

Acharya, N., Nanda, P., Panda, S., and Acharya, S. (2019). A comparative study of stability characteristics of mahua and jatropha biodiesel and their blends. *Journal of King Saud University - Engineering Sciences, 31*(2), 184-190.

Adhvaryu, A., and Erhan, S. (2002). Epoxidized soybean oil as a potential source of high-temperature lubricants. *Industrial Crops and Products, 15*(3), 247-254.

Adhvaryu, A., Erhan, S. Z., and Perez, J. M. (2004). Tribological studies of thermally and chemically modified vegetable oils for use as environmentally friendly lubricants. *Wear, 257*(3), 359-367.

Adu-Mensah, D., Mei, D., Zuo, L., Zhang, Q., and Wang, J. (2019). A review on partial hydrogenation of biodiesel and its influence on fuel properties. *Fuel, 251*, 660-668.

Aguilera, A. F., Tolvanen, P., Wärnå, J., Leveneur, S., and Salmi, T. (2019). Kinetics and reactor modelling of fatty acid epoxidation in the presence of heterogeneous catalyst. *Chemical Engineering Journal*, 121936.

Ahmed, W. A., Yarmo, A., Salih, N., Derawi, M. D., Yusop, M. R., and Salimon, J. (2015). Synthesis and Lubricity Properties Analysis of Branched Dicarboxylate Esters Based Lubricant. *Malaysian Journal of Analytical Sciences, 19*(1), 106-117.

Al-Bukhaiti, M., Al-Hatab, K., and Gabbert, U. (2011). The influence af high contact stresses and lubricant type an the rolling contact fatigue life and failure mode of Aisi 52100 Steel Balls. *Emirates Journal for Engineering Research, 16*(1), 9-22.

Allen, M. M., and Stanier, R. (1968). Selective isolation of blue-green algae from water and soil. *Microbiology, 51*(2), 203-209.

Altunoz, M., Pirrotta, O., Forti, L., Allesina, G., Pedrazzi, S., Obali, O., Tartarini, P., and Arru, L. (2017). Combined effects of LED lights and chicken manure on Neochloris oleoabundans growth. *Bioresource Technology, 244*, 1261-1268.

Amiril, S. A. S., Rahim, E. A., Embong, Z., and Syahrullail, S. (2018). Tribological investigations on the application of oil-miscible ionic liquids additives in modified Jatropha-based metalworking fluid. *Tribology International, 120*, 520-534.

Anastopoulos, G., Kaligeros, S., Schinas, P., Zannikou, Y., Karonis, D., and Zannikos, F. (2017). The Impact of Fatty Acid Diisopropanolamides on Marine Gas Oil Lubricity. *Lubricants, 5*(3), 28.

Andersen, R. A. (2005). *Algal culturing techniques*: Academic press.

Anez-Bustillos, L., Dao, D. T., Fell, G. L., Baker, M. A., Gura, K. M., Bistrian, B. R., and Puder, M. (2018). Redefining essential fatty acids in the era of novel intravenous lipid emulsions. *Clinical Nutrition, 37*(3), 784-789.

Ansari, A. A., Khoja, A. H., Nawar, A., Qayyum, M., and Ali, E. (2017). Wastewater treatment by local microalgae strains for CO 2 sequestration and biofuel production. *Applied Water Science, 7*(7), 4151-4158.

Anto, S., Pugazhendhi, A., and Mathimani, T. (2019). Lipid enhancement through nutrient starvation in Chlorella sp. and its fatty acid profiling for appropriate bioenergy feedstock. *Biocatalysis and Agricultural Biotechnology, 20*, 101179.

Aravind, A., Joy, M. L., and Nair, K. P. (2015). Lubricant properties of biodegradable rubber tree seed (Hevea brasiliensis Muell. Arg) oil. *Industrial Crops and Products, 74*, 14-19.

Archard, J. (1953). Contact and rubbing of flat surfaces. *Journal of applied physics, 24*(8), 981-988.

Askwith, T., Cameron, A., and Crouch, R. (1966). Chain length of additives in relation to lubricants in thin film and boundary lubrication. *Proc. R. Soc. Lond. A, 291*(1427), 500-519.

Aziz, N. A. M., Yunus, R., Rashid, U., and Zulkifli, N. W. M. (2016). Temperature effect on tribological properties of polyol ester-based environmentally adapted lubricant. *Tribology International, 93*, 43-49.

Baldisserotto, C., Popovich, C., Giovanardi, M., Sabia, A., Ferroni, L., Constenla, D., Leonardi, P., and Pancaldi, S. (2016). Photosynthetic aspects and lipid profiles in the mixotrophic alga Neochloris oleoabundans as useful parameters for biodiesel production. *Algal Research, 16*, 255-265.

Ball, K. F., Bostick, J. G., and Brennan, T. J. (1999). Fuel lubricity from blends of a diethanolamine derivative and biodiesel. In: Google Patents.

Bayer, R. G. (1994). Mechanical wear prediction and prevention. *Marcel! Dekker, Inc, P. O. Box 5005, Monticello, NY 12701-5185, USA, 1994. 657*.

Bayramoğlu, G., Tuzun, I., Celik, G., Yilmaz, M., and Arica, M. Y. (2006). Biosorption of mercury(II), cadmium(II) and lead(II) ions from aqueous system by microalgae Chlamydomonas reinhardtii immobilized in alginate beads. *International Journal of Mineral Processing, 81*(1), 35-43.

Bayramoğlu, G., and Yakup Arıca, M. (2009). Construction a hybrid biosorbent using Scenedesmus quadricauda and Ca-alginate for biosorption of Cu(II), Zn(II) and Ni(II): Kinetics and equilibrium studies. *Bioresource Technology, 100*(1), 186-193.

Bhaumik, S., Maggirwar, R., Datta, S., and Pathak, S. D. (2018). Analyses of anti-wear and extreme pressure properties of castor oil with zinc oxide nano friction modifiers. *Applied Surface Science, 449*, 277-286.

Bhushan, B. (2013). *Introduction to tribology*: John Wiley & Sons.

Bin Sayeed, M. S., Karim, S. M. R., Sharmin, T., and Morshed, M. M. (2016). Critical Analysis on Characterization, Systemic Effect, and Therapeutic Potential of Beta-Sitosterol: A Plant-Derived Orphan Phytosterol. *Medicines, 3*(4), 29.

Biresaw, G., Adhvaryu, A., and Erhan, S. Z. (2003). Friction properties of vegetable oils. *Journal of the American Oil Chemists' Society, 80*(7), 697.

Bischoff, H. W., and Bold, H. C. (1963). *Some soil algae from Enchanted Rock and related algal species*: University of Texas.

Blanco, A., Sanz, B., Llama, M. a. J., and Serra, J. L. (1999). Biosorption of heavy metals to immobilised Phormidium laminosum biomass. *Journal of Biotechnology, 69*(2), 227-240.

Boidi, G., Tertuliano, I. S., Profito, F. J., de Rossi, W., and Machado, I. F. (2019). Effect of laser surface texturing on friction behaviour in elastohydrodynamically lubricated point contacts under different sliding-rolling conditions. *Tribology International*, In press, corrected proof.

Booser, E. R. (1997). *Tribology Data Handbook: An Excellent Friction, Lubrication, and Wear Resource*: CRC Press.

Borugadda, V. B., Dalai, A. K., and Ghosh, S. (2018). Effects of natural additives on performance of canola biodiesel and its structurally modified derivatives. *Industrial Crops and Products, 125*, 303-313.

Boshui, C., Kecheng, G., Jianhua, F., Jiang, W., Jiu, W., and Nan, Z. (2015). Tribological characteristics of monodispersed cerium borate nanospheres in biodegradable rapeseed oil lubricant. *Applied Surface Science, 353*, 326-332.

Bringi, N. V. (1987). *Non-traditional oilseeds and oils in India*: Oxford and IBH Pub. Co.

Brown Jr, E. (1971). Friction and wear testing with the modern four-ball apparatus. *Wear, 17*(5-6), 381-388.

Cañizares-Villanueva, R. O., Martínez-Jerónimo, F., and Espinosa-Chávez, F. (2000). Acute toxicity to Daphnia magna of effluents containing Cd, Zn, and a mixture Cd-Zn, after metal removal by Chlorella vulgaris. *Environmental Toxicology, 15*(3), 160-164.

Cavalcanti, E. D. C., Aguieiras, É. C. G., da Silva, P. R., Duarte, J. G., Cipolatti, E. P., Fernandez-Lafuente, R., da Silva, J. A. C., and Freire, D. M. G. (2018). Improved production of biolubricants from soybean oil and different polyols via esterification reaction catalyzed by immobilized lipase from Candida rugosa. *Fuel, 215*, 705-713.

Chan, C.-H., Tang, S. W., Mohd, N. K., Lim, W. H., Yeong, S. K., and Idris, Z. (2018). Tribological behavior of biolubricant base stocks and additives. *Renewable and Sustainable Energy Reviews, 93*, 145-157.

Chang, H. S., Spikes, H., and Bunemann, T. (1992). The shear stress properties of ester lubricants in elastohydrodynamic contacts. *Journal of Synthetic Lubrication, 9*(2), 91-114.

Chapman, R. L. (2013). Algae: the world's most important "plants"—an introduction. *Mitigation and Adaptation Strategies for Global Change, 18*(1), 5-12.

Chen, Y.-C. (2003). Immobilized Isochrysis galbana (Haptophyta) for long-term storage and applications for feed and water quality control in clam (Meretrix lusoria) cultures. *Journal of Applied Phycology, 15*(5), 439-444.

Chen, Z., Ma, W., and Han, M. (2008). Biosorption of nickel and copper onto treated alga (Undaria pinnatifida): Application of isotherm and kinetic models. *Journal of Hazardous Materials, 155*(1), 327-333.

Cheng, J., Li, K., Yang, Z., Lu, H., Zhou, J., and Cen, K. (2016). Gradient domestication of Haematococcus pluvialis mutant with 15% CO2 to promote biomass growth and astaxanthin yield. *Bioresource Technology, 216*, 340-344.

Chethan, K. N., Satish Shenoy, B., and Shyamasunder Bhat, N. (2018). Role of different orthopedic biomaterials on wear of hip joint prosthesis: A review. *Materials Today: Proceedings, 5*(10, Part 1), 20827-20836.

Chi, N. T. L., Duc, P. A., Mathimani, T., and Pugazhendhi, A. (2019). Evaluating the potential of green alga Chlorella sp. for high biomass and lipid production in biodiesel viewpoint. *Biocatalysis and Agricultural Biotechnology, 17*, 184-188.

Chisti, Y. (2007). Biodiesel from microalgae. *Biotechnology Advances, 25*(3), 294-306.

Chiu, S.-Y., Kao, C.-Y., Chen, C.-H., Kuan, T.-C., Ong, S.-C., and Lin, C.-S. (2008). Reduction of CO2 by a high-density culture of Chlorella sp. in a semicontinuous photobioreactor. *Bioresource Technology, 99*(9), 3389-3396.

Chiu, S.-Y., Kao, C.-Y., Huang, T.-T., Lin, C.-J., Ong, S.-C., Chen, C.-D., Chang, J.-S., and Lin, C.-S. (2011). Microalgal biomass production and on-site bioremediation of carbon dioxide, nitrogen oxide and sulfur dioxide from flue gas using Chlorella sp. cultures. *Bioresource Technology, 102*(19), 9135-9142.

Chiu, S.-Y., Tsai, M.-T., Kao, C.-Y., Ong, S.-C., and Lin, C.-S. (2009). The air-lift photobioreactors with flow patterning for high-density cultures of microalgae and carbon dioxide removal. *Engineering in Life Sciences, 9*(3), 254-260.

Crabbe, E., Nolasco-Hipolito, C., Kobayashi, G., Sonomoto, K., and Ishizaki, A. (2001). Biodiesel production from crude palm oil and evaluation of butanol extraction and fuel properties. *Process biochemistry, 37*(1), 65-71.

Credence Research. (2017). *Algae Products Market By Application (Nutraceuticals, Food & Feed Supplements, Pharmaceuticals, Paints & Colorants, Pollution Control, Others) - Growth, Future Prospects, Competitive Analysis, and Forecast 2017 - 2025*. Retrieved from https://www.credenceresearch.com/report/algae-products-market

D'Alessandro, E. B., and Antoniosi Filho, N. R. (2016). Concepts and studies on lipid and pigments of microalgae: A review. *Renewable and Sustainable Energy Reviews, 58*, 832-841.

Damasceno, S. S., Santos, N. A., Santos, I. M. G., Souza, A. L., Souza, A. G., and Queiroz, N. (2013). Caffeic and ferulic acids: An investigation of the effect of antioxidants on the stability of soybean biodiesel during storage. *Fuel, 107*, 641-646.

Danping, W., and Spikes, H. A. (1986). The lubricity of diesel fuels. *Wear, 111*(2), 217-235.

Darriba, D., Taboada, G. L., Doallo, R., and Posada, D. (2012). jModelTest 2: more models, new heuristics and parallel computing. *Nature methods, 9*(8), 772-772.

David, B. (2015). Fats and oils - are all fats the same? Retrieved from https://www.david-bender.co.uk/metabonline/lipids/fats/fats14.html

de-Bashan, L. E., Moreno, M., Hernandez, J.-P., and Bashan, Y. (2002). Removal of ammonium and phosphorus ions from synthetic wastewater by the microalgae Chlorella vulgaris coimmobilized in alginate beads with the microalgae growth-promoting bacterium Azospirillum brasilense. *Water Research, 36*(12), 2941-2948.

de Sousa, L. S., de Moura, C. V. R., de Oliveira, J. E., and de Moura, E. M. (2014). Use of natural antioxidants in soybean biodiesel. *Fuel, 134*, 420-428.

Delgado, M. A., Quinchia, L. A., Spikes, H. A., and Gallegos, C. (2017). Suitability of ethyl cellulose as multifunctional additive for blends of vegetable oil-based lubricants. *Journal of Cleaner Production, 151*, 1-9.

Devan, P. K., and Mahalakshmi, N. V. (2009). Study of the performance, emission and combustion characteristics of a diesel engine using poon oil-based fuels. *Fuel Processing Technology, 90*(4), 513-519.

Devi, A., Das, V. K., and Deka, D. (2017a). Ginger extract as a nature based robust additive and its influence on the oxidation stability of biodiesel synthesized from non-edible oil. *Fuel, 187*, 306-314.

Devi, A., Das, V. K., and Deka, D. (2017b). Ginger extract as a nature based robust additive and its influence on the oxidation stability of biodiesel synthesized from non-edible oil. *Fuel, 187*(Supplement C), 306-314.

Dinda, S., Patwardhan, A. V., Goud, V. V., and Pradhan, N. C. (2008). Epoxidation of cottonseed oil by aqueous hydrogen peroxide catalysed by liquid inorganic acids. *Bioresource Technology, 99*(9), 3737-3744.

Doucha, J., Straka, F., and Lívanský, K. (2005). Utilization of flue gas for cultivation of microalgae Chlorella sp.) in an outdoor open thin-layer photobioreactor. *Journal of Applied Phycology, 17*(5), 403-412.

Duarte, J. H., de Morais, E. G., Radmann, E. M., and Costa, J. A. V. (2017). Biological CO2 mitigation from coal power plant by Chlorella fusca and Spirulina sp. *Bioresource Technology, 234*, 472-475.

Dwyer-Joyce, R. S., Sayles, R. S., and Ioannides, E. (1994). An investigation into the mechanisms of closed three-body abrasive wear. *Wear, 175*(1), 133-142.

El Boulifi, N., Bouaid, A., Martinez, M., and Aracil, J. (2010). Process optimization for biodiesel production from corn oil and its oxidative stability. *International Journal of Chemical Engineering, 2010*.

Elmhurst College. (2003). Virtual Chembook. Retrieved from http://chemistry.elmhurst.edu/vchembook/213organicfcgp.html

Enamala, M. K., Enamala, S., Chavali, M., Donepudi, J., Yadavalli, R., Kolapalli, B., Aradhyula, T. V., Velpuri, J., and Kuppam, C. (2018). Production of biofuels from microalgae - A review on cultivation, harvesting, lipid extraction, and numerous applications of microalgae. *Renewable and Sustainable Energy Reviews, 94*, 49-68.

Erhan, S. Z., Sharma, B. K., and Perez, J. M. (2006). Oxidation and low temperature stability of vegetable oil-based lubricants. *Industrial Crops and Products, 24*(3), 292-299.

Errichello, R., and Cardis, A. B. (2014). Additives: Anti-wear vs. anti-scuff. Is one better? *Gear Technology*. August 2014. Retrieved from https://www.geartechnology.com/articles/0814/Additives:_Anti-Wear_vs_Anti-Scuff/

Farfan-Cabrera, L. I., Gallardo-Hernández, E. A., Pérez-González, J., Marín-Santibáñez, B. M., and Lewis, R. (2019). Effects of Jatropha lubricant thermo-oxidation on the tribological behaviour of engine cylinder liners as measured by a reciprocating friction test. *Wear, 426-427*, 910-918.

Faried, M., Samer, M., Abdelsalam, E., Yousef, R. S., Attia, Y. A., and Ali, A. S. (2017). Biodiesel production from microalgae: Processes, technologies and recent advancements. *Renewable and Sustainable Energy Reviews, 79*(Supplement C), 893-913.

Fazal, M. A., Haseeb, A., and Masjuki, H. H. (2011). Effect of temperature on the corrosion behavior of mild steel upon exposure to palm biodiesel. *Energy, 36*(5), 3328-3334.

Fazal, M. A., Haseeb, A., and Masjuki, H. H. (2013). Investigation of friction and wear characteristics of palm biodiesel. *Energy Conversion and Management, 67*, 251-256.

Fazal, M. A., Suhaila, N. R., Haseeb, A. S. M. A., Rubaiee, S., and Al-Zahrani, A. (2018). Influence of copper on the instability and corrosiveness of palm biodiesel and its blends: An assessment on biodiesel sustainability. *Journal of Cleaner Production, 171*, 1407-1414.

Fernandes, D. M., Sousa, R. M. F., de Oliveira, A., Morais, S. A. L., Richter, E. M., and Muñoz, R. A. A. (2015). Moringa oleifera: A potential source for production of biodiesel and antioxidant additives. *Fuel, 146*, 75-80.

Fernandes, K. V., Papadaki, A., da Silva, J. A. C., Fernandez-Lafuente, R., Koutinas, A. A., and Freire, D. M. G. (2018). Enzymatic esterification of palm fatty-acid distillate for the production of polyol esters with biolubricant properties. *Industrial Crops and Products, 116*, 90-96.

Fernández-Linares, L. C., Guerrero Barajas, C., Durán Páramo, E., and Badillo Corona, J. A. (2017). Assessment of Chlorella vulgaris and indigenous microalgae biomass with treated wastewater as growth culture medium. *Bioresource Technology, 244*, 400-406.

Fettes, E. M. (1964). *Chemical reactions of polymers* (Vol. 19): Interscience Publishers.

Folch, J., Ascoli, I., Lees, M., Meath, J., and LeBaron, F. (1951). Preparation of lipide extracts from brain tissue. *J. biol. Chem, 191*(2), 833-841.

Fox, N., and Stachowiak, G. (2007). Vegetable oil-based lubricants—a review of oxidation. *Tribology International, 40*(7), 1035-1046.

Fox, N., Tyrer, B., and Stachowiak, G. (2004). Boundary lubrication performance of free fatty acids in sunflower oil. *Tribology letters, 16*(4), 275-281.

Frankel, E. N. (2014). *Lipid Oxidation*: Elsevier Science.

Freitas, B. C. B., Morais, M. G., and Costa, J. A. V. (2017). Chlorella minutissima cultivation with CO2 and pentoses: Effects on kinetic and nutritional parameters. *Bioresource Technology, 244*, 338-344.

Gabay, O., Sanchez, C., Salvat, C., Chevy, F., Breton, M., Nourissat, G., Wolf, C., Jacques, C., and Berenbaum, F. (2010). Stigmasterol: a phytosterol with potential anti-osteoarthritic properties. *Osteoarthritis and Cartilage, 18*(1), 106-116.

Garnham, G. W., Codd, G. A., and Gadd, G. M. (1992). Accumulation of cobalt, zinc and manganese by the estuarine green microalga Chlorella salina immobilized in alginate microbeads. *Environmental science & technology, 26*(9), 1764-1770.

Geller, D. P., and Goodrum, J. W. (2004). Effects of specific fatty acid methyl esters on diesel fuel lubricity. *Fuel, 83*(17-18), 2351-2356.

George, B., Pancha, I., Desai, C., Chokshi, K., Paliwal, C., Ghosh, T., and Mishra, S. (2014). Effects of different media composition, light intensity and photoperiod on morphology and physiology of freshwater microalgae Ankistrodesmus falcatus – A potential strain for bio-fuel production. *Bioresource Technology, 171*, 367-374.

Gharavi, N., and El-Kadi, A. O. S. (2005). Tert-butylhydroquinone is a novel aryl hydrocarbon receptor ligand. *Drug Metabolism and Disposition, 33*(3), 365.

Ghazi, T. I. M., Resul, M. F. G., and Idris, A. (2009). Bioenergy II: production of biodegradable lubricant from jatropha curcas and trimethylolpropane. *International Journal of Chemical Reactor Engineering, 7*(1).

Goh, B. H. H., Ong, H. C., Cheah, M. Y., Chen, W.-H., Yu, K. L., and Mahlia, T. M. I. (2019). Sustainability of direct biodiesel synthesis from microalgae biomass: A critical review. *Renewable and Sustainable Energy Reviews, 107*, 59-74.

Gokhale, S. V., Jyoti, K. K., and Lele, S. S. (2009). Modeling of chromium (VI) biosorption by immobilized Spirulina platensis in packed column. *Journal of Hazardous Materials, 170*(2), 735-743.

Goldman, J. C., Azov, Y., Riley, C. B., and Dennett, M. R. (1982). The effect of pH in intensive microalgal cultures. I. Biomass regulation. *Journal of experimental marine biology and ecology, 57*(1), 1-13.

Golshokouh, I., Syahrullail, S., Ani, F. N., and Masjuki, H. (2014). Investigation of Palm Fatty Acid Distillate Oil as an Alternative to Petrochemical Based Lubricant. *Journal of Oil Palm Research, 26*(1), 25-36.

Griffiths, M. J., van Hille, R. P., and Harrison, S. T. L. (2012). Lipid productivity, settling potential and fatty acid profile of 11 microalgal species grown under nitrogen replete and limited conditions. *Journal of Applied Phycology, 24*(5), 989-1001.

Gryglewicz, S., Piechocki, W., and Gryglewicz, G. (2003). Preparation of polyol esters based on vegetable and animal fats. *Bioresource Technology, 87*(1), 35-39.

Gulzar, M., Masjuki, H. H., Varman, M., Kalam, M. A., Mufti, R. A., Zulkifli, N. W. M., Yunus, R., and Zahid, R. (2015). Improving the AW/EP ability of chemically modified palm oil by adding CuO and MoS2 nanoparticles. *Tribology International, 88*, 271-279.

Gupta, V. K., and Rastogi, A. (2008). Biosorption of lead(II) from aqueous solutions by non-living algal biomass Oedogonium sp. and Nostoc sp.—A comparative study. *Colloids and Surfaces B: Biointerfaces, 64*(2), 170-178.

Gupta, V. K., Rastogi, A., and Nayak, A. (2010). Biosorption of nickel onto treated alga (Oedogonium hatei): Application of isotherm and kinetic models. *Journal of Colloid and Interface Science, 342*(2), 533-539.

Habibullah, M., Masjuki, H. H., Kalam, M. A., Zulkifli, N. W. M., Masum, B. M., Arslan, A., and Gulzar, M. (2015). Friction and wear characteristics of Calophyllum inophyllum biodiesel. *Industrial Crops and Products, 76*, 188-197.

Halim, R., Gladman, B., Danquah, M. K., and Webley, P. A. (2011). Oil extraction from microalgae for biodiesel production. *Bioresource Technology, 102*(1), 178-185.

Hamrock, B. J., and Dowson, D. (1981). Ball bearing lubrication: the elastohydrodynamics of elliptical contacts.

Hamrock, B. J., Schmid, S. R., and Jacobson, B. O. (2004). *Fundamentals of fluid film lubrication*: CRC press.

Haseeb, A., Sia, S. Y., Fazal, M. A., and Masjuki, H. H. (2010). Effect of temperature on tribological properties of palm biodiesel. *Energy, 35*(3), 1460-1464.

Hasenhuettl, G. L. (2000). Fats and fatty oils. *Kirk‐Othmer Encyclopedia of Chemical Technology*, 1-37.

Hashem, A. I., Abou Elmagd, W. S. I., Salem, A. E., El-Kasaby, M., and El-Nahas, A. M. (2013). Conversion of Some Vegetable Oils into Synthetic Lubricants. *Energy Sources, Part A: Recovery, Utilization, and Environmental Effects, 35*(5), 397-400.

Hazrat, M. A., Rasul, M. G., and Khan, M. M. K. (2015). Lubricity Improvement of the Ultra-low Sulfur Diesel Fuel with the Biodiesel. *Energy Procedia, 75*, 111-117.

Hong, I. K., Lee, J. R., and Lee, S. B. (2015). Fuel properties of canola oil and lard biodiesel blends: Higher heating value, oxidative stability, and kinematic viscosity. *Journal of Industrial and Engineering Chemistry, 22*, 335-340.

Hughes, J. M., Mushrush, G. W., and Hardy, D. R. (2003). The Relationship between the Base Extractable Species Found in Middle Distillate Fuel and Lubricity. *Energy & Fuels, 17*(2), 444-449.

Humood, M., Ghamary, M. H., Lan, P., Iaccino, L. L., Bao, X., and Polycarpou, A. A. (2019). Influence of additives on the friction and wear reduction of oil-based drilling fluid. *Wear, 422-423*, 151-160.

Hunter, W., and Zienkiewicz, O. (1960). Effect of temperature variations across the lubricant films in the theory of hydrodynamic lubrication. *Journal of Mechanical Engineering Science, 2*(1), 52-58.

Hutchings, I. (1992). Tribology: friction and wear of engineering materials. *Mater. Des, 13*(3), 187.

Hwang, H.-S., and Erhan, S. Z. (2006). Synthetic lubricant basestocks from epoxidized soybean oil and Guerbet alcohols. *Industrial Crops and Products, 23*(3), 311-317.

Imran, A., Masjuki, H. H., Kalam, M. A., Varman, M., Hasmelidin, M., Al Mahmud, K. A. H., Shahir, S. A., and Habibullah, M. (2013). Study of Friction And Wear Characteristic of Jatropha Oil Blended Lube Oil. *International Tribology Conference Malaysia 2013, 68*, 178-185.

Jain, D., Ghonse, S. S., Trivedi, T., Fernandes, G. L., Menezes, L. D., Damare, S. R., Mamatha, S. S., Kumar, S., and Gupta, V. (2019). CO2 fixation and production of biodiesel by Chlorella vulgaris NIOCCV under mixotrophic cultivation. *Bioresource Technology, 273*, 672-676.

Jaiswar, S., Balar, N., Kumar, R., Patel, M. K., and Chauhan, P. S. (2017). Morphological and molecular characterization of newly isolated microalgal strain Neochloris aquatica SJ-1 and its high lipid productivity. *Biocatalysis and Agricultural Biotechnology, 9*, 108-112.

James, G. O., Hocart, C. H., Hillier, W., Price, G. D., and Djordjevic, M. A. (2013). Temperature modulation of fatty acid profiles for biofuel production in nitrogen deprived Chlamydomonas reinhardtii. *Bioresource Technology, 127*, 441-447.

Jamshaid, M., Masjuki, H. H., Kalam, M. A., Zulkifli, N. W. M., Arslan, A., Alwi, A., Khuong, L. S., Alabdulkarem, A., and Syahir, A. Z. (2019). Production optimization and tribological characteristics of cottonseed oil methyl ester. *Journal of Cleaner Production, 209*, 62-73.

Jayadas, N. H., and Nair, K. P. (2006). Coconut oil as base oil for industrial lubricants—evaluation and modification of thermal, oxidative and low temperature properties. *Tribology International, 39*(9), 873-878.

JGS LLC. (2014). Corrosive Wear. Retrieved from https://www.jgs-nitriding.com/index.php/2014-09-09-14-47-03/methods-of-surface-failure/24-corrosive-wear

Jiang, S., Li, S., Liu, L., Wang, L., and Mominou, N. (2015). The tribological properties and tribochemical analysis of blends of poly alpha-olefins with neopentyl polyol esters. *Tribology International, 86*, 42-51.

Jinqi, L., and Houtian, L. (1992). Degradation of azo dyes by algae. *Environmental Pollution, 75*(3), 273-278.

Kahoul, N., Chenni, R., Cheghib, H., and Mekhilef, S. (2017). Evaluating the reliability of crystalline silicon photovoltaic modules in harsh environment. *Renewable Energy, 109*, 66-72.

Kalam, M. A., Masjuki, H. H., Cho, H. M., Mosarof, M. H., Mahmud, M. I., Chowdhury, M. A., and Zulkifli, N. W. M. (2017). Influences of thermal stability, and lubrication performance of biodegradable oil as an engine oil for improving the efficiency of heavy duty diesel engine. *Fuel, 196*, 36-46.

Kamalakar, K., Rajak, A. K., Prasad, R. B. N., and Karuna, M. S. L. (2013). Rubber seed oil-based biolubricant base stocks: A potential source for hydraulic oils. *Industrial Crops and Products, 51*, 249-257.

Kania, D., Yunus, R., Omar, R., Abdul Rashid, S., and Mohamad Jan, B. (2015). A review of biolubricants in drilling fluids: Recent research, performance, and applications. *Journal of Petroleum Science and Engineering, 135*, 177-184.

Kania, D., Yunus, R., Omar, R., Abdul Rashid, S., Mohamed Jan, B., and Arsanjani, N. (2018). Nonionic polyol esters as thinner and lubricity enhancer for synthetic-based drilling fluids. *Journal of Molecular Liquids, 266*, 846-855.

Kardash, E., and Tur'yan, Y. I. (2005). Acid value determination in vegetable oils by indirect titration in aqueous-alcohol media. *Croatica Chemica Acta, 78*(1), 99-103.

Katırcıoğlu, H., Aslım, B., Rehber Türker, A., Atıcı, T., and Beyatlı, Y. (2008). Removal of cadmium(II) ion from aqueous system by dry biomass, immobilized live and heat-inactivated Oscillatoria sp. H1 isolated from freshwater (Mogan Lake). *Bioresource Technology, 99*(10), 4185-4191.

Khan, M. S., Sisodia, M. S., Gupta, S., Feroskhan, M., Kannan, S., and Krishnasamy, K. (2019). Measurement of tribological properties of Cu and Ag blended coconut oil nanofluids for metal cutting. *Engineering Science and Technology, an International Journal*, In Press, Corrected Proof.

Knothe, G. (2005). Dependence of biodiesel fuel properties on the structure of fatty acid alkyl esters. *Fuel Processing Technology, 86*(10), 1059-1070.

Knothe, G., Krahl, J., and Van Gerpen, J. (2015). *The biodiesel handbook*: Elsevier.

Knothe, G., and Steidley, K. R. (2005). Kinematic viscosity of biodiesel fuel components and related compounds. Influence of compound structure and comparison to petrodiesel fuel components. *Fuel, 84*(9), 1059-1065.

Knothe, G., and Steidley, K. R. (2011). Kinematic viscosity of fatty acid methyl esters: Prediction, calculated viscosity contribution of esters with unavailable data, and carbon–oxygen equivalents. *Fuel, 90*(11), 3217-3224.

Koh, M. Y., Mohd. Ghazi, T. I., and Idris, A. (2014). Synthesis of palm based biolubricant in an oscillatory flow reactor (OFR). *Industrial Crops and Products, 52*, 567-574.

Kondo, Y., Koyama, T., and Sasaki, S. (2013). Tribological properties of ionic liquids. In Ionic liquids-New aspects for the future: IntechOpen. Retrieved from https://www.intechopen.com/books/ionic-liquids-new-aspects-for-the-future/tribological-properties-of-ionic-liquids.

Kong, Q., Chen, P., and Ruan, R. (2007). *High oil content microalgae selection for biodiesel production.* Paper presented at the 2007 ASAE Annual Meeting.

Konishi, T., and Perez, J. (1997). Properties of Polyol Esters—-Lubrication of an Aluminum Silicon Alloy. *Tribology Transactions, 40*(3), 500-506.

Kopeliovich, D. (2012, June 2). Additives in lubricating oils. *Materials Engineering.* Retrieved from https://www.substech.com/dokuwiki/doku.php?id=additives_in_lubricating_oils

Kopeliovich, D. (2018, February 3). Mechanisms of wear. *Materials Engineering.* Retrieved from http://www.substech.com/dokuwiki/doku.php?id=mechanisms_of_wear

Kraft, K. (2011). *Biolubricant.* State of Washingthon, USA.

Kulkarni, R. D., Deshpande, P. S., Mahajan, S. U., and Mahulikar, P. P. (2013). Epoxidation of mustard oil and ring opening with 2-ethylhexanol for biolubricants with enhanced thermo-oxidative and cold flow characteristics. *Industrial Crops and Products, 49*, 586-592.

Kumar, A., and Sharma, S. (2011). Potential non-edible oil resources as biodiesel feedstock: An Indian perspective. *Renewable and Sustainable Energy Reviews, 15*(4), 1791-1800.

Kumar, D., Rai, J., and Gaur, J. P. (2012). Removal of metal ions by Phormidium bigranulatum (Cyanobacteria)-dominated mat in batch and continuous flow systems. *Bioresource Technology, 104*, 202-207.

Kumar, N. (2017). Oxidative stability of biodiesel: Causes, effects and prevention. *Fuel, 190*, 328-350.

Kusano, Y., and Hutchings, I. M. (2003). Modelling the entrainment and motion of particles in a gap: Application to abrasive wear. *Proceedings of the Institution of Mechanical Engineers, Part J: Journal of Engineering Tribology, 217*(6), 427-433.

Kusumo, F., Silitonga, A. S., Masjuki, H. H., Ong, H. C., Siswantoro, J., and Mahlia, T. M. I. (2017). Optimization of transesterification process for Ceiba pentandra oil: A comparative study between kernel-based extreme learning machine and artificial neural networks. *Energy, 134*, 24-34.

Kusumoto, K., Shimizu, K., Efremenko, V. G., Hara, H., Shirai, M., ito, J., Hatate, M., gaqi, Y., and Purba, R. H. (2019). Three body type abrasive wear characteristics of multi-component white cast irons. *Wear, 426-427*, 122-127.

Lam, M. K., and Lee, K. T. (2013). Catalytic transesterification of high viscosity crude microalgae lipid to biodiesel: Effect of co-solvent. *Fuel Processing Technology, 110*, 242-248.

Lam, M. K., Yusoff, M. I., Uemura, Y., Lim, J. W., Khoo, C. G., Lee, K. T., and Ong, H. C. (2017). Cultivation of Chlorella vulgaris using nutrients source from domestic wastewater for biodiesel production: Growth condition and kinetic studies. *Renewable Energy, 103*, 197-207.

Lane, T. (1957). The flash temperature parameter: A criterion for assessing EP performance in the four-ball machine. *Journal of the Institute of Petroleum, 43*, 181-188.

Leite, G. B., Paranjape, K., and Hallenbeck, P. C. (2016). Breakfast of champions: Fast lipid accumulation by cultures of Chlorella and Scenedesmus induced by xylose. *Algal Research, 16*, 338-348.

Li, T., Gargouri, M., Feng, J., Park, J.-J., Gao, D., Miao, C., Dong, T., Gang, D. R., and Chen, S. (2015). Regulation of starch and lipid accumulation in a microalga Chlorella sorokiniana. *Bioresource Technology, 180*, 250-257.

Li, W., and Wang, X. (2015). Bio-lubricants derived from waste cooking oil with improved oxidation stability and low-temperature properties. *Journal of Oleo Science, 64*(4), 367-374.

Li, Y., Han, D., Sommerfeld, M., and Hu, Q. (2011). Photosynthetic carbon partitioning and lipid production in the oleaginous microalga Pseudochlorococcum sp. (Chlorophyceae) under nitrogen-limited conditions. *Bioresource Technology, 102*(1), 123-129.

Li, Y., Horsman, M., Wang, B., Wu, N., and Lan, C. Q. (2008). Effects of nitrogen sources on cell growth and lipid accumulation of green alga Neochloris oleoabundans. *Applied microbiology and biotechnology, 81*(4), 629-636.

Liang, Y., Sarkany, N., and Cui, Y. (2009). Biomass and lipid productivities of Chlorella vulgaris under autotrophic, heterotrophic and mixotrophic growth conditions. *Biotechnology letters, 31*(7), 1043-1049.

Liu, S., Tan, S., Li, W., Song, J., Yu, H., Liu, Y., Wu, Q., Yu, S., Liu, F., and Song, Z. (2018). Hydrogenation of fatty acid methyl ester over Pd nanoparticles stabilized by thermoregulated ionic liquid. *Molecular Catalysis, 458*, 106-111.

Lorenz, R. T. (1999). A technical review of Haematococcus algae. *NatuRoseTM Technical Bulletin, 60*, 1-12.

Lubeletter, N. (2016). All About Additives - The Role of Antioxidants February 17, 2016. Retrieved from https://www.nyelubricants.com/all-about-additives---the-role-of-antioxidants

Lv, F., Jiao, C., Ta, N., and Rao, Z. (2018). Mixed-lubrication analysis of misaligned bearing considering turbulence. *Tribology International, 119*, 19-26.

Machinery Lubrication. (2018). Lubricant Additives - A Practical Guide. Retrieved from https://www.machinerylubrication.com/Read/31107/oil-lubricant-additives

Macias-Rodriguez, B. A., and Marangoni, A. A. (2018). Linear and nonlinear rheological behavior of fat crystal networks. *Critical Reviews in Food Science and Nutrition, 58*(14), 2398-2415.

Madanhire, I., and Mbohwa, C. (2016). Lubricant Additive Impacts on Human Health and the Environment. In *Mitigating Environmental Impact of Petroleum Lubricants* (pp. 17-34): Springer.

Madankar, C. S., Dalai, A. K., and Naik, S. N. (2013). Green synthesis of biolubricant base stock from canola oil. *Industrial Crops and Products, 44*, 139-144.

Maity, J. P., Bundschuh, J., Chen, C.-Y., and Bhattacharya, P. (2014). Microalgae for third generation biofuel production, mitigation of greenhouse gas emissions and wastewater treatment: Present and future perspectives – A mini review. *Energy, 78*, 104-113.

Mannekote, J. K., Kailas, S. V., Venkatesh, K., and Kathyayini, N. (2017). Environmentally friendly functional fluids from renewable and sustainable sources-A review. *Renewable and Sustainable Energy Reviews*.

Markets and Markets. (2018). *Bio-Lubricant Market worth 3.36 Billion USD by 2022*. Retrieved from https://www.marketsandmarkets.com/PressReleases/biolubricants.asp

Markou, G., and Georgakakis, D. (2011). Cultivation of filamentous cyanobacteria (blue-green algae) in agro-industrial wastes and wastewaters: A review. *Applied Energy, 88*(10), 3389-3401.

Martins, R., Seabra, J., Brito, A., Seyfert, C., Luther, R., and Igartua, A. (2006). Friction coefficient in FZG gears lubricated with industrial gear oils: Biodegradable ester vs. mineral oil. *Tribology International, 39*(6), 512-521.

Maru, M. M., Almeida, C. M., Silva, R. F., and Achete, C. A. (2013). Assessment of boundary lubrication in biodiesels by nanotribological tests. *Energy, 55*, 273-277.

Masjuki, H., Maleque, M., Kubo, A., and Nonaka, T. (1999). Palm oil and mineral oil based lubricants—their tribological and emission performance. *Tribology International, 32*(6), 305-314.

McNutt, J., and He, Q. (2016). Development of biolubricants from vegetable oils via chemical modification. *Journal of Industrial and Engineering Chemistry, 36*, 1-12.

Medina-Meza, I. G., Barnaba, C., and Barbosa-Cánovas, G. V. (2014). Effects of high pressure processing on lipid oxidation: A review. *Innovative Food Science & Emerging Technologies, 22*, 1-10.

Meher, L. C., Vidya Sagar, D., and Naik, S. N. (2006). Technical aspects of biodiesel production by transesterification—a review. *Renewable and Sustainable Energy Reviews, 10*(3), 248-268.

Menegazzo, M. L., and Fonseca, G. G. (2019). Biomass recovery and lipid extraction processes for microalgae biofuels production: A review. *Renewable and Sustainable Energy Reviews, 107*, 87-107.

Mihaela, P., Josef, R., Monica, N., and Rudolf, Z. (2013). Perspectives of safflower oil as biodiesel source for South Eastern Europe (comparative study: Safflower, soybean and rapeseed). *Fuel, 111*, 114-119.

Mobarak, H. M., Mohamad, E. N., Masjuki, H. H., Kalam, M. A., Al Mahmud, K. A. H., Habibullah, M., and Ashraful, A. M. (2014). The prospects of biolubricants as alternatives in automotive applications. *Renewable & Sustainable Energy Reviews, 33*, 34-43.

Mobarak, H. M., Niza Mohamad, E., Masjuki, H. H., Kalam, M. A., Al Mahmud, K. A. H., Habibullah, M., and Ashraful, A. M. (2014). The prospects of biolubricants as alternatives in automotive applications. *Renewable and Sustainable Energy Reviews, 33*(0), 34-43.

Mohd Noor, C. W., Noor, M. M., and Mamat, R. (2018). Biodiesel as alternative fuel for marine diesel engine applications: A review. *Renewable and Sustainable Energy Reviews, 94*, 127-142.

Monirul, I., Masjuki, H., Kalam, M., Zulkifli, N., Rashedul, H., Rashed, M., Imdadul, H., and Mosarof, M. (2015). A comprehensive review on biodiesel cold flow properties and oxidation stability along with their improvement processes. *Rsc Advances, 5*(105), 86631-86655.

Monirul, I. M., Masjuki, H. H., Kalam, M. A., Mosarof, M. H., Zulkifli, N. W. M., Teoh, Y. H., and How, H. G. (2016). Assessment of performance, emission and combustion characteristics of palm, jatropha and Calophyllum inophyllum biodiesel blends. *Fuel, 181*, 985-995.

Mosarof, M. H., Kalam, M. A., Masjuki, H. H., Alabdulkarem, A., Habibullah, M., Arslan, A., and Monirul, I. M. (2016). Assessment of friction and wear characteristics of Calophyllum inophyllum and palm biodiesel. *Industrial Crops and Products, 83*, 470-483.

Mostafa, S. S. M., and El-Gendy, N. S. (2013). Evaluation of fuel properties for microalgae *Spirulina platensis* bio-diesel and its blends with Egyptian petro-diesel. *Arabian Journal of Chemistry, 10*, s2040-s2050.

Muraki, M. (1987). Molecular structure of synthetic hydrocarbon oils and their rheological properties governing traction characteristics. *Tribology International, 20*(6), 347-354.

Muratore, C., Bultman, J. E., Aouadi, S. M., and Voevodin, A. A. (2011). In situ Raman spectroscopy for examination of high temperature tribological processes. *Wear, 270*(3), 140-145.

Nagappan, S., Devendran, S., Tsai, P.-C., Dahms, H.-U., and Ponnusamy, V. K. (2019). Potential of two-stage cultivation in microalgae biofuel production. *Fuel, 252*, 339-349.

Nahidian, B., Ghanati, F., Shahbazi, M., and Soltani, N. (2018). Effect of nutrients on the growth and physiological features of newly isolated Haematococcus pluvialis TMU1. *Bioresource Technology, 255*, 229-237.

Nakajima, A., Horikoshi, T., and Sakaguchi, T. (1982). Recovery of uranium by immobilized microorganisms. *European journal of applied microbiology and biotechnology, 16*(2), 88-91.

Ng, W., and Law, H. (2017). *The New Lubricant Trade In Asean. A Promising New Era*. Retrieved from http://www.ipsosconsulting.com/en/node/612

Ngangkham, M., Ratha, S. K., Prasanna, R., Saxena, A. K., Dhar, D. W., Sarika, C., and Prasad, R. B. N. (2012). Biochemical modulation of growth, lipid quality and productivity in mixotrophic cultures of Chlorella sorokiniana. *SpringerPlus, 1*(1), 33.

Ni, Z.-h., Li, F.-s., Wang, H., Wang, S., Gao, S.-y., and Zhou, L. (2020). Antioxidative performance and oil-soluble properties of conventional antioxidants in rubber seed oil biodiesel. *Renewable Energy, 145*, 93-98.

Nohair, B., Especel, C., Lafaye, G., Marécot, P., and Barbier, J. (2005). Palladium supported catalysts for the selective hydrogenation of sunflower oil. *Journal of Molecular Catalysis A: Chemical, 229*(1-2), 117-126.

Oh, J., Yang, S., Kim, C., Choi, I., Kim, J. H., and Lee, H. (2013). Synthesis of biolubricants using sulfated zirconia catalysts. *Applied Catalysis A: General, 455*, 164-171.

Onay, M., Sonmez, C., Oktem, H. A., and Yucel, A. M. (2014). Thermo-resistant green microalgae for effective biodiesel production: Isolation and characterization of unialgal species from geothermal flora of Central Anatolia. *Bioresource Technology, 169*, 62-71.

Orives, J. R., Galvan, D., Pereira, J. L., Coppo, R. L., and Borsato, D. (2014). Experimental Design Applied for Cost and Efficiency of Antioxidants in Biodiesel. *Journal of the American Oil Chemists' Society, 91*(10), 1805-1811.

Packer, A., Li, Y., Andersen, T., Hu, Q., Kuang, Y., and Sommerfeld, M. (2011). Growth and neutral lipid synthesis in green microalgae: a mathematical model. *Bioresource Technology, 102*(1), 111-117.

Pancha, I., Chokshi, K., George, B., Ghosh, T., Paliwal, C., Maurya, R., and Mishra, S. (2014). Nitrogen stress triggered biochemical and morphological changes in the microalgae Scenedesmus sp. CCNM 1077. *Bioresource Technology, 156*, 146-154.

Pancha, I., Chokshi, K., Maurya, R., Trivedi, K., Patidar, S. K., Ghosh, A., and Mishra, S. (2015). Salinity induced oxidative stress enhanced biofuel production potential of microalgae Scenedesmus sp. CCNM 1077. *Bioresource Technology, 189*, 341-348.

Pandarus, V., Gingras, G., B land, F. o., Ciriminna, R., and Pagliaro, M. (2012). Selective hydrogenation of vegetable oils over Silia Cat Pd (0). *Organic Process Research & Development, 16*(7), 1307-1311.

Pavlostathis, S. G., and Jackson, G. H. (2002). Biotransformation of 2,4,6-trinitrotoluene in a continuous-flow Anabaena sp. system. *Water Research, 36*(7), 1699-1706.

Pecchia, P., Galasso, I., Mapelli, S., Bondioli, P., Zaccheria, F., and Ravasio, N. (2013). Stabilisation of camelina oil methyl esters through selective hydrogenation. *Industrial Crops and Products, 51*, 306-309.

Peng, Y., Xu, Y., Geng, J., Dearn, K. D., and Hu, X. (2017). Tribological assessment of coated piston ring-cylinder liner contacts under bio-oil lubricated conditions. *Tribology International, 107*, 283-293.

Pullen, J., and Saeed, K. (2012). An overview of biodiesel oxidation stability. *Renewable and Sustainable Energy Reviews, 16*(8), 5924-5950.

Quinchia, L. A., Delgado, M. A., Franco, J. M., Spikes, H. A., and Gallegos, C. (2012). Low-temperature flow behaviour of vegetable oil-based lubricants. *Industrial Crops and Products, 37*(1), 383-388.

Ra, C.-H., Kang, C.-H., Jung, J.-H., Jeong, G.-T., and Kim, S.-K. (2016). Effects of light-emitting diodes (LEDs) on the accumulation of lipid content using a two-phase culture process with three microalgae. *Bioresource Technology, 212*, 254-261.

Rabinowicz, E., and Tanner, R. (1966). Friction and wear of materials. *Journal of Applied Mechanics, 33*, 479.

Ramos, M. J., Fernández, C. M., Casas, A., Rodríguez, L., and Pérez, Á. (2009). Influence of fatty acid composition of raw materials on biodiesel properties. *Bioresource Technology, 100*(1), 261-268.

Rani, S., Joy, M. L., and Nair, K. P. (2015). Evaluation of physiochemical and tribological properties of rice bran oil – biodegradable and potential base stoke for industrial lubricants. *Industrial Crops and Products, 65*, 328-333.

Rastogi, R. B., and Yadav, M. (2003). Suspension of molybdenum–sulphur complexes in paraffin oil as extreme pressure lubricants. *Tribology International, 36*(7), 511-516.

Reddy, M. S., Sharma, N., and Agarwal, A. K. (2016). Effect of straight vegetable oil blends and biodiesel blends on wear of mechanical fuel injection equipment of a constant speed diesel engine. *Renewable Energy, 99*, 1008-1018.

Reddy, S. M., Sharma, N., Gupta, N., and Agarwal, A. K. (2018). Effect of non-edible oil and its biodiesel on wear of fuel injection equipment components of a genset engine. *Fuel, 222*, 841-851.

Ren, H.-Y., Liu, B.-F., Ma, C., Zhao, L., and Ren, N.-Q. (2013). A new lipid-rich microalga *Scenedesmus* sp. strain R-16 isolated using Nile red staining: effects of carbon and nitrogen sources and initial pH on the biomass and lipid production. *Biotechnology for Biofuels, 6*(1), 143.

Research Grand View. (2018). *Lubricants Market Size & Share, Industry Analysis Report, 2018-2025*. Retrieved from https://www.grandviewresearch.com/industry-analysis/lubricants-market

Rippka, R., and Herdman, M. (1992). Pasteur culture collection of cyanobacteria catalog and taxonomic handbook: catalog of strains. *Institut Pasteur, Paris*.

Rosenkranz, A., Costa, H. L., Profito, F., Gachot, C., Medina, S., and Dini, D. (2019). Influence of surface texturing on hydrodynamic friction in plane converging bearings - An experimental and numerical approach. *Tribology International, 134*, 190-204.

Rudnick, L. R. (2009). *Lubricant additives: chemistry and applications*: CRC press.

Rudnick, L. R. (2013). *Synthetics, mineral oils, and bio-based lubricants: chemistry and technology*: CRC press.

Ruggiero, A., D'Amato, R., Merola, M., Valašek, P., and Müller, M. (2017). Tribological characterization of vegetal lubricants: Comparative experimental investigation on Jatropha curcas L. oil, Rapeseed Methyl Ester oil, Hydrotreated Rapeseed oil. *Tribology International, 109*, 529-540.

Ruhul, M. A., Abedin, M. J., Rahman, S. M. A., Masjuki, B. H., Alabdulkarem, A., Kalam, M. A., and Shancita, I. (2016). Impact of fatty acid composition and physicochemical properties of Jatropha and Alexandrian laurel biodiesel blends: An analysis of performance and emission characteristics. *Journal of Cleaner Production, 133*, 1181-1189.

Saber, M., Nakhshiniev, B., and Yoshikawa, K. (2016). A review of production and upgrading of algal bio-oil. *Renewable and Sustainable Energy Reviews, 58*, 918-930.

Sadvakasova, A. K., Akmukhanova, N. R., Bolatkhan, K., Zayadan, B. K., Usserbayeva, A. A., Bauenova, M. O., Akhmetkaliyeva, A. E., and Allakhverdiev, S. I. (2019). Search for new strains of microalgae-producers of lipids from natural sources for biodiesel production. *International Journal of Hydrogen Energy, 44*(12), 5844-5853.

Sajjadi, B., Raman, A. A. A., and Arandiyan, H. (2016). A comprehensive review on properties of edible and non-edible vegetable oil-based biodiesel: Composition, specifications and prediction models. *Renewable and Sustainable Energy Reviews, 63*, 62-92.

Sankara narayanan, T. S. N. (2012). 8 - Nanocoatings to improve the tribocorrosion performance of materials. In V. S. Saji ,R. Cook (Eds.), *Corrosion Protection and Control Using Nanomaterials* (pp. 167-212): Woodhead Publishing.

Saranya, D., and Shanthakumar, S. (2019). Green microalgae for combined sewage and tannery effluent treatment: Performance and lipid accumulation potential. *Journal of Environmental Management, 241*, 167-178.

Sarı, A., and Tuzen, M. (2008). Biosorption of Pb(II) and Cd(II) from aqueous solution using green alga (Ulva lactuca) biomass. *Journal of Hazardous Materials, 152*(1), 302-308.

Sarin, A., Arora, R., Singh, N., Sarin, R., Malhotra, R., and Sarin, S. (2010). Blends of biodiesels synthesized from non-edible and edible oils: effects on the cold filter plugging point. *Energy & Fuels, 24*(3), 1996-2001.

Sarin, A., Arora, R., Singh, N. P., Sarin, R., Malhotra, R. K., and Kundu, K. (2009). Effect of blends of Palm-Jatropha-Pongamia biodiesels on cloud point and pour point. *Energy, 34*(11), 2016-2021.

Schneider, A. C., Mutterlose, J., Blumenberg, M., Heimhofer, U., and Luppold, F. W. (2019). Palynofacies, micropalaeontology, and source rock evaluation of non-marine Jurassic–Cretaceous boundary deposits from northern Germany - Implications for palaeoenvironment and hydrocarbon potential. *Marine and Petroleum Geology, 103*, 526-548.

Sebayang, A. H., Masjuki, H. H., Ong, H. C., Dharma, S., Silitonga, A. S., Kusumo, F., and Milano, J. (2017). Optimization of bioethanol production from sorghum grains using artificial neural networks integrated with ant colony. *Industrial Crops and Products, 97*, 146-155.

Seebens, H., Schwartz, N., Schupp, P. J., and Blasius, B. (2016). Predicting the spread of marine species introduced by global shipping. *Proceedings of the National Academy of Sciences, 113*(20), 5646-5651.

Semple, K. T., and Cain, R. B. (1996). Biodegradation of phenols by the alga Ochromonas danica. *Applied and Environmental Microbiology, 62*(4), 1265-1273.

Serrano, M., Bouaid, A., Martínez, M., and Aracil, J. (2013). Oxidation stability of biodiesel from different feedstocks: Influence of commercial additives and purification step. *Fuel, 113*, 50-58.

Shakib, S., and Mekhilef, S. (2017). A Frequency Adaptive Phase Shift Modulation Control Based LLC Series Resonant Converter for Wide Input Voltage Applications. *Ieee Transactions on Power Electronics, 32*(11), 8360-8370.

Shanta, S. M., Molina, G. J., and Soloiu, V. (2011). Tribological Effects of Mineral-Oil Lubricant Contamination with Biofuels: A Pin-on-Disk Tribometry and Wear Study. *Advances in Tribology, 2011*.

Sheehan, J., Dunahay, T., Benemann, J., and Roessler, P. (1998). *Look back at the US department of energy's aquatic species program: biodiesel from algae; close-out report*. Retrieved from

Shi, J., Podola, B., and Melkonian, M. (2007). Removal of nitrogen and phosphorus from wastewater using microalgae immobilized on twin layers: an experimental study. *Journal of Applied Phycology, 19*(5), 417-423.

Silitonga, A. S., Masjuki, H. H., Mahlia, T. M. I., Ong, H. C., Chong, W. T., and Boosroh, M. H. (2013). Overview properties of biodiesel diesel blends from edible and non-edible feedstock. *Renewable & Sustainable Energy Reviews, 22*, 346-360.

Silitonga, A. S., Masjuki, H. H., Ong, H. C., Kusumo, F., Mahlia, T. M. I., and Bahar, A. H. (2016). Pilot-scale production and the physicochemical properties of palm and Calophyllum inophyllum biodiesels and their blends. *Journal of Cleaner Production, 126*, 654-666.

Singh, P., and Goel, V. (2018). Effect of bio-lubricant on wear characteristics of cylinder liner-piston ring and cam-tappet combination in simulated environment. *Fuel, 233*, 677-684.

Singh, P., Guldhe, A., Kumari, S., Rawat, I., and Bux, F. (2015). Investigation of combined effect of nitrogen, phosphorus and iron on lipid productivity of microalgae Ankistrodesmus falcatus KJ671624 using response surface methodology. *Biochemical Engineering Journal, 94*, 22-29.

Smith, P. C., Ngothai, Y., Dzuy Nguyen, Q., and O'Neill, B. K. (2010). Improving the low-temperature properties of biodiesel: Methods and consequences. *Renewable Energy, 35*(6), 1145-1151.

Song, D., Fu, J., and Shi, D. (2008). Exploitation of Oil-bearing Microalgae for Biodiesel. *Chinese Journal of Biotechnology, 24*(3), 341-348.

Srinivasan, R., Mageswari, A., Subramanian, P., Suganthi, C., Chaitanyakumar, A., Aswini, V., and Gothandam, K. M. (2018). Bicarbonate supplementation enhances growth and biochemical composition of Dunaliella salina V-101 by reducing oxidative stress induced during macronutrient deficit conditions. *Scientific Reports, 8*(1), 6972.

Sripada, P. K., Sharma, R. V., and Dalai, A. K. (2013). Comparative study of tribological properties of trimethylolpropane-based biolubricants derived from methyl oleate and canola biodiesel. *Industrial Crops and Products, 50*, 95-103.

Srivastava, A., and Prasad, R. (2000). Triglycerides-based diesel fuels. *Renewable and Sustainable Energy Reviews, 4*(2), 111-133.

Stachowiak, G., and Batchelor, A. W. (2013). *Engineering tribology*: Butterworth-Heinemann.

Stachowiak, G. W. (2017). How tribology has been helping us to advance and to survive. *Friction, 5*(3), 233-247.

Stachowiak, G. W., and Batchelor, A. W. (2005). *Engineering Tribology*. Oxford, UK: Elsevier Butterworth-Heinemann.

Starr, R. C. (1971). [2] Algal cultures—sources and methods of cultivation. *Methods in Enzymology, 23*, 29-53.

Sukjit, E., Tongroon, M., Chollacoop, N., Yoshimura, Y., Poapongsakorn, P., Lapuerta, M., and Dearn, K. D. (2019). Improvement of the tribological behaviour of palm biodiesel via partial hydrogenation of unsaturated fatty acid methyl esters. *Wear, 426-427*, 813-818.

Sun, J., Xiong, X., Wang, M., Du, H., Li, J., Zhou, D., and Zuo, J. (2019). Microalgae biodiesel production in China: A preliminary economic analysis. *Renewable and Sustainable Energy Reviews, 104*, 296-306.

Suresh Kumar, K., Dahms, H.-U., Won, E.-J., Lee, J.-S., and Shin, K.-H. (2015). Microalgae – A promising tool for heavy metal remediation. *Ecotoxicology and Environmental Safety, 113*(Supplement C), 329-352.

Syahir, A. Z., Zulkifli, N. W. M., Masjuki, H. H., Kalam, M. A., Alabdulkarem, A., Gulzar, M., Khuong, L. S., and Harith, M. H. (2017). A review on bio-based lubricants and their applications. *Journal of Cleaner Production, 168*(Supplement C), 997-1016.

Sydney, E. B., Sturm, W., de Carvalho, J. C., Thomaz-Soccol, V., Larroche, C., Pandey, A., and Soccol, C. R. (2010). Potential carbon dioxide fixation by industrially important microalgae. *Bioresource Technology, 101*(15), 5892-5896.

Tam, N. F. Y., Chong, A. M. Y., and Wong, Y. S. (2002). Removal of tributyltin (TBT) by live and dead microalgal cells. *Marine Pollution Bulletin, 45*(1), 362-371.

Tan, C. H., Chen, C.-Y., Show, P. L., Ling, T. C., Lam, H. L., Lee, D.-J., and Chang, J.-S. (2016). Strategies for enhancing lipid production from indigenous microalgae isolates. *Journal of the Taiwan Institute of Chemical Engineers, 63*, 189-194.

Tang, D., Han, W., Li, P., Miao, X., and Zhong, J. (2011). CO2 biofixation and fatty acid composition of Scenedesmus obliquus and Chlorella pyrenoidosa in response to different CO2 levels. *Bioresource Technology, 102*(3), 3071-3076.

Taştan, B. E., Duygu, E., and Dönmez, G. (2012). Boron bioremoval by a newly isolated Chlorella sp. and its stimulation by growth stimulators. *Water Research, 46*(1), 167-175.

Teoh, M.-L., Phang, S.-M., and Chu, W.-L. (2013). Response of Antarctic, temperate, and tropical microalgae to temperature stress. *Journal of Applied Phycology, 25*(1), 285-297.

The Freedonia Group. (2015). World Lubricants. Retrieved from https://www.freedoniagroup.com/industry-study/world-lubricants-3364.htm

Uddin, M., Ibatan, T., and Shankar, S. (2017). Influence of surface texture shape, geometry and orientation on hydrodynamic lubrication performance of plane - to - plane slider surfaces. *Lubrication Science, 29*(3), 153-181.

Upadhyay, R. K., and Kumar, A. (2019). Boundary lubrication properties and contact mechanism of carbon/MoS2 based nanolubricants under steel/steel contact. *Colloid and Interface Science Communications, 31*, 100186.

Vaičiulytė, S., Padovani, G., Kostkevičienė, J., and Carlozzi, P. (2014). Batch growth of *Chlorella vulgaris* CCALA 896 versus semi-continuous regimen for enhancing oil-rich biomass productivity. *Energies, 7*(6), 3840-3857.

van der Westhuizen, I., and Focke, W. W. (2018). Stabilizing sunflower biodiesel with synthetic antioxidant blends. *Fuel, 219*, 126-131.

Van Gerpen, J. H., Soylu, S., and Tat, M. (1999). *Evaluation of the lubricity of soybean oil-based additives in diesel fuel.* Paper presented at the Proceedings, Annual International Meeting of the ASAE.

Varatharajan, K., and Pushparani, D. S. (2018). Screening of antioxidant additives for biodiesel fuels. *Renewable and Sustainable Energy Reviews, 82*, 2017-2028.

Vigani, M., Parisi, C., Rodríguez-Cerezo, E., Barbosa, M. J., Sijtsma, L., Ploeg, M., and Enzing, C. (2015). Food and feed products from micro-algae: Market opportunities and challenges for the EU. *Trends in Food Science & Technology, 42*(1), 81-92.

Wagner, H., Luther, R., and Mang, T. (2001). Lubricant base fluids based on renewable raw materials: their catalytic manufacture and modification. *Applied Catalysis A: General, 221*(1-2), 429-442.

Wang, C.-Y., Fu, C.-C., and Liu, Y.-C. (2007). Effects of using light-emitting diodes on the cultivation of Spirulina platensis. *Biochemical Engineering Journal, 37*(1), 21-25.

Wang, H., Zhou, C., Lei, Y., and Liu, Z. (2019). An adhesive wear model for helical gears in line-contact mixed elastohydrodynamic lubrication. *Wear, 426-427*, 896-909.

Wang, J., and Zhou, C. (2018). Finite element analysis of the wear fatigue of rails with gradient structures. *Materials Letters, 231*, 35-37.

Wedeen, R. P., and Qian, L. F. (1991). Chromium-induced kidney disease. *Environmental Health Perspectives, 92*, 71-74.

Wright, J. (2008). Extreme Pressure Additives in Gear Oils. *Machinery Lubrication*(September 2008).

Wu, J., Alam, M. A., Pan, Y., Huang, D., Wang, Z., and Wang, T. (2017). Enhanced extraction of lipids from microalgae with eco-friendly mixture of methanol and ethyl acetate for biodiesel production. *Journal of the Taiwan Institute of Chemical Engineers, 71*, 323-329.

Xiao, H., Zou, H., Liu, S., and Li, C. (2019). An investigation of the friction and wear behavior of soybean biodiesel. *Tribology International, 131*, 377-385.

Xiao, Y., Lu, Y., Dai, J., and Wu, Q. (2015). Industrial Fermentation of Auxenochlorella protothecoides for Production of Biodiesel and Its Application in Vehicle Diesel Engines. *Frontiers in Bioengineering and Biotechnology, 3*(164).

Xin, L., Hong-ying, H., Ke, G., and Ying-xue, S. (2010). Effects of different nitrogen and phosphorus concentrations on the growth, nutrient uptake, and lipid accumulation of a freshwater microalga Scenedesmus sp. *Bioresource Technology, 101*(14), 5494-5500.

Xu, H., Miao, X., and Wu, Q. (2006). High quality biodiesel production from a microalga *Chlorella protothecoides* by heterotrophic growth in fermenters. *Journal of Biotechnology, 126*(4), 499-507.

Xu, Y., Hu, X., Yuan, K., Zhu, G., and Wang, W. (2014). Friction and wear behaviors of catalytic methylesterified bio-oil. *Tribology International, 71*, 168-174.

Xu, Y., Zheng, X., Hu, X., Dearn, K. D., and Xu, H. (2014). Effect of catalytic esterification on the friction and wear performance of bio-oil. *Wear, 311*(1–2), 93-100.

Yadav, G., Karemore, A., Dash, S. K., and Sen, R. (2015). Performance evaluation of a green process for microalgal CO2 sequestration in closed photobioreactor using flue gas generated in-situ. *Bioresource Technology, 191*, 399-406.

Yan, X. D., Sun, J. L., Xiong, S., and Hou, Y. Q. (2017). Insights into the sliding wear behavior of a copper-steel pair with oils containing extreme-pressure additives. *Wear, 386-387*(Supplement C), 211-217.

Yang, H.-Y., Lu, W.-J., Chen, Y.-C., Chen, K.-T., Teng, J.-C., and Wan, H.-P. (2017). New algal lipid extraction procedure using an amphiphilic amine solvent and ionic liquid. *Biomass and Bioenergy, 100*(Supplement C), 108-115.

Yang, J., Li, X., Hu, H., Zhang, X., Yu, Y., and Chen, Y. (2011). Growth and lipid accumulation properties of a freshwater microalga, Chlorella ellipsoidea YJ1, in domestic secondary effluents. *Applied Energy, 88*.

Yang, Z., Hollebone, B. P., Wang, Z., Yang, C., and Landriault, M. (2013). Factors affecting oxidation stability of commercially available biodiesel products. *Fuel Processing Technology, 106*, 366-375.

Yao, L. (2009). *Synthesis of fatty acid derivatives as potential biolubricants and their physical properties and boundary lubrication performances.* (Doctoral dissertation), Iowa State University, Ames, Iowa. Retrieved from https://lib.dr.iastate.edu/etd/10212

Young, I., and McEneny, J. (2001). Lipoprotein oxidation and atherosclerosis. In: Portland Press Limited.

Yuan, M.-H., Chen, Y.-H., Chen, J.-H., and Luo, Y.-M. (2017). Dependence of cold filter plugging point on saturated fatty acid profile of biodiesel blends derived from different feedstocks. *Fuel, 195*, 59-68.

Yunus, R., Fakhru'l‐Razi, A., Ooi, T. L., Iyuke, S. E., and Perez, J. M. (2004). Lubrication properties of trimethylolpropane esters based on palm oil and palm kernel oils. *European journal of lipid science and technology, 106*(1), 52-60.

Zaccheria, F., Psaro, R., Ravasio, N., and Bondioli, P. (2012). Standardization of vegetable oils composition to be used as oleochemistry feedstock through a selective hydrogenation process. *European journal of lipid science and technology, 114*(1), 24-30.

Zahid, R., Hassan, M. B., Alabdulkarem, A., Varman, M., Mufti, R. A., Kalam, M. A., Zulkifli, N., Gulzar, M., and Lee, T. (2017). Investigation of the tribochemical interactions of a tungsten-doped diamond-like carbon coating (W-DLC) with formulated palm trimethylolpropane ester (TMP) and polyalphaolefin (PAO). *Rsc Advances, 7*(43), 26513-26531.

Zainal, N. A., Zulkifli, N. W. M., Gulzar, M., and Masjuki, H. H. (2018). A review on the chemistry, production, and technological potential of bio-based lubricants. *Renewable and Sustainable Energy Reviews, 82*, 80-102.

Zhang, G., Xu, Y., Xiang, X., Zheng, G., Zeng, X., Li, Z., Ren, T., and Zhang, Y. (2018). Tribological performances of highly dispersed graphene oxide derivatives in vegetable oil. *Tribology International, 126*, 39-48.

Zhang, J., Tan, A., and Spikes, H. (2016). Effect of Base Oil Structure on Elastohydrodynamic Friction. *Tribology Letters, 65*(1), 13.

Zhao, B., and Su, Y. (2014). Process effect of microalgal-carbon dioxide fixation and biomass production: a review. *Renewable and Sustainable Energy Reviews, 31*, 121-132.

Zhou, J., Xiong, Y., and Liu, X. (2017). Evaluation of the oxidation stability of biodiesel stabilized with antioxidants using the Rancimat and PDSC methods. *Fuel, 188*, 61-68.

Zhu, L. D., Li, Z. H., Guo, D. B., Huang, F., Nugroho, Y., and Xia, K. (2017). Cultivation of Chlorella sp. with livestock waste compost for lipid production. *Bioresource Technology, 223*, 296-300.

Zuleta, E. C., Baena, L., Rios, L. A., and Calderón, J. A. (2012). The oxidative stability of biodiesel and its impact on the deterioration of metallic and polymeric materials: a review. *Journal of the Brazilian Chemical Society, 23*(12), 2159-2175.

Zulkifli, N. W. M., Azman, S. S. N., Kalam, M. A., Masjuki, H. H., Yunus, R., and Gulzar, M. (2016). Lubricity of bio-based lubricant derived from different chemically modified fatty acid methyl ester. *Tribology International, 93*, 555-562.

Zulkifli, N. W. M., Kalam, M. A., Masjuki, H. H., Shahabuddin, M., and Yunus, R. (2013). Wear prevention characteristics of a palm oil-based TMP (trimethylolpropane) ester as an engine lubricant. *Energy, 54*(Supplement C), 167-173.

Zulkifli, N. W. M., Kalam, M. A., Masjuki, H. H., and Yunus, R. (2013). Experimental analysis of tribological properties of biolubricant with nanoparticle additive. *International Tribology Conference Malaysia 2013, 68*, 152-157.

LIST OF PUBLICATIONS AND PAPERS PRESENTED

Presentation:

Cheah Mei Yee, Nurin Wahidah Mohd Zulkifli & Masjuki Hj. Hassan (2017). Anti-Wear Characteristics of Chemically Modified Microalgae Oil presented at Persidangan Kebangsaan Staf Kumpulan Profesional dan Pelaksana Universiti-Universiti Kejuruteraan (PPPRO'17), Kuala Lumpur, Malaysia, 2 August 2017.

Cheah Mei Yee, Ong Hwai Chyuan, Nurin Wahidah Mohd Zulkifli, Masjuki Hj. Hassan & Prof. Datin Seri Dr. Aishah Salleh (2017). Lubricity Evaluation of Upgraded *Chlorella* sp. Oil presented at the 3rd International Conference on the Science and Engineering of Materials (ICOSEM 2017), Kuala Lumpur, Malaysia, 24-25 October 2017.

Cheah Mei Yee, Ong Hwai Chyuan, Nurin Wahidah Mohd Zulkifli, Masjuki Hj. Hassan & Aishah Salleh (2018). Lubricity of chemically modified Chlorella sp. Oil blends presented at the International Conference on Sustainable Energy and Green Technology (SEGT 2018), Kuala Lumpur, Malaysia, 11-14 December 2018.

Journal articles:

Cheah MY, Ong HC, Zulkifli NWM, Masjuki HH, Salleh A. Evaluation of physicochemical and tribological properties of microalgae oil as biolubricant for used in hydrogen-powered internal combustion engine. International Journal of Hydrogen Energy (under revision).

Cheah MY, Ong HC, Zulkifli NWM, Masjuki HH, Salleh A. Chemically modified microalgae oil as green additive for anti-wear and extreme pressure properties enhancement. Wear (under review).